Utrecht University

Graduate school of natural sciences

Institute for theoretical physics

Mass Hierarchies and Scaling Scenarios for Perturbatively Flat Flux Vacua

Maarten Rottier

July 2022

Master's thesis

under the supervision of

Dr. Erik Plauschinn

Daily Supervisor

Dr. Umut Gürsoy

First Supervisor

Prof. dr. Thomas Grimm

Second Supervisor

Utrecht University

Abstract

Within the setting type IIB string theory compactifications on a Calabi-Yau orientifold, we systematically analyze the scaling behavior of the superpotential W_0 and the moduli masses with respect to the flux-induced tadpole charge N_{flux}. We do this for a set of explicit geometries in the large complex structure regime. In particular, we use a recipe proposed by Demirtas, Kim, McAllister, and Moritz (DKMM) in combination with a recent statistical analysis of Carta, Mininno, and Shukla (CMS) to solve the F-term equations for this set of geometries. We will go beyond the effective approach taken in this recipe, allowing us to explicitly compute the masses of the moduli. We furthermore stabilize a single Kähler modulus utilizing the KKLT-recipe. For all models investigated by CMS, we find that the bounding region of the distribution of W_0 with respect to N_{flux} can be described by an exponential scaling. Furthermore, we find that the mass of the lightest modulus scales as a power law with respect to W_0, indicating that smaller values of W_0 give rise to lighter moduli. The most interesting finding is that the mass scale of the heaviest modulus competes with, or drastically exceeds, the Kaluza-Klein scale of the compactification for all of these models. We consequently compute the scaling of the ratio between the heaviest modulus and the Kaluza-Klein scale with respect to N_{flux}, indicating that these models need unrealistically large flux numbers in order to give a correct mass hierarchy. We extend the analysis to a handful of models with three complex structure moduli, one of which admits a flux vacuum with a correct mass hierarchy.

Acknowledgements

First and foremost I would like to thank my daily supervisor Erik Plauschinn. Not only has he introduced me to the fascinating world of string theory research, but he has also been an extremely involved supervisor. We have had many interesting and engaging discussions from which I have learned a great deal. His advice about both the research as well as the more general aspects of life has been of tremendous help. I would also like to thank Umut and Thomas for taking up the role of being my official supervisors.

I would like to thank my friends and family for supporting me throughout this year, especially during the last months of the project. I would like to specifically thank Ima Meijer, Aylon Pinto, Artim Bassant, Hanne Leeuwen and Thomas Bakx for our times on the 7'th floor and the many much-needed coffee breaks.

Contents

Introduction

Why String Theory?

Many of the great achievements in theoretical physics have been unification schemes, in which two theories turned out to be part of some greater, *unified*, theory. Maxwell unified the theories of electricity and magnetism into electromagnetism, while Dirac first combined special relativity and quantum mechanics into quantum field theory. All these unifications eventually led to two extremely successful theories describing nature: general relativity and the standard model of particle physics. One of the most pressing challenges in theoretical physics today is to find a consistent theory of *quantum gravity* (QG), unifying the two.

In quantum field theory forces are described by particles. These so-called gauge bosons mediate the force between interacting matter. The (curved) spacetime only serves as the background on which the theory is defined. On the other hand, Einstein's theory of general relativity describes the force of gravity not in terms of particles, but as a consequence of the curved nature of spacetime itself. This seemingly very different nature of the concept of force within the two theories hints at the tremendous difficulty of this unification problem. At first attempts were made to "translate" one description into the other. For example, considering gravity to be a force mediated by a particle (called the *graviton*) allows one to quantize the classical, Einstein formulation of gravity. It turns out that this approach gives rise to a theory with an incurable sickness: non-predictability (or, in more technical terms, non-renormalizability).

String theory is a theory that addresses this difficult unification problem. As the name suggests, it is built on the following extremely simple premise: the fundamental building blocks of nature are not point-like particles, but extended objects called strings. When strings move through space, they sweep out a *worldsheet* (in contrast to the worldline of a point particle). Particles in the target space arise, after quantization, as excited states of the string. Remarkably, this spectrum of particle states naturally contains a symmetric, rank two tensor field: the *graviton*. The non-renormalizability one encounters in the quantization of Einstein's gravity is naturally cured through an infinite spectrum of states. These extra degrees of freedom tame the UV-divergencies, and predictive power is restored. These are all hints that string theory could indeed be the unifying theory of quantum gravity.

A Quick Look at (Super)strings

The replacement of point-like particles with one-dimensional, extended objects is the starting point of string theory. We choose a coordinate system such that we have one time-like coordinate τ and one space-like coordinate σ. We can furthermore demand that σ has periodic boundary conditions. This gives rise to *closed* strings, where we otherwise get open strings. We consequently embed the worldsheet into a d-dimensional target space using the embedding coordinates X^μ. For a visualization of this worldsheet embedding, see Figure 1.

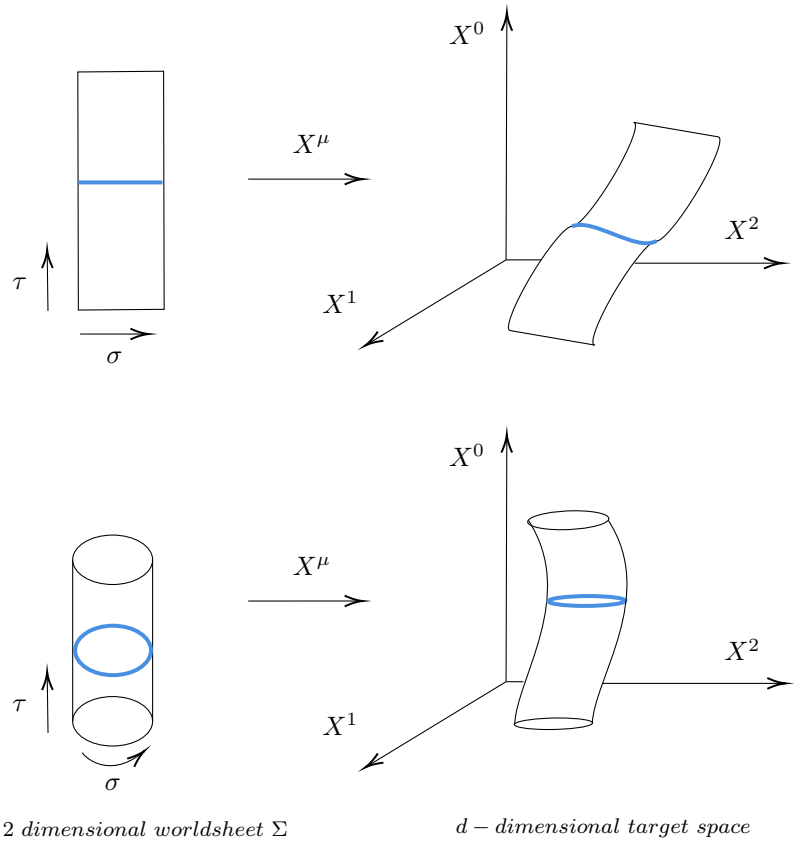

Figure 1: Illustration of the two dimensional worldsheet Σ with open string (above) and closed string (below) boundary conditions under the target space embedding X^μ. Depicted in blue is a time slice of the worldsheet, representing a particular string configuration.

Using the embedding coordinates we can write down an action for the worldsheet. This is the famous *Polyakov*-action

$$S = \frac{-1}{4\pi\alpha'} \int_\Sigma d^2\sigma \sqrt{-h} h^{\alpha\beta} \partial_\alpha X^\mu \partial_\beta X^\nu \eta_{\mu\nu},$$

where $h^{\alpha\beta}$ is an internal metric on the worldsheet, $\eta_{\mu\nu}$ is the flat Minkowski metric on the d-dimensional target space, and α' is a convenient parameter that is related to the fundamental length scale of the string as $l_s = 2\pi\sqrt{\alpha'}$. From this action a plethora of results follow, which we will mostly skip. We mention a couple of important features:

- For this theory to be consistent, it turns out that we need $d = 26$.
- The string spectrum contains a tachyon.
- There are no fermions in the spectrum.

We can quite easily remedy the last two problems by adding internal, fermionic degrees of freedom to the worldsheet theory. This brings us to the string theories that are actively being investigated today, the so-called *superstring theories*. It turns out that there are multiple constructions possible, leading to a total of five superstring theories. All of these constructions

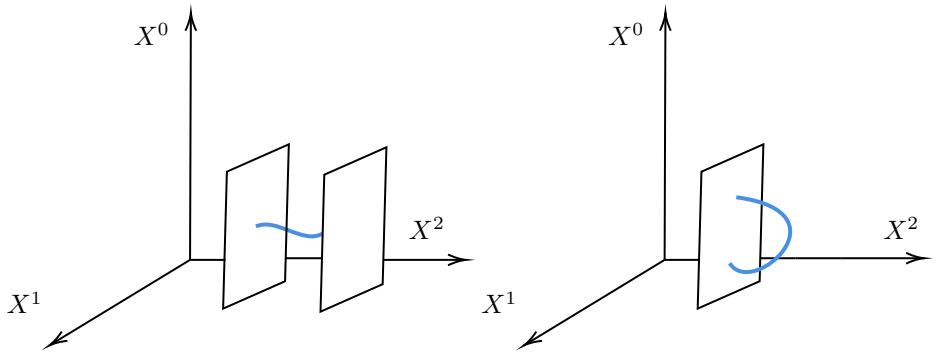

Figure 2: Illustration of an open string stretching between two different branes and an open string with both endpoints on the same brane.

lead to a supersymmetric spectrum of states in the target space [1]. In this thesis, we will focus on one particular type of string theory, called type IIB superstring theory. There are two type II string theories, known as type IIA and type IIB. They both describe closed, oriented [2] strings with internal fermionic degrees of freedom on the worldsheet. To make these theories consistent, it turns out that we need to project certain states out of the spectrum. This can be achieved through the so-called GSO projection. There are two inequivalent ways by which this can be done, leading to the two type II string theories. We again skip the details of these important constructions, and only comment on the important features:

- For the superstring theories to be consistent we find that $d = 10$.
- There is no tachyonic mode anymore, and the target space spectrum of states is supersymmetric.
- The spacetime dynamics of the massless mode are described by a supergravity theory, known as type IIB supergravity [3].

It is important to mention that string theory is not just a theory of strings, but also a theory of higher-dimensional extended objects called *branes*. These branes initially arise as objects on which open strings can end, see Figure 2. It turns out that these branes are dynamical in their own right, and they play a tremendously important role in phenomenology as they naturally support (non-Abelian) gauge fields.

String Phenomenology

As we have seen, string theory could be a unified theory of quantum gravity. There are, however, still problems to be overcome. The most obvious one concerns the number of dimensions of the target space. If string theory turns out to be the correct unified theory of nature, we would need the standard model to emerge within a particular limit. The standard model, however, is a theory that lives in four spacetime dimensions. This is in sharp contrast with the ten predicted dimensions of the superstring. This begs the question: what happens to the six extra dimensions that the superstring needs?

[1] Supersymmetry is a symmetry that exchanges bosons and fermions. The amount of supersymmetry is often denoted by an integer N, referring to the number of superpartners of one particular particle.

[2] Oriented strings arise from embedding an oriented worldsheet into the target space. One can also consider unoriented strings, arising from embedding unorientable surfaces (like the Möbius strip).

[3] Supergravity is a theory that combines gravity and with supersymmetry, necessarily making supersymmetry local. A priori it has nothing to do with string theory, and it is quite remarkable that the low energy limit of the superstring can be described by a supergravity theory.

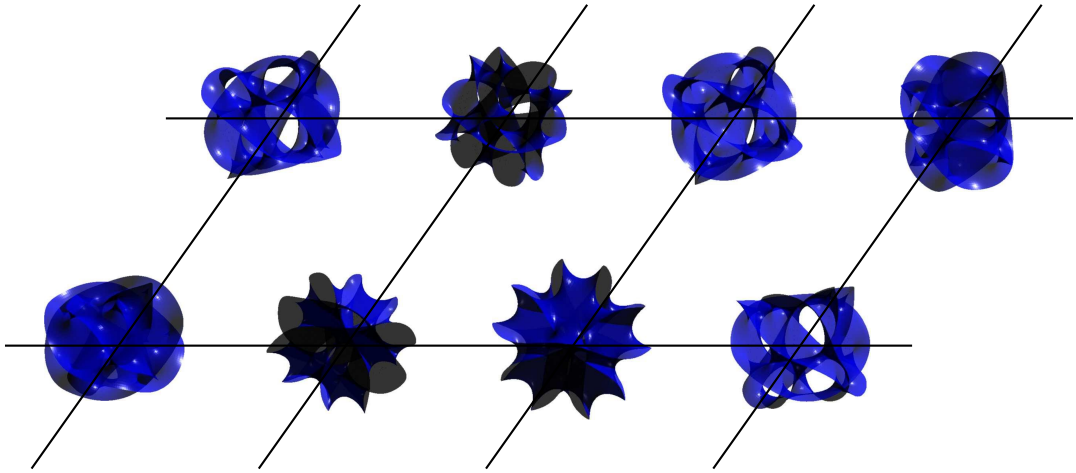

Figure 3: A visualization of a Calabi-Yau compactification. Spacetime is represented as a grid, and at each point the remaining six dimensions are represented by a compact Calabi-Yau manifold. Picture credits: Artim Bassant.

One possibility is that these six extra dimensions are not large, but compact and extremely small. Together they make up the *internal* space, and if we make them sufficiently small they are beyond the reach of current particle physics experiments. Besides compactness, there are some physically motivated conditions these internal spaces need to satisfy. The first one is the admittance of a Ricci flat metric. Secondly, we want (some) supersymmetry to survive the compactification. Together, these conditions fix the internal space to be a so-called *Calabi-Yau* manifold. For a visualization of this, see Figure 3.

Compactifying our ten-dimensional string theory on a Calabi-Yau manifold solves our problem concerning the number of dimensions. There are, however, new issues that arise. The most important one is that from the four dimensional perspective, the parameters that describe the size and shape of the internal space are left unfixed. From a particle physics perspective, this means that we obtain a bunch of massless scalar fields in four dimensions called *moduli*. These are phenomenologically problematic, as they lead to additional (unobserved) forces. This introduces the necessity to generate a potential for these fields that generates a mass that is high enough to overcome any possible conflicts with experimentally observed facts. Various procedures can establish this, collectively known as *moduli stabilization*.

A particular attractive model via which moduli can be stabilized is by allowing certain fields in the spectrum to attain background values on the internal manifold. These background values are known as *fluxes*, and including them in the compactification procedure leads to *flux compactifications*. Valid solutions are known as *flux vacua*. Flux compactifications form the central theme of this thesis. In particular, we will look for flux vacua of explicit Calabi-Yau backgrounds and see if some general patterns emerge.

However attractive flux compactifications may be, there are still many things to consider. First of all, fluxes cannot be arbitrarily tuned. Consistency conditions constrain the total amount of flux, which can be represented by an integer $N_{\text{flux}} \geq 0$, to be constrained from above. At the same time, the potential that the fluxes generate for the moduli is described in terms of a holomorphic function W. The precise numerical value of W in the minimum of the potential, denoted W_0, plays an important role in many phenomenological models. In this thesis we will consider one particular model building technique that requires W_0 to be exponentially small . This immediately poses an interesting question. We have two parameters that have to satisfy particular restrictions. The flux charge N_{flux} is bounded from above, while we need $W_0 \ll 1$. One aspect of this thesis is to investigate if there is some scaling behaviour of W_0 with respect

to N_{flux} for a set of explicit compactification models.

As we noted above, the spacetime dynamics of the massless mode of the type IIB superstring are described by type IIB supergravity. It turns out, however, that upon compactification of the string theory we obtain additional massive degrees of freedom that scale as $(\frac{1}{R})^n$, where R is the length scale associated with the compactification space. If these massive modes are sufficiently heavy we can effectively discard them. The upshot of this is that the four-dimensional action we are left with is again of a standard supergravity form. The masses of these modes therefore set an energy scale, known as the Kaluza-Klein (KK) scale. If we consequently turn on fluxes to give the remaining massless moduli a mass we have to make sure that these moduli masses, denoted M_{mod}, are smaller than this KK scale M_{KK}. The necessity of this scale separation is is another aspect of this thesis. For the particular models we investigate we will be able to compare the masses of the moduli with the KK-scale.

Outline of Thesis

This thesis serves a dual goal. In the first place is it a document in which we explain what our research is about. Secondly, it serves as a document that explains, in a self-contained way, the prerequisites that are necessary to read, understand and work with the papers we have used to perform this research. String theory is a vast subject, and ever growing-still. It can become highly mathematical, drawing on new research from the frontiers of mathematics, but it can also be more computational. For that reason, it is impossible to cover all the "basics". An extremely brief overview of some of the core concepts of string theory has been provided in the above introduction. For more material the interested reader can consult any introductory string theory textbook, of which the author particularly liked [1, 2, 3, 4, 5].

We start with the spectrum of type IIB string theory and its low energy supergravity description. We consequently introduce the necessary ingredients to understand the various aspects of our research. In Chapter 1 we introduce the procedure of compactifying type IIB supergravity on a Calabi-Yau manifold. In Chapter 2 we perform the so-called orientifold projection, partially breaking supersymmetry. In Chapter 3 we introduce background fluxes and look at their consequences. In particular, we will see how they generate a potential for (some) of the massless moduli fields. It turns out that at first order there is no potential generated for the modulus parametrizing the volume of the compactification space. We discuss a famous procedure for stabilizing this volume modulus as well, the so-called KKLT-scenario. In the remaining chapters, we will explicitly build upon the theoretical aspects above, looking for particular flux vacua. We will investigate the scaling behavior of W_0 as a function of N_{flux} as well as the scaling behavior of the moduli masses. This will allow us to comment on the observed hierarchy of masses, drawing conclusions about the validity of this procedure.

Chapter 1

Compactification of Type IIB on Calabi-Yau Threefolds

One of the most striking features of superstring theory is that the spacetime through which the string propagates has to be ten-dimensional. In contrast, our most celebrated physical theories, the standard model and Einstein's theory of gravity, are both formulated on a four-dimensional spacetime. If string theory is the fundamental theory of nature that encompasses both gravity and the standard model, these theories must arise within a particular limit. The discrepancy between the critical string dimension and the dimensions in which we have our well-established physical theories is the first motivation for considering string compactifications.

In particular, compactifying a string theory means taking the target space background of the string to be of the form $M_4 \times Y$. Here, M_4 denotes four-dimensional Minkowski space and Y is a compact six-dimensional manifold. We have to pick Y to be of small enough size such that probing these six extra dimensions is a task that, at present, cannot be achieved by experiments. The internal, compact, manifold Y can initially chosen to be anything, but the physically motivated condition to have a minimal amount of supersymmetry in the four-dimensional theory forces us to pick Y to be a Calabi-Yau manifold [1]. For type II theories this results in an effective four-dimensional theory with $N = 2$ supersymmetry.

We use the following *ansatz* for the metric that preserves the symmetries of M_4

$$g_{MN}(x^\mu, y^m) = \begin{pmatrix} g_{\mu\nu}(x) & 0 \\ 0 & g_{mn}(y) \end{pmatrix}, \tag{1.1}$$

where x^μ, $\mu = 0, \ldots 3$ denote the coordinates on M_4 and y^m denotes the coordinates on the internal manifold Y. Since string theory naturally incorporates gravity, the metric itself is a dynamical object. Upon compactification, we will see that the effective four-dimensional theory hosts a bunch of scalar fields that parametrize distinct Calabi-Yau backgrounds also compatible with the compactification conditions. These fields are called *moduli* and they appear in the action without a potential. Driving them to a particular vacuum expectation value (a vev) is an important problem, and is called *moduli stabilization*.

This chapter provides a review of the compactification of type IIB string theory on a Calabi-Yau background. We start with the ten-dimensional effective supergravity action, describing the massless modes of the type IIB string. We consequently compactify six large dimensions resulting in an effective action in four dimensions. Coupling constants appearing in this action encode the properties of the internal manifold, as they correspond to metrics on the moduli

spaces of the Calabi-Yau. In Section 1.1 we will briefly discuss some of the generic features arising upon compactifications of field theories. After that, we will compactify ten-dimensional type IIB supergravity on a Calabi-Yau threefold. Some additional background concerning Calabi-Yau manifolds is provided in Appendix B. The computations done in this section mainly follow the work of [6], as well as its review in [7]. Concise treatments can also be found in [8, 9]. For a well-written introduction concerning general string compactifications see [10].

1.1 Elements of Compactifications

Of particular interest in field theory compactifications are the ways in which the features of the internal space get encoded in the reduced action. In order to develop a feeling for the workings of this, we will consider the example of compactifying a massless, free scalar field $\phi(x^M)$ in five dimensions onto $\mathcal{M}^4 \times S^1$. This follows the discussion in Section 14.3 of [1]. The action describing such a theory is given by

$$S \propto \int_{\mathcal{M}^5} d^5x\, \eta^{MN} \partial_M \phi \partial_N \phi. \tag{1.2}$$

The capital letters M, N denote coordinates on the five-dimensional space. We can consequently split the coordinates according to $X^M = (x^\mu, y)$, where $y \in [0, 2\pi R]$ describes the coordinate on the circle $S^1 = \mathbb{R}/2\pi R$ with radius R. Upon variation of this action the equation of motion for ϕ reads

$$\Delta_5 \phi = \partial_\mu \partial^\mu \phi + \partial_y^2 \phi = 0. \tag{1.3}$$

We see that, due to the diagonal form of the metric, the differential operator Δ splits into its four- and one-dimensional part according to $\Delta_5 = \Delta_4 + \Delta_1 = \partial_\mu \partial^\mu + \partial_y^2$. To have a well-defined compactification ϕ must satisfy a periodicity condition on the fifth large dimension $\phi(x^\mu, y) = \phi(x^\mu, y + 2\pi R)$. Using this we find the Fourier expansion of ϕ

$$\phi(x^\mu, y) = \frac{1}{\sqrt{2\pi R}} \sum_{n=-\infty}^{\infty} \phi_n(x) e^{iny/R}. \tag{1.4}$$

It is important to note that the the Fourier coefficients $\frac{1}{\sqrt{2\pi R}} e^{iny/R}$ are eigenfunctions of ∂_y^2 on S^1. Plugging this expansion back into the equation of motion we obtain

$$\partial_\mu \partial^\mu \phi_n - \frac{n^2}{R^2} \phi_n = 0. \tag{1.5}$$

We see that we found an infinite set of four-dimensional scalar fields ϕ_n with masses n^2/R^2. We can learn a great deal about the general features concerning compactifications from this toy example. Generally, we will make a similar *ansatz* for the higher dimensional metric to decompose diagonally. When this is the case, the differential operator will split into an internal and external part. The eigenvalues of the internal Laplace operator will then generate the mass terms from the 4-dimensional perspective. The masses will generically be of the form $(n/R)^k$, with R denoting the typical size of the internal manifold. Due to phenomenological reasons, we are interested in the limit in which R becomes extremely small. Then all modes, except for

the Laplace zero mode, become extremely heavy and beyond the reach of detection of current experimental methods. We are left with only the massless modes, corresponding to the zero modes of the internal Laplacian.

Consider now a theory defined in some critical dimension $d_c = d + D$. Suppose we wish to compactify this theory onto a D-dimensional manifold Y leaving an effective d-dimensional theory. Consider a p-form $A^p(x^\mu, y^m)$ in the d_c-dimensional theory. If this p-form is massless, it satisfies the following equation of motion

$$\Delta_{d_c} A^p = 0. \tag{1.6}$$

Under a decomposition of the d_c-dimensional metric as in Equation 1.1 the Laplacian splits over the product manifold as $\Delta_{d_c} = \Delta_d + \Delta_D$. Each index of the p-form either lies in M_d or Y. This allows us to write

$$A^p = \sum_n \tilde{A}^{p-n} \wedge \omega_n,\ \omega_n \in \Omega^n(X),\ \tilde{A}^{p-n} \in \Omega^{p-n}(M_{d_c}). \tag{1.7}$$

Using the splitting of the Laplace operator and considering only the 4-dimensional massless modes, it follows that we are looking for forms ω_n satisfying

$$\Delta_D \omega_n = 0. \tag{1.8}$$

Differential forms satisfying 1.8 are called *harmonic*, and the discussion above illustrates that finding these harmonic forms of the internal manifold corresponds to finding the massless modes in the d-dimensional theory. Due to the Hode decomposition theorem, finding the Laplace zero modes is a cohomology problem on Calabi-Yau manifolds (cf. Appendix A).

1.2 Type IIB Spectrum and its Effective Action

The bosonic sector of type IIB string theory in $d_c = 10$ consists of the following NS-NS fields: the scalar dilaton $\hat{\phi}$, the metric $\hat{g}$ and the anti-symmetric two form $\hat{B}_2$. In the R-R sector (the sector distinguishing it from type IIA) we find the scalar axion $\hat{C}_0$, a two form $\hat{C}_2$ and a self-dual four form $\hat{C}_4$. Supersymmetry fixes the fermionic sector, and we will not make any reference to them here. The low energy effective action is a ten-dimensional supergravity action that, in the Einstein frame, takes the following form [4]:

$$\begin{aligned} S^{(10)}_{IIB} = \int & -\frac{1}{2}\hat{R} * 1 - \frac{1}{4} d\hat{\phi} \wedge * d\hat{\phi} - \frac{1}{4} e^{-\hat{\phi}} \hat{H}_3 \wedge * \hat{H}_3 \\ & - \frac{1}{4} e^{2\hat{\phi}} d\hat{C}_0 \wedge * d\hat{C}_0 - \frac{1}{4} e^{\hat{\phi}} \hat{F}_3 \wedge * \hat{F}_3 - \frac{1}{8} \hat{F}_5 \wedge * \hat{F}_5 - \frac{1}{4} \hat{C}_4 \wedge \hat{H}_3 \wedge \hat{F}_3, \end{aligned} \tag{1.9}$$

where the three field strengths are defined as

$$\begin{aligned} \hat{H}_3 &= d\hat{B}_2 \\ \hat{F}_3 &= d\hat{C}_2 - \hat{C}_0 d\hat{B}_2 \\ \hat{F}_5 &= d\hat{C}_4 - d\hat{B}_2 \wedge \hat{C}_2. \end{aligned} \tag{1.10}$$

The self duality condition on the four-form field strength $\hat{F}_5 = *\hat{F}_5$ is only imposed on the equations of motion and does not follow from the action. We consequently imagine that the ten-dimensional critical space of the superstring decomposes as $M_4 \times Y$, with Y Calabi-Yau threefold. Since Calabi-Yau manifolds are most naturally described as complex manifolds, we split coordinates accordingly. This means that we decompose the ten-dimensional coordinates X^M as

$$X^M = (x^\mu, y^\alpha, \bar{y}^{\bar{\alpha}}), \tag{1.11}$$

where the y's collectively denote the coordinates of the internal Calabi-Yau manifold, and x^μ the coordinates of M_4. In these coordinates the Kaluza-Klein *ansatz* for the metric, Equation 1.1, takes the form

$$\hat{g}_{MN} = g_{\mu\nu}(x)dx^\mu dx^\nu + g_{\alpha\bar{\beta}}dy^\alpha d\bar{y}^{\bar{\beta}}. \tag{1.12}$$

In general, quantum field theory describes the fluctuations of fields around their vacuum expectation value (vev). If we insist on a Minkowski vacuum in the four-dimensional theory we are highly restricted in the possibility of turning on vevs. In particular, since only $\eta_{\mu\nu}$ and the epsilon tensor $\epsilon_{\mu_1\ldots\mu_p}$ are invariant tensors, only the metric $g_{\mu\nu}$ and a p-form F^p are allowed to acquire a non trivial vev, restricted to be $\overline{g}_{\mu\nu} = \eta_{\mu\nu}$ and $\bar{F}_{\mu_1\ldots\mu_p} \propto \epsilon_{\mu_1\ldots\mu_p}$, respectively.

On the internal Calabi-Yau manifold we can turn on vevs for various fields in some specific way. This leads in so-called *flux compactifications*, which we will consider Chapter 3. As for now, we will only consider perturbations of the metric $g_{\alpha\bar{\beta}}$ on the Calabi-Yau manifold. These fluctuations describe the topologically equivalent class of Calabi-Yau threefolds and are called the *moduli* of the metric. They come in two flavors, called the Kähler moduli and the complex structure moduli (for more information, see Appendix B).

1.3 Expansion of the fields

The reduction of Equation 1.9 appears like a rather daunting task. It is wise to outline the general strategy and think about the expansion of the fields. Every field in the IIB spectrum lives in the critical dimension $d_c = 10$. As an example, we can consider the metric, g_{MN}. The first step is to decompose the metric under $GL(10,\mathbb{R}) \to GL(4,\mathbb{R}) + GL(6,\mathbb{R})$. This gives the decomposition $g_{MN} = g_{\mu\nu} + g_{\mu\alpha} + g_{\alpha\bar{\beta}}$, which we recognize as a scalar, a vector and the metric from the six-dimensional internal perspective. Upon the splitting of the Laplace operator, we wish to expand *each piece* of this decomposition into Laplace zero modes, discarding the massive modes. Via the Hodge decomposition theorem, this turns out to be a cohomology problem. Since we know a great deal about the cohomology spaces of Calabi-Yau threefolds (cf. Appendix B), we can fix the basis as in Table 1.1. These cohomology representatives are defined such that they intersect according to

$$\int_Y \omega_A \wedge \tilde{\omega}^B = \delta_A^B, \quad \int_Y \alpha_{\hat{K}} \wedge \beta^{\hat{L}} = \delta_{\hat{K}}^{\hat{L}}. \tag{1.13}$$

As mentioned in the previous section, we consider fluctuations around the fixed Calabi-Yau metric $g_{\alpha\bar{\beta}}$. As explained in Appendix B, the fluctuations of g decouple into the complex structure fluctuations $\delta g_{\alpha\beta}$ (pure index structure) and the Kähler fluctuations $\delta g_{\alpha\bar{\beta}}$ (mixed index structure). For the Kähler fluctuations there is no problem, and we can simply expand

Cohomology group	Dimension	Basis
$H^{(0,0)}$	1	1
$H^{(1,1)}$	$h^{(1,1)}$	$\omega_A,\ A = 1, \ldots, h^{(1,1)}$
$H^{(2,2)}$	$h^{(1,1)}$	$\tilde{\omega}_A\ A = 1, \ldots, h^{(1,1)}$
$H^{(2,1)}$	$h^{(2,1)}$	$\chi_K,\ K = 1, \ldots, K = h^{(2,1)}$
$H^{(3)}$	$2h^{(1,2)} + 2$	$\left(\alpha_{\hat{K}}, \beta^{\hat{K}}\right),\ K = 0, \ldots, h^{(2,1)}$
$H^{(3,3)}$	1	$\mathrm{vol}_6 \sim \Omega \wedge \overline{\Omega}$

Table 1.1: Cohomology basis of a Calabi-Yau threefold.

them in the basis ω. The complex structure fluctuations actually correspond to harmonic forms with values in the tangent bundle $H^{(2,0)}(Y, TY)$ [1]. Using the unique holomorphic three form Ω we can define

$$(b_K)_{\bar{\alpha}\bar{\beta}} := -\frac{i}{\|\Omega\|^2} (\chi_K)_{\bar{\alpha}\gamma\delta}\, \Omega^{\gamma\delta}_{\bar{\beta}}. \tag{1.14}$$

This pairing provides an isomorphism $H^{(2,0)}(Y, TY) \simeq H^{(2,1)}$, and gives us a suitable basis of $(0,2)$-forms to expand the complex structure deformations in. The other fields are expanded using the basis elements of Table 1.1. We will do this in two steps. First expanding the gravity sector and consequently the matter fields.

1.3.1 Gravity

The metric on the Calabi-Yau threefold is given by $\mathring{g}_{\alpha\bar{\beta}}$. On top of this, we have the fluctuations, comprised of the change in Kähler structure and the complex structure variations. These are denoted $\delta g_{\alpha\bar{\beta}}$ and $\delta g_{\alpha\beta}$, respectively. Expanding them in the relevant cohomology basis gives

$$g_{\alpha\bar{\beta}} = \mathring{g}_{\alpha\bar{\beta}} - iv^A(\omega_A)_{\alpha\bar{\beta}} \tag{1.15a}$$
$$g_{\alpha\beta} = \bar{z}^K(\bar{b}_K)_{\alpha\beta}. \tag{1.15b}$$

From the relation $g^{MN}g_{NK} = \delta^M_K$ we can find the expansion of the inverse metric. Here M, N, K do not denote ten-dimensional indices, but holomorphic or anti-holomorphic indices. In particular, we can pick M to be holomorphic and K to be anti-holomorphic. Doing this we find the expansion for the inverse metric

$$g^{\alpha\beta} = -\mathring{g}^{\alpha\bar{\alpha}}\mathring{g}^{\beta\bar{\beta}} z^K (b_K)_{\alpha\beta}. \tag{1.16}$$

In the same spirit we can consider M and K to be both (anti-)holomorphic. Such a combination results in

$$g^{\alpha\bar{\beta}} = \mathring{g}^{\alpha\bar{\beta}} + iv^A(\omega_A)_{\bar{\alpha}\bar{\beta}}\mathring{g}^{\bar{\alpha}\alpha}\mathring{g}^{\bar{\beta}\beta}. \tag{1.17}$$

1.3.2 Matter fields

The expansion of the matter fields consequently reads

$$\begin{aligned}
\hat{B}_2(x,y) &= B_2(x) + b^A\omega_A \\
\hat{C}_2(x,y) &= C_2(x) + c^A\omega_A \\
\hat{C}_4(x,y) &= D_2^A \wedge \omega_A + \rho_A \wedge \tilde{\omega}^A + V^{\hat{A}} \wedge \alpha_{\hat{A}} - U_{\hat{A}} \wedge \beta^{\hat{A}} \\
\hat{\phi}(x,y) &= \phi(x) \\
\hat{C}_0(x,y) &= C_0(x).
\end{aligned} \tag{1.18}$$

Here $B_2(x)$, $C_2(x)$ and $D_2^A(x)$ are $\mathcal{M}_4$ two-forms, $V^{\hat{A}}(x)$ and $U_{\hat{A}}(x)$ are $\mathcal{M}_4$ one-forms and and $b^A(x)$, $c^A(x)$ and $\rho_A(x)$ are $\mathcal{M}_4$ scalars. For the expansion of the field strengths we obtain

$$\begin{aligned}
d\hat{B}_2 &= dB_2 + db^A \wedge \omega_A \\
d\hat{C}_2 &= dC_2 + dc^A \wedge \omega_A \\
d\hat{C}_4 &= dD_2^A \wedge \omega_A + d\rho_A \wedge \tilde{\omega}^A + F^{\hat{K}} \wedge \alpha_{\hat{K}} - G_{\hat{K}} \wedge \beta^{\hat{K}} \\
\hat{F}_5 &= F^{\hat{K}} \wedge \alpha_{\hat{K}} - G_{\hat{K}} \wedge \beta^{\hat{K}} + \left(dD_2^A - db^A \wedge C_2 - c^A H_3\right) \wedge \omega_A \\
&\quad + d\rho_A \wedge \tilde{\omega}^A - c^A db^B \wedge \omega_A \wedge \omega_B \\
\hat{F}_3 &= dC_2 + dc^A \wedge \omega_A - C_0(dB_2 + db^A \wedge \omega_A).
\end{aligned} \tag{1.19}$$

Where we have defined the $\mathcal{M}_4$ two-forms $F^{\hat{K}} = dV^{\hat{K}}$ and $G_{\hat{K}} = dU_{\hat{K}}$.

1.4 Reduction of gravity

We have decomposed all the fields appearing in the ten-dimensional IIB supergravity action into their harmonic cohomology representatives. We consequently plug these expansions into the ten-dimensional supergravity action and perform the integrals over the Calabi-Yau manifold. We will do this according to the same two-step procedure. First reducing the gravity sector, after which we will turn to the matter part. The Einstein-Hilbert term is given by

$$S_{\text{EH}} = \int_{M_4 \times Y} \hat{R} * 1 = \int_{M_4 \times Y} \sqrt{|\hat{g}|}\hat{R}, \tag{1.20}$$

where $\hat{g} = \det(\hat{g}_{MN})$. We therefore turn to the task of dimensionally reducing the Ricci scalar. The full Ricci scalar is given by the following expression:

$$\begin{aligned}
R_{10} =& R_4 + g^{\mu\nu}R^{\alpha}_{\mu\alpha\nu} + g^{\alpha\beta}\left(R^{\mu}_{\alpha\mu\beta} + R^{\gamma}_{\alpha\gamma\beta} + R^{\bar{\gamma}}_{\alpha\bar{\gamma}\beta}\right) \\
&+ g^{\alpha\bar{\beta}}\left(R^{\mu}_{\alpha\mu\bar{\beta}} + R^{\gamma}_{\alpha\gamma\bar{\beta}} + R^{\bar{\gamma}}_{\alpha\bar{\gamma}\bar{\beta}}\right) + \text{ conjugate terms },
\end{aligned} \tag{1.21}$$

where we have denoted the Ricci scalar in four dimensions by R_4.

If we have the Christoffel symbols with at least one spacetime index, we can perform the computationlly tedious task of reducing the Ricci scalar. The explicit computation of one of the terms is relegated to Appendix A. The rest of the terms follow via similar computations (see also [6]). The dimensionally reduced Einstein-Hilbert term consequently takes the form

$$S_{\text{EH}} = \int \mathrm{d}^4x\sqrt{-g_4}\left(\mathcal{K}R + P_{AB}\partial_\mu v^A\partial^\mu v^B + Q_{AB}\partial_\mu z^A\partial^\mu \bar{z}^B\right), \tag{1.22}$$

where we have employed the same definitions as in [6]

$$\begin{aligned}(\omega_A g) &= (\omega_A)_{\alpha\bar{\beta}}\,\mathring{g}^{\alpha\bar{\beta}}\\ \omega_A\omega_B &= (\omega_A)_{\alpha\bar{\alpha}}\,(\omega_B)_{\beta\bar{\beta}}\,\mathring{g}^{\alpha\bar{\beta}}\mathring{g}^{\beta\bar{\alpha}}\\ b_A\bar{b}_B &= (b_A)_{\bar{\alpha}\bar{\beta}}\left(\bar{b}_B\right)_{\alpha\beta}\mathring{g}^{\alpha\bar{\beta}}\mathring{g}^{\beta\bar{\alpha}}.\end{aligned} \tag{1.23}$$

The coefficients appearing in front of the moduli are given by

$$\begin{aligned}P_{AB} &= \int_Y \mathrm{d}^6y\sqrt{g_6}\left[(\omega_A g)\,(\omega_B g) - \frac{1}{2}\,(\omega_A\omega_B)\right]\\ Q_{AB} &= \frac{1}{2}\int_Y \mathrm{d}^6y\sqrt{g_6}\,\left(b_A\bar{b}_B\right).\end{aligned} \tag{1.24}$$

Furthermore $\mathcal{K}$ represents the volume of the Calabi-Yau (cf. Appendix B)

$$\mathcal{K} = \int_Y d^6y\sqrt{g_6}. \tag{1.25}$$

Taking a closer look at Equation 1.22 we see that, as promised, we obtain a bunch of (complex) scalar fields v^A and z^A that dynamically parametrize the size and shape of our Calabi-Yau manifold.

1.5 Reduction of matter content

Having the expansions of Equations 1.18 and 1.19 at our disposal, we can now, term by term, reduce the matter part of the ten-dimensional IIB supergravity action. To do the computation, we again split the ten-dimensional integration according to

$$\int_{\mathcal{M}_4\times Y} = \int_{\mathcal{M}_4}\int_Y \tag{1.26}$$

and we consequently perform the integral over Y. Furthermore, we will repeatedly use the distributive property of the Hodge star $*$ over the wedge product

$$*_{10}\left(E_n\wedge I_p\right) = (-1)^{np}\left(*_4E_n\right)\wedge\left(*_6I_p\right), \tag{1.27}$$

where $E_n\in\Omega^n(\mathcal{M}_\triangle)$ and $I_p\in\Omega^p(Y)$. Using this identity together with Equations 1.18 and 1.19 we find:

$$\begin{aligned}
\int_Y d\hat{\phi}\wedge *d\hat{\phi} &= d\phi\wedge *d\phi\int_Y *1 \\
&= \mathcal{K}d\phi\wedge *d\phi && (1.28)\\
\int_Y d\hat{C}_0\wedge *d\hat{C}_0 &= dC_0\wedge *dC_0\int_Y *1 \\
&= \mathcal{K}dC_0\wedge *dC_0 && (1.29)\\
\int_Y \hat{H}_3\wedge *\hat{H}_3 &= \mathcal{K}dB_2\wedge *dB_2 + 4g_{AB}db^A\wedge *db^B && (1.30)\\
\int_Y \hat{F}_3\wedge *\hat{F}_3 &= \mathcal{K}\left(dC_2 - C_0dB_2\right)\wedge *(dC_2 - C_0dB_2) && (1.31)\\
\int_Y \hat{F}_5\wedge *\hat{F}_5 &= -\left(\mathrm{Im}\mathcal{M}^{-1}\right)^{AB}\left(G_A - \mathcal{M}_{AC}F^C\right)\wedge *\left(G_B - \overline{\mathcal{M}}_{BD}F^D\right)\\
&\quad + 4\mathcal{K}g_{ij}d\tilde{D}_2^i\wedge *d\tilde{D}_2^j + \frac{1}{4\mathcal{K}}g^{ij}d\tilde{\rho}_i\wedge *d\tilde{\rho}_j && (1.32)\\
\int_Y \hat{C}_4\wedge\hat{H}_3\wedge d\hat{C}_2 &= \mathcal{K}_{ijk}D_2^i\wedge db^j\wedge dc^k - \rho_i\left(dB_2\wedge dc^i + db^i\wedge dC_2\right), && (1.33)
\end{aligned}$$

where we have defined $d\tilde{D}_2^i = dD_2^i - db^i\wedge C_2 - c^i dB_2$ and $d\tilde{\rho}_i = d\rho_i - \mathcal{K}_{ijk}c^j db^k$. The matrix $\mathcal{M}$ is defined in terms of the intersections of α and β, and is related to the metric on $H^3(Y)$. The couplings that appear in the various terms of the action all encode properties of the internal Calabi-Yau. Their definitions are given in Appendix B.

1.6 Effective 4-Dimensional Action of Type IIB

We have reduced both the gravity and the matter section of the ten-dimensional supergravity action. At this point we still have to impose the self-duality of F_5. Furthermore, we have to canonically normalise the Einstein-Hilbert term through a suitable redefinition of some of the fields. These are details that are not important for the rest of the thesis, and for that reason we will omit them here. The interested reader can check the computations in [6]. We will simply state the result of the full action in four dimensions to conclude this chapter. It is given by

$$\begin{aligned}
S_{IIB}^{(4)} = \int_{\mathcal{M}_4} &-\frac{1}{2}R*1 - d\phi\wedge *d\phi - \frac{1}{2\mathcal{K}}Q_{AB}dz^A\wedge *d\bar{z}^B - g_{AB}dv^A\wedge *dv^B\\
&- \frac{1}{4}e^{-4\phi}dB_2\wedge *dB_2 - g_{AB}db^A\wedge *db^B\\
&- \frac{1}{4}e^{2\phi}\mathcal{K}dC_0\wedge *dC_0 - \frac{1}{4}e^{-2\phi}\mathcal{K}\left(dC_2 - C_0dB_2\right)\wedge *\left(dC_2 - C_0dB_2\right)\\
&- \mathcal{K}e^{2\phi}g_{AB}\left(dc^A - C_0db^B\right)\wedge *\left(dc^A - C_0db^B\right)\\
&- \frac{e^{2\phi}}{16\mathcal{K}}g^{AB}\left(d\rho_A - \mathcal{K}_{Akl}c^k db^l\right)\wedge *\left(d\rho_B - \mathcal{K}_{Bmn}c^m db^n\right)\\
&+ \left(db^i\wedge C_2 + c^i dB_2\right)\wedge\left(d\rho_i - \mathcal{K}_{ijk}c^j db^k\right) + \frac{1}{4}\mathcal{K}_{ijk}c^i c^j dB_2\wedge db^k\\
&+ \frac{1}{4}Re\mathcal{M}_{AB}F^A\wedge F^B + \frac{1}{4}Im\mathcal{M}_{AB}F^A\wedge *F^B.
\end{aligned} \tag{1.34}$$

Finally we can combine v and b to form the complex Kähler moduli defined by $T^A = b^A + iv^A$.

Combining the fields in the appropriate multiplets indicates that we end up with an $N = 2$ supersymmetric theory in four dimensions [11].

Chapter 2

Compactification of Type IIB on Calabi-Yau Orientiefolds

In the previous chapter, we have seen that the compactification of ten-dimensional type IIB supergravity gives us a $N = 2$ supersymmetric theory in four dimensions. We would like to break this supersymmetry to obtain a $N = 1$ theory. The reason we want this minimal amount of supersymmetry is to have more computational control. At the same time it is not too mathematically restrictive [11] [1]. The breaking of supersymmetry can be accomplished by dividing the total IIB action by a so-called orientifold projection $\mathcal{O}$. This reduces the degrees of freedom, as we only keep the fields that are symmetric under $\mathcal{O}$. Additionally, we would like to include Dp-branes into our supergravity theory to engineer non-Abelian gauge theories. As it turns out, Dp-branes are charged under certain field strengths appearing in the massless spectrum. Since the compactification space is a compact manifold, these charges must be canceled. The fixed point set of the orientifold projection naturally provides us with a new class of extended objects called O-planes. These O-planes can offset the Dp-brane charges.

The goal of this chapter is to introduce the orientifold action $\mathcal{O}$ and consider the ramifications of dividing out the symmetries defined by $\mathcal{O}$ in the effective IIB action we have found in the previous section. The material presented in this chapter closely follows the discussion in [11] and [12].

2.1 Orientifold projection and $O3/O7$-planes

In this section, we introduce the definition of the orientifold projection in the particular setting of type IIB supergravity with so-called $O3/O7$-planes. Starting from the $N = 2$ supergravity action in Equation 1.9, we want to divide out a symmetry $\mathcal{O}$ truncating the spectrum in such a way that we obtain an effective $N = 1$ theory. It turns out that in this particular setting $\mathcal{O}$ consists of various parts. Describing them is what we will turn to now.

The first piece of $\mathcal{O}$ consists of the parity operator Ω_p that acts on the level of the worldsheet. In particular, it exchanges the left-moving and the right-moving sector and thereby alters the fields we find in the critical dimension by only keeping the ones that are symmetric under this

[1] Not only gives some amount of supersymmetry us more computational control, it used to be a physically motivated condition. Reason for this is the fact that we know that the standard model is not yet complete. A supersymmetric extension of the standard model could be the explanation for this incompleteness, but no evidence of supersymmetry has been found in experiments so far.

exchange. In addition to this worldsheet operation, we also introduce a geometric symmetry operator σ. For consistency reasons, σ must act as a holomorphic involution on the internal space [13, 14]. It acts as the identity operator on $\mathcal{M}_4$. The action of σ on the cohomology basis elements is defined through its pull-back σ^*. Finally, we also need $(-1)^{F_L}$, where F_L counts the fermion number in the left-moving sector. Including this counting factor ensures that $\mathcal{O}^2 = \mathrm{Id}$.

The fact that σ is a holomorphic involution on the internal manifold Y means that it leaves the metric (and as a consequence, the Kähler form) invariant:

$$\sigma^* J = J. \tag{2.1}$$

The holomorphicity of σ ensures that it respects the Hodge decomposition of the cohomology groups. In particular, $\sigma^* H^{(3,0)}(Y) = H^{(3,0)}(Y)$. Picking Ω as cohomology representative of $H^{(3,0)}(Y)$ we can distinguish two different theories by considering the action of σ on Ω [15, 13, 14, 16]. These two possibilities are characterized by

$$\sigma^*\Omega = -\Omega \quad \text{or} \quad \sigma^*\Omega = \Omega. \tag{2.2}$$

In this section, we will focus on the former condition. As we will see momentarily, this condition gives rise to $O3$- and $O7$-planes. Combining all elements we find the full *orientifold projection* $\mathcal{O}$

$$\mathcal{O} = (-1)^{F_L}\Omega_p\sigma^*. \tag{2.3}$$

As we will see in the next sections, modding out the low energy effective action from the previous section by $\mathcal{O}$ truncates the spectrum and modifies the couplings in such a way that we obtain the standard $N = 1$ supergravity action in four dimensions.

Orientifold planes (O-planes) are defined as the fixed point set of the entire ten-dimensional space $M_4 \times Y$ under σ. Since σ acts trivially on $\mathcal{M}_4$, the orientifold plane fills up the entire four-dimensional Minkowski space. As a consequence of the involutive property $\sigma^2 = 1$, the dimensionality of these planes has to be even. This leaves the possibility of $O3, O5, O7$- and $O9$-planes (O-planes always fill the time direction, which we do not count in this convention). Using the fact that in local holomorphic coordinates z^m the holomorphic three form is given by $\Omega \sim dz^1 \wedge dz^2 \wedge dz^3$ and $\sigma^*\Omega = -\Omega$, we see that σ^* changes the sign of either one or three holomorphic basis forms. This indicates the possibility of a 2- or 0-dimensional fixed point set. Combining this with the Minkowski dimension, we conclude that this particular choice of involution indeed gives rise to $O3$- and $O7$-planes [2].

At this point it is important to note that in order to build phenomenological realistic models, we also have to include D-branes. These are extended objects that first appear in the geometrical string picture as places where the endpoints of open strings can end [4, 17, 1]. Branes naturally support non-Abelian gauge theories [18] and since type IIB does not come equipped with such gauge fields, this inclusion is indeed necessary for realistic model building. As it turns out, however, D-branes are charged under certain fields of the type IIB spectrum [1]. This presents a problem, as flux lines induced by the charge have nowhere to end on a compact manifold. It turns out the inclusion of orientifold planes naturally cures this problem. Indeed, O-planes can carry a negative charge with respect to their field couplings and can therefore cancel the

[2] An equivalent way to think about O-planes is as D-branes on which open strings can end, only now with un*oriented* worldsheets. This explains the name orientifold planes.

contribution from the D-branes [16]. So, to have a consistent and realistic theory, we have to incorporate both. If we were to do this properly we would have to consider the action governing the brane dynamics, the so-called Dirac-Born-Infeld (DBI) action. We will not consider the implication of this in this thesis. The interested reader is referred to [4, 17, 19]. We pick the same route as in [11] and choose to freeze the moduli that would appear in the low energy description of D-branes, such that these subtle issues are not manifest in the computation of the low energy effective action we will consider in this thesis.

2.2 Expansion in massless modes

Our goal now is to impose the projection 2.3 on the type IIB supergravity theory in ten dimensions, truncating the expansion of the fields and therefore reducing the four-dimensional spectrum. We will then perform an analysis similar to the one in the previous section. In particular, we will see how the spectrum gets truncated such that we end up with an effective $N = 1$ supergravity theory. It turns out that the coupling constants (that appear as metrics on the moduli spaces) are also altered, as we will discuss in the next section. For now, let us first investigate the surviving field content after modding out $\mathcal{O}$ in Equation 1.9.

Under the action of Ω_p the dilaton $\hat{\phi}$, the axion $\hat{C}_0$ and the metric $\hat{g}$ are even. The magnetic field $\hat{B}_2$ and the self-dual four form $\hat{C}_4$ are odd. Furthermore, $(-1)^{F_L}$ acts as the identity on the NS-NS fields $\hat{\phi}$, $\hat{g}$ and $\hat{B}_2$ but flips the sign of the R-R fields $\hat{C}_0$, $\hat{C}_2$ and $\hat{C}_4$. Combining this we find that under $(-1)^{F_L}\Omega_p$ the fields $\hat{\phi}, \hat{C}_0, \hat{C}_4$ and $\hat{g}$ are even, while $\hat{B}_2$ and $\hat{C}_2$ are odd. Demanding symmetry under the total orientifold operator 2.3, it follows that the σ action on the fields is given by

$$\begin{aligned} \sigma^*\hat{\phi} &= \hat{\phi}, & \sigma^*\hat{C}_0 &= \hat{C}_0 \\ \sigma^*\hat{g} &= \hat{g}, & \sigma^*\hat{C}_2 &= -\hat{C}_2 \\ \sigma^*\hat{B}_2 &= -\hat{B}_2, & \sigma^*\hat{C}_4 &= \hat{C}_4. \end{aligned} \tag{2.4}$$

We furthermore recall that in the setting we are working in we have the additional condition $\sigma^*\Omega = -\Omega$. Using σ^* we can split the Dolbeault-cohomology groups into the σ^*-eigenspaces according to

$$H^{(p,q)}(Y) = H^{(p,q)}_+(Y) \oplus H^{(p,q)}_-(Y), \tag{2.5}$$

where for $\omega_\pm \in H^{(p,q)}_\pm$ we thus have $\sigma^*\omega_\pm = \pm\omega_\pm$. We also denote $\dim_{\mathbb{C}}(H^{(p,q)}_\pm(Y)) = h^{(p,q)}_\pm$. Since $*$ and σ commute ([11]) and using the fact that σ is holomorphic, the Hodge diamond splits in the natural way and we find $h^{(1,1)}_\pm = h^{(2,2)}_\pm$ and $h^{(2,1)}_\pm = h^{(1,2)}_\pm$. The action on Ω consequently translates into $h^{(3,0)}_+ = h^{(0,3)}_+ = 0$ and $h^{(3,0)}_- = h^{(0,3)}_- = 1$. By invariance of the volume form $\text{vol}_6 \sim \Omega \wedge \overline{\Omega}$ under the action of σ^* we deduce that $h^{(0,0)}_+ = h^{(3,3)}_+ = 1$ and $h^{(0,0)}_- = h^{(3,3)}_- = 0$. The splitting of the Dolbeault cohomology groups alters Table 1.1. We summarize the results in Table 2.1 where, for later reference, we also introduce a basis for the dual homology groups.

With the new basis of harmonic representatives we can expand the fields in a way similar to what we have done in the previous chapter. It is important that we only keep the expansions that obey the constraints resulting from the specific orientifold projection, given by Equation 2.4. In particular, from Equation 2.2 we know that J is even under the orientifold action, and therefore the odd forms are projected out, resulting in

Cohomology	Basis	Homology	Basis	Dimension
$H^{(1,1)}$	ω_A	$H_2(\mathbb{Z})$	Σ^A	$A = 1, \ldots, h^{(1,1)}$
$H^{(1,1)}_+$	ω_a	$H_{2+}(\mathbb{Z})$	Σ^a	$a = 1, \ldots, h^{(1,1)}_+$
$H^{(1,1)}_-$	$\omega_{\hat{a}}$	$H_{2-}(\mathbb{Z})$	$\Sigma^{\hat{a}}$	$\hat{a} = 1, \ldots, h^{(1,1)}_-$
$H^{(2,2)}$	$\tilde{\omega}^A$	$H_4(\mathbb{Z})$	Γ^A	$A = 1, \ldots, h^{(1,1)}$
$H^{(2,2)}_+$	$\tilde{\omega}^a$	$H_{4+}(\mathbb{Z})$	Γ^a	$a = 1, \ldots, h^{(1,1)}_+$
$H^{(2,2)}_-$	$\tilde{\omega}^{\hat{a}}$	$H_{4-}(\mathbb{Z})$	$\Gamma^{\hat{a}}$	$\hat{a} = 1, \ldots, h^{(1,1)}_-$
$H^{(2,1)}$	χ_K	-	-	$K = 1, \ldots, h^{(2,1)}$
$H^{(2,1)}_+$	χ_k	-	-	$k = 1, \ldots, h^{(2,1)}_+$
$H^{(2,1)}_-$	$\chi_{\hat{k}}$	-	-	$\hat{k} = 1, \ldots, h^{(2,1)}_-$
$H^{(3)}$	$(\alpha_{\hat{K}}, \beta^{\hat{K}})$	$H_3(\mathbb{Z})$	$(\rho_{\hat{K}}, \sigma^{\hat{K}})$	$\hat{K} = 0, \ldots, h^{(2,1)}$
$H^{(3)}_+$	$(\alpha_{\hat{k}}, \beta^{\hat{k}})$	$H_{3+}(\mathbb{Z})$	$(\rho_{\hat{k}}, \sigma^{\hat{k}})$	$\hat{k} = 1, \ldots, h^{(2,1)}_+$
$H^{(3)}_-$	(α_k, β^k)	$H_{3-}(\mathbb{Z})$	(ρ_k, σ^k)	$\hat{k} = 0, \ldots, h^{(2,1)}_-$

Table 2.1: Relevant bases of both the cohomology and their homology duals for a (orientifold of) a Calabi-Yau threeform. This table is adapted from [20].

$$J = v^a \omega_a. \tag{2.6}$$

Noting that the graviton is even under the orientifold projection while Ω is odd, we see that from Equations 1.14 1.15b it follows that

$$\delta g_{ij} = \frac{i}{\|\Omega\|^2} \bar{z}^k \left(\bar{\chi}_k\right)_{i\bar{i}\bar{j}} \Omega^{\bar{i}\bar{j}}_j, \quad k = 1, \ldots, h^{(1,2)}_-. \tag{2.7}$$

In the matter sector, we have the $\hat{B}_2$ and the $\hat{C}_2$ field that both transform odd under the orientifold action. Since $H^{(0,0)}$ is one-dimensional we conclude that that the B_2 and C_2 part in Equation 1.18 are projected out, and we are left with

$$\begin{aligned} \hat{B}_2(x,y) &= b^{\hat{a}} \omega_{\hat{a}} \\ \hat{C}_2(x,y) &= c^{\hat{a}} \omega_{\hat{a}}. \end{aligned} \tag{2.8}$$

Since both the dilaton $\hat{\phi}$ and $\hat{C}_0$ are σ-even they remain in the spectrum. Finally $\hat{C}_4$ is even and is expanded as

$$\hat{C}_4 = D_2^\alpha(x) \wedge \omega_\alpha + V^{\hat{\kappa}}(x) \wedge \alpha_{\hat{\kappa}} + U_{\hat{\kappa}}(x) \wedge \beta^{\hat{\kappa}} + \rho_\alpha(x) \tilde{\omega}^\alpha. \tag{2.9}$$

2.3 Effective Action and Moduli Space

With this truncation of the fields after the orientifold projection we can again perform the entire Kaluza-Klein reduction, revealing the coupling matrices and the metrics on the moduli spaces. We will not repeat the procedure of explicitly reducing the Kaluza-Klein action. Instead we note we can obtain the reduced action by inserting the truncated spectrum into Equation 1.34

[12]. The exact result is not immediately relevant, and for the entire expanded action in four dimensions, we refer to [12, 11].

It turns out that the orientifold projection does have some serious implications for the form of the metrics on the moduli space. In particular, we have to make some redefinitions of the fields to reveal the Kähler structure on the moduli space. The complex structure deformations are still good Kähler coordinates even after the truncation. The first thing to do is combine the dilaton ϕ and the axion C_0 into the axio-dilaton τ

$$\tau = C_0 + ie^{-\phi}. \tag{2.10}$$

With the definition of the axio-dilaton we can take a combination of the c and b moduli to form the new coordinate G^a, as well as the redefined Kähler coordinates T_a

$$\begin{aligned} G^a &= c^a - \tau b^a \\ T_\alpha &= i\left(\rho_\alpha - \frac{1}{2}\mathcal{K}_{\alpha ab}c^a b^b\right) + \frac{1}{2}e^{-\phi}\mathcal{K}_\alpha - \zeta_\alpha - \frac{i}{2(\tau-\bar{\tau})}\mathcal{K}_{\alpha bc}G^b(G-\bar{G})^c, \end{aligned} \tag{2.11}$$

where we defined

$$\mathcal{K}_\alpha = \mathcal{K}_{\alpha\beta\gamma}v^\beta v^\gamma. \tag{2.12}$$

As has been explicitly computed in [12] these coordinates are indeed good Kähler coordinates on the moduli space and the total Kähler potential now takes the form

$$K = K_{\text{cs}}(z,\bar{z}) + K^{\text{Q}}(\tau, T, G). \tag{2.13}$$

We conclude that, locally, the moduli space of the $N = 1$ orientifolded theory decomposes as a direct product $\mathcal{M} = \mathcal{M}_{\text{cs}} \times \mathcal{M}_{\tau,T,G}$, with the second factor denoting the moduli space of all but the complex structure moduli. We have encountered this direct product structure in the $N = 2$ theory from the previous chapter. As the complex structure moduli are still good Kähler coordinates, the Kähler potential describing $\mathcal{M}_{\text{cs}}$ remains unchanged and reads

$$K_{\text{cs}} = -\ln\left[-i\int_Y \Omega(z)\wedge\bar{\Omega}(\bar{z})\right]. \tag{2.14}$$

The remaining part K^{Q} consists of a potential for the axio-dilaton given by

$$K_{\text{ad}} = -\ln\left[-i(\tau-\bar{\tau})\right], \tag{2.15}$$

and a part for the new Kähler moduli that, roughly speaking, depends on the volume of the compactification space:

$$K_T = -2\ln\left[\text{Vol}_E(\tau, T, G)\right]. \tag{2.16}$$

The precise form of this general Kähler potential is not important in this thesis. For later reference, we mention that in the case of one Kähler modulus T parametrizing the volume of the Calabi-Yau, the Kähler potential reduces to

Multiplet	Multiplicity	Moduli	Origin
Gravity Multiplet	1	$g_{\mu\nu}$	The 4-dimensional part of the 10-dimensional metric
Vector Multiplet	$h_+^{(2,1)}$	V^k	The expansion of $\hat{C}_4$ in the σ-even χ_k
Chiral Multiplet	$h_-^{(2,1)}$	$z^{\hat{k}}$	Complex structure moduli, from the internal part of the 10-dimensional metric
Chiral Multiplet	$h_+^{(1,1)}$	T^a	Redefined Kähler moduli, partly from the internal part of the 10-dimensional metric
Chiral Multiplet	$h_-^{(1,1)}$	$G^{\hat{a}}$	The G-moduli
Chiral Multiplet	1	τ	Axio-dilaton

Table 2.2: Arrangement of the fields into $N = 1$ multiplets as originating from the compactification of the type IIB spectrum on a Calabi-Yau orientifold. This table is adapted from [20].

$$K_T = -3 \ln \left[T + \bar{T} \right] . \tag{2.17}$$

With these new coordinates, we can appropriately arrange the field content into $N = 1$ multiplets, see Table 2.2. The action governing the dynamics of these fields consequently takes the form of the standard $N = 1$ supergravity action in 4 dimensions [21, 20]

$$- \int \frac{1}{2} R * \mathbf{1} + K_{I\bar{J}} D M^I \wedge * D \bar{M}^{\bar{J}} + \frac{1}{2} \operatorname{Re} f_{\kappa\lambda} F^\kappa \wedge * F^\lambda + \frac{1}{2} \operatorname{Im} f_{\kappa\lambda} F^\kappa \wedge F^\lambda . \tag{2.18}$$

The D's are gauge covariant derivatives and the M^I denote all the complex moduli fields that appear in the compactification. The f's are holomorphic gauge kinetic coupling functions. Their exact meaning and definition are not of importance to us.

Chapter 3

Flux Compactifications

We have found that the effective description of the low-energy dynamics of the type IIB spectrum hosts a variety of scalar fields, including the axio-dilaton, the Kähler- and complex structure moduli. It is a phenomenological problem that there are no mass terms for these scalar fields. Massless scalar degrees of freedom would correspond to additional long-range forces not observed in nature. To engineer a setting in which we can build phenomenologically realistic models we have to generate a potential for these massless fields, driving them to a particular vacuum expectation value (and thus fixing their masses). There are multiple mechanisms known that can accomplish this task, see e.g. [22], [23], [24]. In this section, we will consider a particular example making use of *fluxes*, meaning that we allow for non-trivial background values of the R-R and NS-NS two forms on the internal manifold. Including them in the low energy action yields a potential fixing (some) of the moduli.

As we have seen in the previous chapter, the Lagrangian without fluxes takes the form of a standard $N = 1$ supergravity theory in four dimensions. In order to fit a potential in this standard format, we need to find a holomorphic superpotential W. As we will see, it is remarkable that this superpotential exists. Finally, we will introduce the KKLT scenario to stabilize moduli by turning on background fluxes combined with non-perturbative corrections. Flux compactifications were originally described in [22] but have become standard work now. Useful discussions can be found in [10], [25], [2], [16], [1], [26].

3.1 Background Fluxes and their Quantization

Without further ado, we turn to the definition of background fluxes. *A flux* is a non-trivial vacuum expectation value for a field strength. As discussed in Section 1.2, maintaining four-dimensional Poincaré invariance restricts these field strengths to only having a non-zero vev on the internal manifold. In particular, we turn on background fluxes for the NS-NS en R-R field strengths [22]. Compare this to electromagnetism, where the flux enclosed by a surface is proportional to the amount of electric or magnetic field lines passing through. For the background values of the field strength, the integral over the appropriate homology cycles quantifies the amount of background flux. More precisely, we define

$$F = \langle dC_2 \rangle \text{ and } H = \langle dB_2 \rangle. \tag{3.1}$$

It turns out that the fluxes of Equation 3.1 are quantized. This can be shown via a construction

that is similar to the Dirac quantization procedure of magnetic monopoles in electrodynamics. In particular, it follows from the fact that the quantum mechanical transition amplitude of a D-brane coupled to a gauge field has to be well defined. The interested reader is referred to [10], [26], [2]. We simply state the result that the integration of these fluxes over certain homology cycles are quantized according to

$$\begin{aligned} \int_{\rho^{\hat{K}}} F = 2\pi F^{\hat{K}} \in 2\pi\mathbb{Z}, \quad \int_{\sigma_{\hat{K}}} F = 2\pi F_{\hat{K}} \in 2\pi\mathbb{Z}, \\ \int_{\rho^{\hat{K}}} H = 2\pi H^{\hat{K}} \in 2\pi\mathbb{Z}, \quad \int_{\sigma_{\hat{K}}} H = 2\pi H_{\hat{K}} \in 2\pi\mathbb{Z}, \end{aligned} \tag{3.2}$$

where we have used the basis homology elements from Table 2.1. Employing the dual basis of cohomology forms, we can write the quantized fluxes as

$$F = -F^{\hat{A}}\alpha_{\hat{A}} + F_{\hat{A}}\beta^{\hat{A}}, \quad H = -H^{\hat{A}}\alpha_{\hat{A}} + H_{\hat{A}}\beta^{\hat{A}}. \tag{3.3}$$

With the knowledge that fluxes are quantized background values for the three-form field strengths defined on the relevant three-cycles of our compactification space, we would alter the expansions of Equation 1.19 to include these additional background components

$$\begin{aligned} d\hat{B}_2 &= dB_2 + db^A \wedge \omega_A + \left(-F^{\hat{A}}\alpha_{\hat{A}} + F_{\hat{A}}\beta^{\hat{A}}\right) \\ d\hat{C}_2 &= dC_2 + dc^A \wedge \omega_A + \left(-H^{\hat{A}}\alpha_{\hat{A}} + H_{\hat{A}}\beta^{\hat{A}}\right). \end{aligned} \tag{3.4}$$

With these expansions at hand, we can play the same game as before [1]. We can plug these extended flux expansions into our ten-dimensional supergravity action and integrate them over our internal manifold. If we wish we can also include branes and perform an orientifold projection [2]. It is important to remember that F^A, F_A, H_A and H^A are all integrally quantized for the rest of this thesis.

3.2 The Gukov-Vafa-Witten Superpotential

We have already seen the kinetic term of the standerd $N = 1$ supergravity action in four dimensions in Equation 2.18. Using the expansion of Equation 3.4 and plugging this into the ten-dimensional supergravity would add an additional scalar potential to this action, arising from the following term

$$S = -\frac{1}{4}\int e^{-\hat{\phi}}\hat{H}_3 \wedge *\hat{H}_3 + e^{\hat{\phi}}\hat{F}_3 \wedge *\hat{F}_3. \tag{3.5}$$

Introducing the expansions of Equation 3.4 into Equation 3.5 and combining the F and H fluxes into the so-called G-flux term $G_3 = F - \tau H$ introduces the following potential into the action

[1] Actually, not entirely. The fact that we include fluxes forces us to make a different *Ansatz* for the metric, including a so-called warp factor. This is because fluxes contribute non-trivially to the energy-momentum tensor and therefore alter the geometry of the space. Observe that localized sources such as D-branes and O-planes also source the energy-momentum tensor. In our derivation, however, we ignore this warping

[2] Note: the orientifold projection also projects out some of the flux components. In particular: only fluxes can only be defined on the Poincaré duals of the surviving cohomology classes.

$$V = -\frac{1}{4} e^{\phi} \int_Y G_3 \wedge *\bar{G}_3, \tag{3.6}$$

where the integration over Minkowski space has been performed. We can split G_3 conveniently into its imaginary (anti)-self dual [20] G_3^+ (G_3^-) according to

$$G_3^{\pm} = \frac{1}{2}\left(G_3 \pm i * G_3\right), \quad *G_3^{\pm} = \mp i G_3^{\pm}. \tag{3.7}$$

The combined flux vector G_3 is a three-form. The imaginary self dual (ISD) part G_3^+ is an element of $H_-^{(3,0)} \oplus H^{(1,2)}$. Recall that the volume form Ω forms a basis for the odd eigenspace H_-^3. Using the relevant basis elements listed in Table 2.1 it can be shown that the scalar potential takes the following form [20]

$$V = \frac{18 i e^{\phi}}{\mathcal{K}^2 \int_Y \Omega \wedge \bar{\Omega}} \left(\int_Y \Omega \wedge \bar{G}_3 \int_Y \bar{\Omega} \wedge G_3 + g^{\hat{k}\hat{l}} \int_Y \chi_{\hat{k}} \wedge G_3 \int_Y \bar{\chi}_{\hat{l}} \wedge \bar{G}_3 \right). \tag{3.8}$$

We want to keep the standard $N = 1$ supergravity description of the theory, meaning that the potential of Equation 3.8 has to fit a standard description. In particular, this means that we have to find a holomorphic superpotential W in addition to the holomorphic gauge coupling function f and the Kähler potential K. Defining the Kähler covariant derivative $D_I W = \partial_I W + W\left(\partial_I K\right)$, the scalar potential is restricted to take the following form [12]:

$$V_{\text{flux}} \overset{!}{=} e^K \left(\underbrace{K^{I\bar{J}} D_I W D_{\bar{J}} \bar{W}}_{\text{F-terms}} - 3|W|^2 \right) + \frac{1}{2} \left((\operatorname{Re} f)^{-1} \right)^{\kappa\lambda} \underbrace{\hat{D}_{\kappa} \hat{D}_{\lambda}}_{\text{D-terms}}. \tag{3.9}$$

where I runs over all the moduli of the theory. We see that the potential in Equation 3.9 consists of two parts, the so-called F- and D-terms. We will not consider the latter and set them to zero from now on. Comparing Equation 3.8 with vanishing D-terms with Equation 3.9 the existence of a superpotential W that gives the correct form of the potential looks like a far fetched assumption. It indeed is remarkable that, in the case of vanishing D-terms, such a potential exists. Named after its founders, W is called the *Gukov-Vafa-Witten superpotential* [27] and it reads

$$W_{\text{GVW}} = \int_Y G_3 \wedge \Omega_3. \tag{3.10}$$

Inserting this form of the superpotential in the scalar potential of Equation 3.9 with vanishing D-terms reproduces Equation 3.8. The details of this procedure can be found in the appendix of [20]. Using the expansion of the holomorphic three form Ω_3

$$\Omega_3 = \mathcal{X}^{\Lambda} \alpha_{\Lambda} - \mathcal{F}_{\Lambda} \beta^{\Lambda}, \tag{3.11}$$

together with the expansion of the fluxes Equation 3.4 and relevant basis elements of Table 2.1 we find that the superpotential can be written in the following way

$$W = \sqrt{\frac{2}{\pi}} \left(F_{\Lambda} - \tau H_{\Lambda} \right) \mathcal{X}^{\Lambda} - \sqrt{\frac{2}{\pi}} \left(F^{\Lambda} - \tau H^{\Lambda} \right) \mathcal{F}_{\Lambda}, \tag{3.12}$$

where we recall that $\mathcal{X}$ are the projective coordinates, and $\mathcal{F}$ is the prepotential defined in Appendix B. We will always consider the gauge choice $\mathcal{X} = (1, z^i)$ in this thesis, making the dependence of W on the complex structure moduli explicit.

3.3 Tadpole Cancellation

As we have briefly discussed in the previous sections, phenomenologically interesting orientifold compactifications host a variety of localized sources coupling to various field strengths. Examples are the Dp-branes that can support gauge fields, as well as the O-planes resulting from the orientifolding. These localized sources alter the Bianchi identities for the three form field-strengths appearing in our ten-dimensional theory. Besides these local sources, the fluxes also contribute to the Bianchi identity. We can consequently look at the integrated version of this Bianchi identity, leading to a global consistency condition called *the tadpole cancellation condition*.

Using the expansion for the field strengths $\hat{F}_5$ and $\hat{F}_3$ from Equation 1.19, the unsourced Bianchi identities can be found by taking the exterior derivative. Doing this yields

$$\begin{aligned} d\hat{F}_3 &= d\left(d\hat{C}_2 - C_0 d\hat{B}_2\right) = -dC_0 \wedge d\hat{B}_2 = \hat{H}_3 \wedge \hat{F}_1, \\ d\hat{F}_5 &= d\left(d\hat{C}_4 - \hat{C}_2 \wedge d\hat{B}_2\right) = d\hat{B}_2 \wedge d\hat{C}_2 = \hat{H}_3 \wedge \hat{F}_3. \end{aligned} \tag{3.13}$$

These Bianchi identies are modified in the presence of the localized branes/planes. Schematically this takes the following form [16]:

$$d\hat{F}_n = \hat{H}_3 \wedge \hat{F}_{n-2} + \rho_{\text{local}}, \tag{3.14}$$

where ρ_{local} is the total charge density of all the localized objects of the theory. We can take this condition for the 5-form field strength and integrate over the Calabi-Yau. Schematically this gives the following condition

$$\underbrace{N_{\text{flux}}}_{>0} + \underbrace{N_{\text{D3}}}_{>0} + \underbrace{Q_3 N_{\text{O3}}}_{<0} = 0. \tag{3.15}$$

Here N_{flux} is called the total flux number and it is given by

$$\int_Y H_3 \wedge F_3. \tag{3.16}$$

The signs in Equation 3.15 are a convention. Of course, we could make the tadpole condition more precise, but only this schematic form will be important for the rest of this work. For a more precise definition of this condition, we refer the interested reader to [20, 1, 16, 28]. Recalling that O-planes arise as the fixed point set of the orientifold action, we see that N_O is fixed once we specify the orientifold. The charge induced from the orientifold planes has to be canceled by the combined charge coming from the D-branes and fluxes. Since these quantities carry the same sign, the flux number cannot become arbitrarily large. This observation plays a central role in the motivation of our research. We will return to this issue in more detail in the next chapter.

3.4 The KKLT Scenario

In this section, we will consider a famous (and controversial) method to simultaneously stabilize the Kähler moduli and find a (meta)stable DeSitter vacuum in string theory via uplifting a AdS vacuum [3]. This is based on the famous paper by Kachru, Kalosh, Linde, and Trivedi [30]. The procedure is named after these authors and is known as the KKLT-scenario. Let us consider a model with one Kähler modulus T, the axio-dilaton τ and several complex structure moduli z. We have seen that the (tree) level Kähler potential for such a model takes the following form

$$K = -3\ln[-i(T-\bar{T})] - \ln[-i(\tau-\bar{\tau})] - \ln\left[-i\int_Y \Omega(z)\wedge\bar{\Omega}(\bar{z})\right]. \tag{3.17}$$

As we have seen in the previous section, turning on background fluxes for the three form field strengths introduces a scalar potential of the form

$$V = e^K\left(K^{I\bar{J}}D_I W D_{\bar{J}}\overline{W} - 3|W|^2\right), \tag{3.18}$$

where the indices run over all the moduli that appear in the Kähler potential of Equation 3.17. We note that this superpotential satisfies a so-called *no-scale* structure

$$K^{\bar{T}T}\partial_T K\partial_{\bar{T}}K = 3. \tag{3.19}$$

Due to this no-scale structure the F-term contribution from the Kähler modulus exactly cancels the second piece of Equation 3.18. The scalar potential consequently reduces to

$$V = e^K\left(K^{I\bar{J}}D_I W D_{\bar{J}}\overline{W}\right), \tag{3.20}$$

where the sum now only includes the axio-dilaton and the complex structure moduli. We conclude that, at least at tree level, the Kähler moduli remain unstabilized. In the KKLT scenario, we first use this tree-level potential to stabilize the complex structure moduli and the axio-dilaton. Consequently, we consider corrections to the superpotential that allow us to stabilize the remaining Kähler modulus.

Step 1 of KKLT

We take the tree-level potential of Equation 3.20 induced by an integral flux configuration of H_3 and F_3. The supersymmetric minimum of this potential is given by the vanishing of the F-terms

$$F_I = D_I W = 0, \tag{3.21}$$

where we recall the definition of the Kähler covariant derivative $D_I W = \partial_I W + W\partial_I K$ [4]. We assume that the fluxes can be tuned in such a way that all complex structure moduli z^i, as

[3] The validty of this procedure has recently been challenged in [29].
[4] An equivalent condition is the imaginary self-duality of the three form flux G_3.

well as the axio-dilaton τ, are driven to a non-zero vacuum expectation value[5]. Consequently, the Gukov-Vafa-Witten superpotential evaluated in this F-term solution will be denoted W_0

$$W_{\text{GVW}}|_{\text{min}} = W_0. \tag{3.22}$$

Step 2 of KKLT

Since the dependence on the Kähler moduli drops out of the scalar potential at tree level, they remain unfixed at this point. It turns out, however, that the inclusion of non-perturbative effects generates a potential for the Kähler moduli[6]. These non-perturbative contributions to the tree level superpotential take the following form

$$W_{\text{np}} = \sum_{\Lambda} \mathcal{A}_{\Lambda}(z^i) e^{-a_{\Lambda} T_{\Lambda}} \quad \text{with} \quad T_{\Lambda} = m^i_{\Lambda} T_i. \tag{3.23}$$

Here m^i_{Λ} are integers corresponding to the amount of wrapping of D-branes on particular homology cycles. The precise meaning is of no concern to us here, but more information can be found in [20, 33]. The coefficients A contain higher-order loop effects and only depend on the complex structure moduli z^i. Solving for a minimum of the F-term including the Kähler moduli yields

$$\partial_T V_F = e^{\mathcal{K}} \left(D_T \left(G^{T\bar{T}} F_T \bar{F}_{\bar{T}} \right) - 3 F_T \bar{W} \right). \tag{3.24}$$

It suffices to solve the F-term equations $F_T = 0$ for all the Kähler moduli. The F-term potential evaluated in the minimum consequently takes the following form

$$V_F|_{\text{min}.} = e^{\mathcal{K}} \left(0 - 3|W|^2 \right) \simeq -3 e^{\mathcal{K}} |W_0|^2 \leq 0. \tag{3.25}$$

An Example

To make the KKLT scenario a bit more concrete, we consider an explicit example also described in Chapter 6 of [20]. We consider a model with one Kähler modulus T. In this case the volume of Y is related to $\rho = \text{Re}(T)$ via

$$\mathcal{V} = \rho^{\frac{3}{2}}. \tag{3.26}$$

We assume that the background fluxes are chosen in such a way that the axio-dilaton τ and all complex structure moduli z^i have been stabilized. We wish to minimize the scalar potential. In particular, we look for solutions of zero F-term. In this case it means that $F_T = 0$, where we take the derivative with respect to the single Kähler modulus. The relevant quantities are given by

[5] This assumption has recently been challenged in the case of a large number of complex structure moduli in [31, 32].

[6] Non-perturbative effects can arise as a consequence of D-brane instantons wrapping four-cycles in Y or from gaugino condensates on multiple $D7$-branes wrapped around four-cycles. This can be made very precise, but this is not of importance to us here. We simply take the view that these effects can arise, and take their contributions into consideration. The interested reader can have a look at [20, 33] for more information.

$$\begin{aligned} W &= W_0 + \mathcal{A}e^{-aT}, \quad W_0 \in \mathbb{R}, \quad \mathcal{A} \in \mathbb{R} \\ \mathcal{K}_T &= -\frac{3}{T+\bar{T}}, \end{aligned} \tag{3.27}$$

such that $F_T = 0$ is solved by

$$a\mathcal{A}e^{-aT} - \frac{3}{T+\bar{T}}W_0. \tag{3.28}$$

A closed form solution to this equation does not exist, but we can use the following convenient parametrization of the solution

$$\mathrm{Im}(T) = 0, \quad \hat{\rho}e^{-a\hat{\rho}} = -\frac{3W_0}{2a\mathcal{A}}. \tag{3.29}$$

Now, in order to trust our supergravity description effects of string-scale order have to be negligible. In particular, the volume must be large enough. This manifests itself by the condition $\rho \gg 1$. The description of the non-perturbative effects needs $a\rho \gg 1$ to be valid. Considering these conditions in light of Equation 3.29 we see that we need

$$W_0 \ll 1. \tag{3.30}$$

Chapter 4

Scaling Scenarios

After an extensive discussion of all preliminary material, we can turn to the central theme of this thesis. The question we set out to answer is the following:

Can we discover some general scaling behaviour of W_0 and the moduli masses as a function of N_{flux}?

It is worthwhile to take a moment and reflect on this question. Let us first comment on why it is an interesting question to ask. In the previous chapters, we have introduced two important quantities that need a particular order of magnitude. The tadpole condition of Equation 3.15 states that N_{flux} cannot become arbitrarily large. Indeed, the negative charge of the orientifold planes is fixed once a particular orientifold projection is chosen. This charge needs to be canceled by the D-branes and the flux number. To give an indication, flux numbers $N_{\text{flux}} > 200$ seem to not be described in the literature [34]. In addition to N_{flux} we have seen W_0. Recall that W_0 is the value of the Gukov-Vafa-Witten superpotential evaluated in the minimum. This minimization fixes (some of) the complex structure moduli and the axio-dilaton, constituting the first step of the KKLT procedure. To stabilize the Kähler moduli we considered corrections to this tree-level superpotential. This could indeed fix the Kähler moduli, but to have computational control over this process $|W_0| \ll 1$ is needed.

We see that there are two simultaneous forces at play here. We want to somehow *minimize* N_{flux} to not exceed the tadpole bound, while we also want an exponentially small W_0. Since higher values of N_{flux} allow for more flux configurations, it would be reasonable to assume that finding lower values of W_0 becomes easier once the flux induced charge is allowed to be higher. It would be nice to capture this scaling behaviour in a function $W_0(N_{\text{flux}})$. Finding such a scaling, at least for a certain class of examples, would allow to qualitatively formulate bounds on the ease by which we can find fluxes potentially leading to physical vacua.

We will also be able to compute, for each combination of fluxes, the eigenvalues of the canonically normalised mass matrix. This will give information about the scaling of the moduli masses with respect to N_{flux}. This is extremely interesting in its own right. Since we are working in a supergravity approximation the moduli masses need to be smaller than the Kaluza-Klein scale set by our supergravity theory. The stringent requirements posed by obtaining the correct mass hierarchy will give us crucial information concerning the actual *physical* validity of our specific compactifications.

Since exponentially small values of W_0 are rare in the vast landscape of string theory [35, 36, 37, 38, 39, 40], and the formulae involved in string compactifications are highly interdependent and therefore quickly become intractable, we need a systematic setting in which we can study the

question posed. Such a setting has been described in the work of McAllister and collaborators [41], which has further been elaborated upon in [42, 43]. They provide a recipe to systematically find vacua exhibiting small W_0 in particular examples. A systematic scan of these vacua has consequently been performed by the group of Carta, as described in [34, 44].

In this chapter, we will first explain the recipe described by the McAllister group. We will reproduce the vacua found by Carta and collaborators for some particular Calabi-Yau geometries. Having these vacua, we build upon this previous work in a couple of ways. Instead of describing the statistics of these vacua, we look for the numerical dependence of W_0 on N_{flux}. We will do this in a more accurate setting, moving away from the effective picture described by the McAllister group by solving the full F-term equations, allowing us to compute additional quantities, such as the moduli masses. We also extend the model by explicitly introducing a single Kähler modulus.

4.1 Realizing Exponentially Small Superpotential

4.1.1 Kähler Potential in the LCS regime

In this section, we will describe the recipe proposed by McAllister and collaborators [41] to perform a systematic search for vacua exhibiting exponentially small W_0. Besides the original paper, this recipe is explained in [45, 34, 44, 43, 42]. All necessary background material has been provided in the previous chapters. For the reader's convenience, we will explicitly mention the used definitions instead of cross-referencing. The discussion of this section closely follows the detailed explanations of [34].

We consider an orientifold projection of a Calabi-Yau threefold with an unspecified number of D-brane and O-plane charges. The Kähler potential was found to be of the following form (Equation 2.13)

$$K = K_{\text{cs}} + K_{\text{rest}}, \tag{4.1}$$

where K_{cs} is the Kähler potential for the complex structure moduli, and K_{rest} the Kähler potential for the remaining fields, including the axio-dilaton and the Kähler moduli. At this point we will not be concerned with the Kähler moduli, but we will return to them shortly. Using the holomorphic three form Ω we can write the Kähler potential on the complex structure side as (Equation 2.14):

$$K_{\text{cs}} = -\log\left[-i\int \Omega\wedge\bar{\Omega}\right]. \tag{4.2}$$

The Kähler potential for the axio-dilaton contained in K_{rest} is given by (Equation 2.15)

$$K_{\text{ad}} = -\log\left[-i\left(\tau-\bar{\tau}\right)\right]. \tag{4.3}$$

Recall that the complex structure moduli space exhibits special Kähler geometry, allowing us the write the Kähler potential in terms of a a holomorphic prepotential $\mathcal{F}$. In the large complex structure (LCS), without any non-perturbative corrections, this prepotential is a degree two polynomial in the projective coordinates [46]. In this recipe we include non-perturbative corrections arising from instantons. The total prepotential consequently takes the form

$$\mathcal{F} = \underbrace{-\frac{\kappa^0_{ijk}\mathcal{X}^i\mathcal{X}^j\mathcal{X}^k}{3!\mathcal{X}^0} + \frac{1}{2}\tilde{p}_{ij}\mathcal{X}^i\mathcal{X}^j + \tilde{p}_i\mathcal{X}^i\mathcal{X}^0 - \frac{i}{2}\tilde{p}_0\left(\mathcal{X}^0\right)^2}_{\text{Perturbative prepotential } \mathcal{F}_{\text{pert}}} + \left(\mathcal{X}^0\right)^2\mathcal{F}_{\text{inst}}\left(\mathcal{X}^i/\mathcal{X}^0\right). \tag{4.4}$$

The projective coordinates form an over-complete basis, and we consider the particular gauge choice in which $\mathcal{X}^0 = 1$. Following the original conventions of the paper, we will denote the complex structure moduli with U^i. The remaining projective coordinates are then related to the CS-moduli simply as $\mathcal{X}^i = U^i$. The κ_{ijk} form the intersection tensor of the mirror threefold $\tilde{X}$

$$\kappa^0_{ijk} = \int_{\tilde{X}_3} J_i \wedge J_j \wedge J_k. \tag{4.5}$$

The parameters $\tilde{p}_0$ and $\tilde{p}_j$ are given by

$$\tilde{p}_j = \frac{1}{4\cdot 3!}\int_{\tilde{X}_3} c_2\left(\tilde{X}_3\right)\wedge J_j, \quad \tilde{p}_0 = -\frac{\zeta(3)\chi\left(X_3\right)}{(2\pi)^3}. \tag{4.6}$$

For $\tilde{p}_{ij}$ we follow the conventions as described in [42], defining them to be symmetric and given by

$$\tilde{p}_{ij} = \frac{1}{2}\begin{cases}\kappa^0_{iij} & \text{for } i \geq j\\ \kappa^0_{ijj} & \text{for } i < j.\end{cases} \tag{4.7}$$

Of crucial importance in this recipe are the (worldsheet)-instanton induced corrections to the perturbative prepotential of Equation 4.4. Using mirror symmetry, these corrections (arising on the mirror side) take on the following form

$$\mathcal{F}_{\text{inst}}\left(\mathcal{X}^i/\mathcal{X}^0\right) = \frac{1}{(2\pi i)^3}\sum_{\beta\in H_2^-\left(\tilde{X}_3,\mathbb{Z}\right)\setminus\{0\}} n_\beta \text{Li}_3\left(e^{2\pi i\left(\mathcal{X}^i/\mathcal{X}^0\right)\beta_i}\right), \tag{4.8}$$

where Li_3 is the trilogarithm enjoying the expansion

$$\text{Li}_3(x) = \sum_{m=1}^{\infty}\frac{x^m}{m^3}. \tag{4.9}$$

The coefficients η_{β_i} appearing in Equation 4.8 are known as the Gopakumar-Vafa invariants. They contain geometrical data of the mirror threefold $\tilde{X}$, counting the number of oriented curves Σ_g of genus g that can be holomorphically embedded into $\tilde{X}$ [34, 46, 47].

4.1.2 The Superpotential

Recall from Equation 3.10 that the Gukov-Vafa-Witten superpotential takes the form

$$W_{\text{GVW}} = \sqrt{\frac{2}{\pi}} \left(F_\Lambda - \tau H_\Lambda\right) \mathcal{X}^\Lambda - \sqrt{\frac{2}{\pi}} \left(F^\Lambda - \tau H^\Lambda\right) \mathcal{F}_\Lambda, \tag{4.10}$$

where $\mathcal{F}_\Lambda$ denotes the derivative of the prepotential with respect to the projective coordinates $\mathcal{X}^\Lambda$,

$$\mathcal{F}_\Lambda = \frac{\partial}{\partial \mathcal{X}^\Lambda} \mathcal{F}. \tag{4.11}$$

The total prepotential $\mathcal{F}$ consists of two pieces, the perturbative polynomial piece described by Equation 4.4 and the instanton induced corrections described by Equation 4.8. Consequently, plugging these into Equation 4.10 splits the superpotential into a polynomial piece (coming from the perturbative effects) and an exponential piece (coming from the non-perturbative effects)

$$W = W_{\text{poly}} + W_{\text{exp}}. \tag{4.12}$$

Taking the appropriate derivatives of the various pieces making up the prepotential and consequently fixing the gauge choice $\mathcal{X}^0 = 1$ we find

$$\begin{aligned}
\mathcal{F}_{\text{pert},0} &= \frac{1}{6}\kappa^0_{ijk} U^i U^j U^k + \tilde{p}_i U^i - i\tilde{p}_0 \\
\mathcal{F}_{\text{pert},i} &= -\frac{1}{2}\kappa^0_{ijk} U^j U^k + \tilde{p}_{ij} U^j + \tilde{p}_i \\
\mathcal{F}_{\text{inst},0} &= 2\mathcal{F}_{\text{inst}} \ - U^i \partial_i \mathcal{F}_{\text{inst}} \\
\mathcal{F}_{\text{inst},i} &= \partial_i \mathcal{F}_{\text{inst}}
\end{aligned} \tag{4.13}$$

where the derivatives appearing are now with respect to the complex structure moduli U^i. It is the first two equations in 4.13 that induce the polynomial part of the superpotential that consequently takes the following form

$$\begin{aligned}
W_{\text{poly}} \ = & \sqrt{\frac{2}{\pi}} \left[\bar{F}_0 + U^i \bar{F}_i + \frac{1}{2}\kappa^0_{ijk} U^i U^j F^k - \frac{1}{6}\kappa^0_{ijk} U^i U^j U^k F^0 - i\tilde{p}_0 F^0\right] + \\
& - \sqrt{\frac{2}{\pi}} \tau \left[\bar{H}_0 + U^i \bar{H}_i + \frac{1}{2}\kappa^0_{ijk} U^i U^j H^k - \frac{1}{6}\kappa^0_{ijk} U^i U^j U^k H^0 - i\tilde{p}_0 H^0\right].
\end{aligned} \tag{4.14}$$

Here we defined the shifted fluxes as in [34]

$$\begin{aligned}
\bar{F}_0 &= F_0 - \tilde{p}_i F^i, \quad & \bar{F}_i &= F_i - \tilde{p}_{ij} F^j - \tilde{p}_i F^0 \\
\bar{H}_0 &= H_0 - \tilde{p}_i H^i, \quad & \bar{H}_i &= H_i - \tilde{p}_{ij} H^i - \tilde{p}_i H^0.
\end{aligned} \tag{4.15}$$

Similarly we can plug in the instanton induced terms of Equation 4.13 to find the exponential part of the superpotential

$$\begin{aligned}
W_{\text{exp}} = & - \sqrt{\frac{2}{\pi}} \left(F^0 - \tau H^0\right) \left(2\mathcal{F}_{\text{inst}} - U^i \partial_i \mathcal{F}_{\text{inst}}\right) + \\
& - \sqrt{\frac{2}{\pi}} \left(F^i - \tau H^i\right) \left(\partial_i \mathcal{F}_{\text{inst}}\right).
\end{aligned} \tag{4.16}$$

4.1.3 Perturbatively Flat Vacua

Having introduced all the necessary expansions, we are in a position to investigate the actual procedure proposed in [41]. The key point is that we can state general conditions under which the polynomial part of the superpotential Equation 4.14 exhibits a flat valley along which $W_{\text{poly}} = 0$. Under the same conditions, the F-term equations along this valley vanish, resulting in an effectively flat vacuum solution. We can consequently lift the minimum to some finite value via the introduction of the instanton-induced corrections.

Let us briefly recall that the global minimum of the scalar potential can be found by solving the F-term equations

$$D_I W = \partial_I W + W\left(\partial_I K\right) = 0, \tag{4.17}$$

where in our case the index I runs of the axio-dilaton and all complex structure moduli. The derivatives of the polynomial piece of the superpotential with respect to these moduli take the form

$$\begin{aligned}\frac{\partial W_{\text{poly}}}{\partial U^i} =& \sqrt{\frac{2}{\pi}}\left[\bar{F}_i + \kappa^0_{ijk}U^j F^k - \frac{1}{2}\kappa^0_{ijk}U^j U^k F^0\right] + \\ &- \sqrt{\frac{2}{\pi}}\tau\left[\bar{H}_i + \kappa^0_{ijk}U^j H^k - \frac{1}{2}\kappa^0_{ijk}U^j U^k H^0\right],\end{aligned} \tag{4.18}$$

for the complex structure moduli and

$$\frac{\partial W_{\text{poly}}}{\partial \tau} = -\sqrt{\frac{2}{\pi}}\left[\bar{H}_0 + U^i\bar{H}_i + \frac{1}{2}\kappa^0_{ijk}U^i U^j H^k - \frac{1}{6}\kappa^0_{ijk}U^i U^j U^k H^0 - i\tilde{p}_0 H^0\right] \tag{4.19}$$

for the axio-dilaton. If we consequently choose the fluxes to be of the form

$$F_0 = \tilde{p}_i F^i, \quad F_i = \tilde{p}_{ij}F^j, \quad F^0 = 0, \quad H_0 = 0, \quad H^i = 0, \quad H^0 = 0, \tag{4.20}$$

the shifted fluxes of Equation 4.15 reduce to

$$\bar{F}_0 = 0, \quad \bar{F}_i = 0, \quad \bar{H}_0 = 0, \quad \bar{H}_i = H_i. \tag{4.21}$$

Plugging these tuned fluxes into Equations 4.18, 4.19 and 4.14 we find the following simplified expressions

$$\begin{aligned}\frac{\partial W_{\text{poly}}}{\partial U^i} &= \sqrt{\frac{2}{\pi}}\left[\kappa^0_{ijk}U^j F^k - \tau H_i\right] \\ \frac{\partial W_{\text{poly}}}{\partial S} &= -\sqrt{\frac{2}{\pi}}U^i\bar{H}_i \\ W_{\text{poly}} &= \sqrt{\frac{2}{\pi}}\left[\frac{1}{2}\kappa^0_{ijk}U^i U^j F^k - \tau U^i\bar{H}_i\right].\end{aligned} \tag{4.22}$$

If we can now find general conditions under which all of the quantities above vanish, we will solve the F-term in Equation 4.17 and thereby find the (perturbative) supersymmetric solutions of the scalar potential. We see that this is precisely the case when $U^i = \tau M^i$, where M^i is a vector satisfying the simultaneous set of constraints

$$\begin{cases} H_i M^i = 0 \\ \kappa^0_{ijk} M^i M^j F^k = 0 \\ \kappa^0_{ijk} M^j F^k = H_i. \end{cases} \tag{4.23}$$

Solving these constraints for M^i then yields

$$M^i = \left(\kappa^0_{ijk} F^k\right)^{-1} H_j. \tag{4.24}$$

A couple of remarks concerning this recipe are in place.

- In Equation 4.20 we have set $F_0 = \tilde{p}_i F^i$ and $F_i = \tilde{p}_{ij} F^j$. From the previous Chapter we know that fluxes must be quantized. For that reason we have to make sure that these contractions are indeed integer valued.
- For Equation 4.26 to work we have to make sure that $\kappa_{ijk} F^k$ is an invertible matrix.
- We need to check the orthogonality condition $H_i M^i = 0$.
- Since the perturbatively flat valley is described by the equation $U^i = \tau M^i$ we have to make sure that M^i lies inside the Kähler cone of the mirror Calabi-Yau.

4.1.4 Lifting Along the Flat Valley

After having found a particular flux combination that results in a perturbatively flat vacuum, we wish to stabilize the axio-dilaton along the flat direction. We can do this by generating a potential along this direction through the instanton induced corrections, see also Figure 4.1. Considering Equation 4.16 evaluated along $U^i = \tau M^i$ we find it reduces to

$$W^{\text{eff}}_{\text{exp}}(\tau) = -\sqrt{\frac{2}{\pi}} F^i \partial_i \mathcal{F}_{\text{inst}}(\tau). \tag{4.25}$$

4.2 Finding the Flux Vacua

The effective picture described in the previous section provides a good way of potentially realizing exponentially small values of W_0 in a controlled setting. The final result, however, is still an effective description. More concretely, we only consider the instanton induced contributions along our flat valley in moduli space in Equation 4.25. There is no guarantee that the actual stabilized value of the axio-dilaton remains close to its effective value, as there is no guarantee that the instanton contributions do not significantly alter the general F-term Equations 4.22.

To ensure that no subtle changes arise when considering the full F-term equations, we implement a three-step algorithm. First, we find the fluxes that generate a perturbatively flat valley, as described in the previous section. This is done in *Python*. For this set of models,

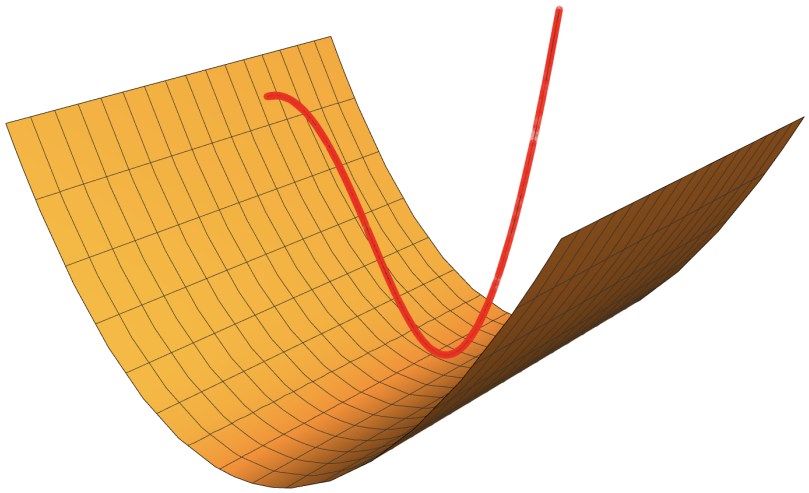

Figure 4.1: Schematic depiction of the lifting of the flat valley. The orange surface represents the superpotential over moduli space. We can lift its flat direction through the inclusion of the instanton induced potential W^{eff}. If this potential only lifts the flat valley (along $W = 0$) a tiny bit we can realize an exponentially small value of W_0.

we use the effective recipe to find the vacuum expectation values of the axio-dilaton and the complex structure moduli. We solve the effective F-term equation for the axio-dilaton using a *FindRoot* algorithm in *Mathematica*. We consequently use this as input for the algorithm that solves the full F-term equations. The upshot is that we obtain reasonable starting values for the *FindRoot* search needed to do the full moduli stabilization. The algorithm then consists of three independent steps, where each step provides input for the next. We will outline them in more detail below.

At this point we remark that we want to investigate these results in light of the KKLT scenario. In particular, we want to stabilize a single Kähler modulus via the addition of the non-perturbative corrections of Equation 3.17. It turns out, however, that the masses we obtain for the Kähler modulus through the application of the two-step procedure are of the same order as the axio-dilaton mass. This means that if we wish to stabilize the Kähler modulus in a KKLT-like fashion, we need to include the non-perturbative corrections for them from the beginning. This is indeed the approach we will take.

We will explicitly investigate 32 distinct Calabi-Yau geometries, of which the topological data associated with each one is collected in Appendix C. We remind the reader that this data is associated with the *mirror* of the Calabi-Yau on which the actual compactification takes place. Reason for this is that the topological data for the prepotential is defined in terms of the topological data of the mirror threefold $\tilde{X}$. The first 26 geometries are models with two complex structure moduli. These are the $K3$-fibred geometries investigated in [34, 44], which yield an abundance of flux vacua. We extend this analysis to six examples with three complex structure moduli. These have not been investigated before. For each of these models, we explicitly compute the vacuum solutions for around 10^9 combinations of fluxes. If we find solutions in the effective picture we consequently investigate if they admit solutions when we incorporate the Kähler modulus and solve the full set of F-term equations. The entire algorithm consists of the following steps.

Step 1: Finding the Vacua

Given the $\tilde{p}_i$, $\tilde{p}_{ij}$ and κ_{ijk} characterizing a particular Calabi-Yau geometry we can compute M^i, which is given by

$$M^i = \left(\kappa^0_{ijk} F^k\right)^{-1} H_j. \tag{4.26}$$

Having M^i we can use the condition $H_i M^i = 0$ to solve for F_1, reducing one independent flux component. After having eliminated the free flux entry F_1, we iterate over the remaining flux entries. For each combination of fluxes that we find we have to check the following conditions:

- The Kähler conde conditions. In the Kähler basis these are defined by $M^i > 0$.
- The various integrality conditions. In particular, we need $F_1, \tilde{p}_i F^i$ and $\tilde{p}_{ij} F^j$ to be integers.
- The flux charge, in our conventions given by $N_{\text{flux}} = -\frac{1}{2} F^i H_i$ must satisfy $0 \leq N_{\text{flux}} \leq N_{\text{max}}$.

The flux vacua that satisfy all these conditions will set Equations 4.22 to zero, leading to a perturbatively flat valley of W. As was pointed out in [34, 44], for cases with two complex structure moduli the Kähler cone conditions take the form

$$M^i = f\left(H_1, H_2, F^2\right) \left(-\frac{H_2}{H_1}, 1\right)^T, \tag{4.27}$$

where $f(H_1, H_2, F^2)$ is some function of the remaining fluxes. Combining this with $M^i H_i = 0$, we can, without loss of generality, restrict the fluxes for these manifolds to be

$$\left\{H_1 < 0, H_2 > 0, F^2 < 0\right\}. \tag{4.28}$$

This automatically satisfies the demand $N_{\text{flux}} \geq 0$ and significantly reduces the amount of flux vacua we iterate over. Furthermore, assuming that $k_{ijk} F^k$ is invertible, the condition $H.(k.F)^{-1}.H = 0$ is solved by

$$F^1 \to \frac{-\kappa_{222} F^2 H_1^2 + 2\kappa_{122} F^2 H_1 H_2 - \kappa_{112} F^2 H_2^2}{\kappa_{122} H_1^2 - 2\kappa_{112} H_1 H_2 + \kappa_{111} H_2^2}. \tag{4.29}$$

Using the conventions 4.28 combined with the fact that for all geometries with $h^{(1,1)} = 2$ the numbers $\{\kappa_{111}, \kappa_{122}, \kappa_{112}, \kappa_{222}\}$ are greater than or equal to 0, we find $F^1 > 0$ in convention 2. Therefore, $F^1 H_1$ and $F^2 H_2$ have the same sign. This means that for any given bound N_{max}, there will be finitely many flux vacua that do not violate the condition. In particular, it will only be relevant to consider the flux components up to $\pm 2N_{\text{max}}$, where the sign corresponds to the convention of Equation 4.28. For the models with two complex structure moduli we will consider vacua with $N_{\text{max}} = 600$. It turns out that a similar condition does not hold for the examples with more complex structure moduli. This means that we have to choose the range of the individual flux entries. For these models we consider the independent flux entries $\{F^2, F^3, H_1, H_2, H_3\} \in (-45, 45)$, meaning we consider around 10^9 vacua for the geometries with three complex structure moduli.

Step 2: Solving the Effective F-term equation

Having the fluxes at our disposal, we can add the instanton induced contributions of Equation 4.25. Since we are interested in stabilizing the moduli in the large complex structure regime, we ignore the non-perturbative corrections to the prepotential in the Kähler potential. The effective Kähler potential, along the flat valley $U^i = M^i\tau$, consequently takes the form

$$K^{\text{eff}}(S) \simeq -4\ln[-i(\tau-\bar{\tau})] - \ln\left[\frac{1}{6}\kappa^0_{ijk}M^iM^jM^k\right]. \tag{4.30}$$

Using this non-perturbative Kähler potential, we can solve the effective F-term equation

$$D_S W^{\text{eff}}(\tau) = \partial_\tau W^{\text{eff}}(\tau) + W^{\text{eff}}(\tau)\left(\partial_\tau K^{\text{eff}}\right) = 0. \tag{4.31}$$

As pointed out already in [34], the axion c can be stabilized to have 0 vev. The other field in the axio-dilaton determines the string coupling, given by $g_s = s_0^{-1}$.

For each combination of fluxes that we have found in Step 1, we compute the instanton induced contributions to the superpotential and consequently solve Equation 4.31 by numerically finding the root. The complex structure moduli are then given by $U^i = M^i\tau$. We do this using a parallelized algorithm in *Mathematica*. At this point we have a list of fluxes that generate a perturbatively flat valley, as well as potential solutions for each combination of fluxes.

Step 3: Adding a Kähler Modulus and Solving the Full F-term equation

The results of Step 2 can be used as proper starting values to solve the full F-term equations, meaning that we consider the Kähler metric with the full non-perturbative contributions induced via the instanton corrections. It turns out that the two step procedure of KKLT does not work with these recipes, as the mass of the Kähler modulus is of the same order of magnitude as the mass of the axio-dilaton. This simply means that we cannot *first* stabilize the axio-dilaton and complex structure moduli and *after* that the Kähler modulus. To circumvent this problem we will simply add the non-perturbative corrections to the superpotential for a single Kähler modulus, defined by Equation 3.27, from the beginning. Doing this we have to solve the coupled system of complex equations, the F-term equations,

$$D_i W(\tau, U^1, \ldots, U^n, T) = \partial_i W(\tau, U^1, \ldots, U^n, T) + W(\tau, U^1, \ldots, U^n, T)\,(\partial_i K) = 0, \tag{4.32}$$

with i running over the axio-dilaton, the single Kähler modulus and all complex structure moduli of the theory. Including all the non-perturbative corrections, the superpotential W reads

$$\begin{aligned} W = &-\sqrt{\frac{2}{\pi}}\left(F^0 - \tau H^0\right)\left(2\mathcal{F}_{\text{inst}} - U^i\partial_i\mathcal{F}_{\text{inst}}\right) + \\ &-\sqrt{\frac{2}{\pi}}\left(F^i - \tau H^i\right)\left(\partial_i\mathcal{F}_{\text{inst}}\right) + e^{-2\pi T}, \end{aligned} \tag{4.33}$$

where we set the constants $\mathcal{A} = 1$ and $a = 2\pi$. The Kähler potential K furthermore contains the part for the single Kähler modulus,

$$K_{\text{Kähler}} = -3\log\left(T + \bar{T}\right). \tag{4.34}$$

Generally speaking, this is a complicated system with many non-perturbative (exponential) contributions. To solve this, we need *good* starting points for the FindRoot. As starting values we use the effective solutions from Step 2. Since this effective computation does not include a Kähler modulus, we still have to make an *ansatz* for its initial value. We choose this to be $T = 1$ in this thesis. We consequently solve the full set of F-term equations for each valid flux combination that we have found in Step 1. We again parallelize the algorithm. The final result is the total set of vacua which lead to stabilized values of all the moduli. For all of these solutions we consequently compute the following quantities.

The Superpotential

For each flux configuration we can compute W_0, which is simply the superpotential of Equation 4.10 evaluated in the minima of the fields.

Canonically normalised mass matrix

We recall that the scalar potential is given by

$$V = e^K \left(K^{I\bar{J}} D_I W D_{\bar{J}} \overline{W} - 3|W|^2 \right). \tag{4.35}$$

The canonically normalised mass matrix is defined as [48, 49]

$$(M^2)^i_j = K^{ik} \partial_k \partial_j V, \tag{4.36}$$

where we choose to take derivatives with respect to the *real* degrees of freedom and we evaluate in the solution to the F-term equation.

Physical Masses

Having the canonically normalised mass matrix at our disposal, we can restore units and powers of the string coupling constant to find the physical masses of the theory. Using [50], we find that the matrix in Equation 4.36 carries units of $\frac{M_{\text{pl}}^2 g_s^3}{4\pi}$. Restoring this prefactor and computing the eigenvalues of the mass matrix, we find the physical moduli masses. We can consequently compare the masses of the moduli with the string- and Kalazu-Klein mass scale, and check if we obtain the correct mass hierarchies.

4.3 Results

In this section, we will present the results of our research. This will be a two-step procedure. In the first step, we will consider the distribution of W_0 and the moduli masses with respect

to N_{flux}. We will visualize these results for two particular Calabi-Yau geometries, allowing us to comment on some of the general behavior we see in all examples. This motivates how we look for various scaling patterns. We consequently present the results of our numerical analysis for all geometries under investigation. As will become clear from the examples, there is a lot of interesting scaling behavior going on. We will find fits for the boundary of the distribution of W_0 with respect to N_{flux}, the mass eigenvalues with respect to N_{flux} and lastly an interesting relation between W_0 and the minimal mass eigenvalue. The volume scale of the compactifications is set through the stabilized value of the Kähler modulus, which will allow us to compare the Kaluza-Klein scale with the moduli masses. These results will be presented in the second part of this section. The topological data associated with each Calabi-Yau (as well as the identifications used in the [34, 44]) are summarized in Appendix C. Here one can also find the reference to the database of the Gopakumar-Vafa invariants. For the models with $h^{(1,1)} = 2$, we have chosen to only consider the $K3$-fibred Calabi-Yau manifolds investigated in [34, 44]. The reason for this is that only these models give rise to an abundance of vacua, allowing for a better analysis. The limited number of geometries with $h^{(1,1)} = 3$ are the ones appearing in the Ross Altman database [51], for which the GV-invariants were computed in [52]. For all examples under consideration we work up to order 4 in the complex structure moduli for the non-perturbative corrections.

4.3.1 An Example with two Complex-Structure Moduli

For illustrative purposes let us consider the results of the entire algorithm for one particular example. We choose this to be Calabi-Yau 11. The reason is that this model admits many effective flux vacua, allowing for a solid analysis of the scaling patterns. In Steps 1 and 2 of the algorithm, we reproduce the results reported in [44]. In particular, we find the lowest value of W_0 for the following combination of fluxes (with $N_{\text{flux}} \leq 500$)

$$\begin{aligned} F^i &= \{29, -10\}, \quad & H_i &= \{-20, 19\}, \quad & N_{\text{flux}} &= 385 \\ \langle g_s \rangle^{-1} &= 17.0661, \quad & \langle U^i \rangle &= \{5.40427, 5.6887\}, \quad & |W_0| &= 2.7117 \cdot 10^{-18}. \end{aligned} \tag{4.37}$$

It turns out that this combination of fluxes also yields a solution to the complete set of F-term equations. The result of this computation (Step 3 of the algorithm) is given by

$$\begin{aligned} F^i &= \{29, -10\}, \quad & H_i &= \{-20, 19\}, \quad & N_{\text{flux}} &= 385 \\ \langle g_s \rangle^{-1} &= 17.06706, \quad & \langle U^i \rangle &= \{5.404570, 5.689021\}, \quad & |W_0| &= 2.711895 \cdot 10^{-18}, \\ T &= 5.98796. \end{aligned} \tag{4.38}$$

While we do not explicitly investigate the accuracy of the effective approach in this thesis, the general finding is comparable with the results of Equations 4.37, 4.38. This means that the effective picture is often accurate in predicting the value of W_0, as well as the stabilized values of the axio-dilaton and complex structure moduli. In order to compute the canonically normalized mass matrices we are forced, however, to go beyond the effective picture. Having the canonically normalized mass matrix we consequently compute the lowest and highest mass eigenvalue for each particular combination of fluxes. We summarize the results of this entire step in Figure 4.2, in which all computed quantities are plotted as a function of N_{flux}.

In Figure 4.2a we see the distribution of W_0 with respect to the flux charge N_{flux}. As one would expect, the higher N_{flux} is allowed to be (and thus the more flux combinations we can consider), the lower possible value of W_0 we find. Of interest to us is to describe the scaling behavior, in particular of the boundary region. This captures the behaviour of $W_0(N_{\text{flux}})$ and indicates how

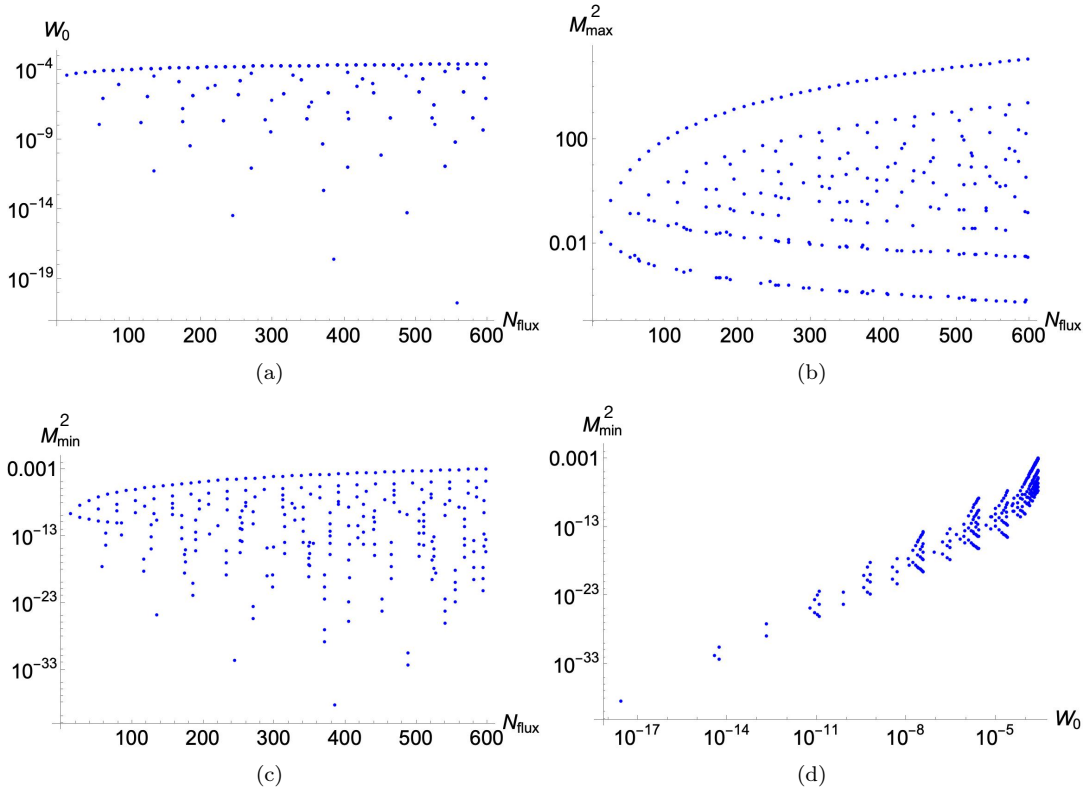

Figure 4.2: (a) The value of the superpotential W_0 for each combination of fluxes as a function of N_{flux}. (b) The value of the maximal mass eigenvalue (squared) of the canonically normalized mass matrix in units of $M_p^2/4\pi$ as a function of N_{flux}. (c) The value of the minimal mass eigenvalue (squared) of the canonically normalized mass matrix in units of $M_p^2/4\pi$ as a function of N_{flux}. (d) The value of the minimal mass eigenvalue (squared) of the canonically normalized mass matrix in units of $M_p^2/4\pi$ plotted as function of the corresponding value of W_0.

low we can make W_0 upon increasing N_{flux}. Since the y-axis is a logarithmic scale, we see that this scaling will roughly be exponential. In Figure 4.2b we see the distribution of the maximal mass eigenvalue squared of the canonically normalised mass matrix Equation 4.36 (in units of $\frac{M^2_{\text{planck}}}{4\pi}$). The resulting scatter plot exhibits two clear bounding regions that together enclose the bulk of the scatter data. These roughly look like logarithmic functions on the logarithmic plot, and we will find the best fit for these bounding regions as well. In Figure 4.2c we see the minimal mass eigenvalue squared with respect to N_{flux}. What is striking is the visual similarity of this figure with the scatter-plot of $W_0(N_{\text{flux}})$ of Figure 4.2a. This is the reason to consider the plot of Figure 4.2d, where we plot the minimal mass eigenvalue against the value of W_0.

It turns out that the general patterns that emerge in all the examples considered in this thesis are rather similar to the ones we have just seen in Calabi-Yau 11. For all these geometries we will fit the relevant boundary regions. The exact fitting functions with the corresponding parameter settings are presented in the subsequent section. The fits for Calabi-Yau 11 are plotted in Figure 4.3.

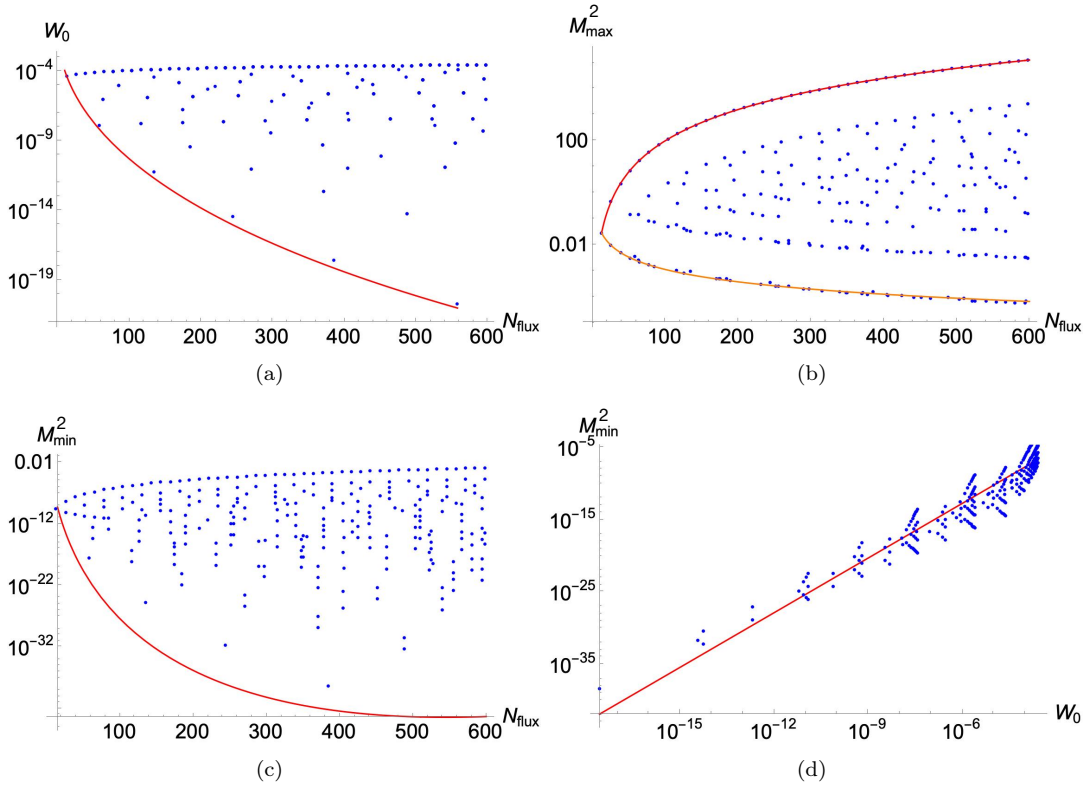

Figure 4.3: (a) The value of the superpotential W_0 for each combination of fluxes as a function of N_{flux}, with the corresponding fit of the boundary in red. (b) The value of the maximal mass eigenvalue (squared) of the canonically normalized mass matrix in units of $M_p^2/4\pi$ as a function of N_{flux}, with the corresponding fits of the upper bound (red) and lower bound (orange). (c) The value of the minimal mass eigenvalue (squared) of the canonically normalized mass matrix in units of $M_p^2/4\pi$ as a function of N_{flux}, with the corresponding fit of the boundary in red. (d) The value of the minimal mass eigenvalue (squared) of the canonically normalized mass matrix in units of $M_p^2/4\pi$ plotted as function of the corresponding value of W_0, with the corresponding fit in red.

4.3.2 An Example with three Complex-Structure Moduli

Since the examples with three or more complex structure moduli have not been considered in the literature, we will also look at one of these models in more detail. The limited number of models with three complex structure moduli that we consider exhibit much of the same structure as we have seen before. We present the results of the algorithm for Calabi-Yau 27 here. For the lowest value of $|W_0|$ we find in the effective picture

$$\begin{aligned} F^i &= \{24, 16, -12\}, & H_i &= \{-18, -1, 22\}, & N_{\text{flux}} &= 356 \\ \langle g_s \rangle^{-1} &= 51.40005, & \langle U^i \rangle &= \{4.85445, 25.700023, 5.14000\}, & |W_0| &= 1.24495 \cdot 10^{-17}. \end{aligned} \tag{4.39}$$

Taking this as input to solve the full F-term equations we find the following solution

$$\begin{aligned} F^i &= \{24, 16, -12\}, \qquad H_i = \{-18, -1, 22\}, \qquad N_{\text{flux}} = 356 \\ \langle g_s \rangle^{-1} &= 51.403886, \qquad \langle U^i \rangle = \{4.854811, 25.70194, 5.14038859\}, \qquad |W_0| = 1.244973 \cdot 10^{-17} \\ T &= 5.514615. \end{aligned} \tag{4.40}$$

Similarly, as in the case of two complex structure moduli, the data seems to indicate that the effective recipe is well-suited to predict the solutions to the full F-term equations. In Figure 4.4 we see the same data plotted in the case for our example that has three complex structure moduli. The emerging patterns are similar to the example we have seen in the previous section. There are, however, also some striking differences. In particular, we note that the structure of the plots in Figure 4.4a and Figure 4.4c are again similar. This also leads to the power-law scaling depicted in Figure 4.4d. We see that the scatter-plot of the maximal mass eigenvalue exhibits less structure than in the case of three complex structure moduli. We will have more to say about this in the discussion. In general, it turns out that for these examples there is no evident upper and lower boundary, and for this reason, we refrain from fitting the boundaries here. For the data that admits a fit we have again plotted the relevant fit functions. These can be seen in Figure 4.5.

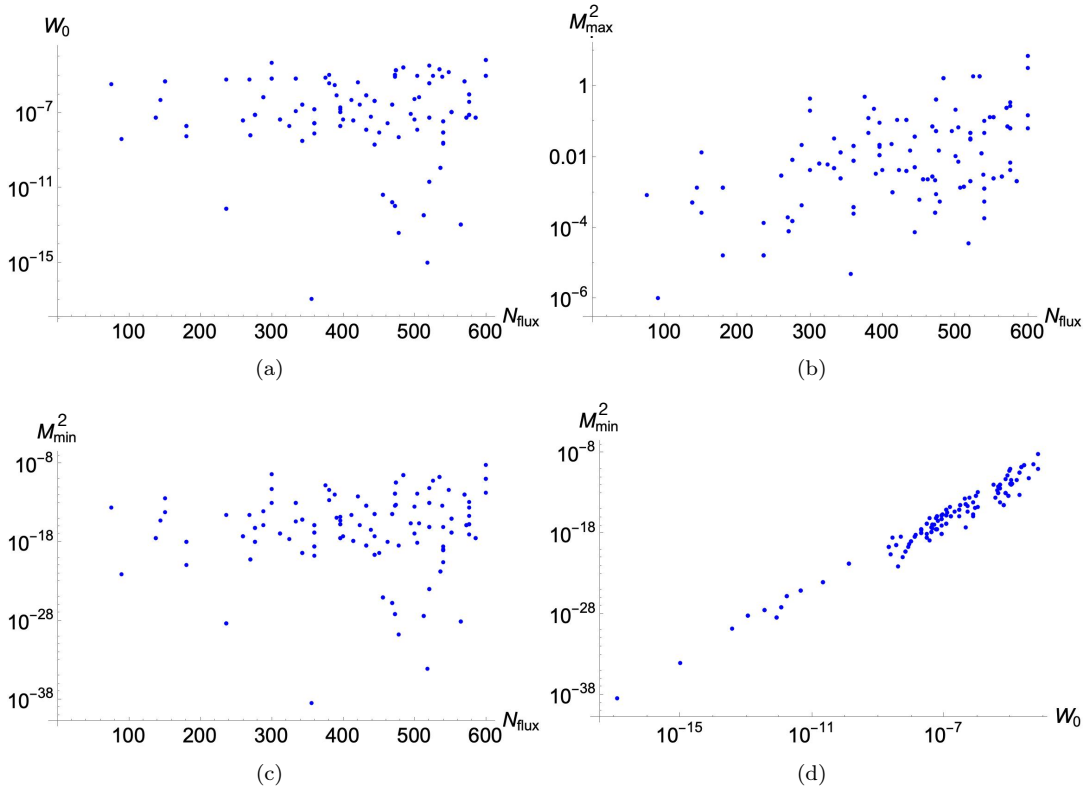

Figure 4.4: (a) The value of the superpotential W_0 for each combination of fluxes as a function of N_{flux}. (b) The value of the maximal mass eigenvalue (squared) of the canonically normalized mass matrix in units of $M_p^2/4\pi$ as a function of N_{flux}. (c) The value of the minimal mass eigenvalue (squared) of the canonically normalized mass matrix in units of $M_p^2/4\pi$ as a function of N_{flux}. (d) The value of the minimal mass eigenvalue (squared) of the canonically normalized mass matrix in units of $M_p^2/4\pi$ plotted as function of the corresponding value of W_0.

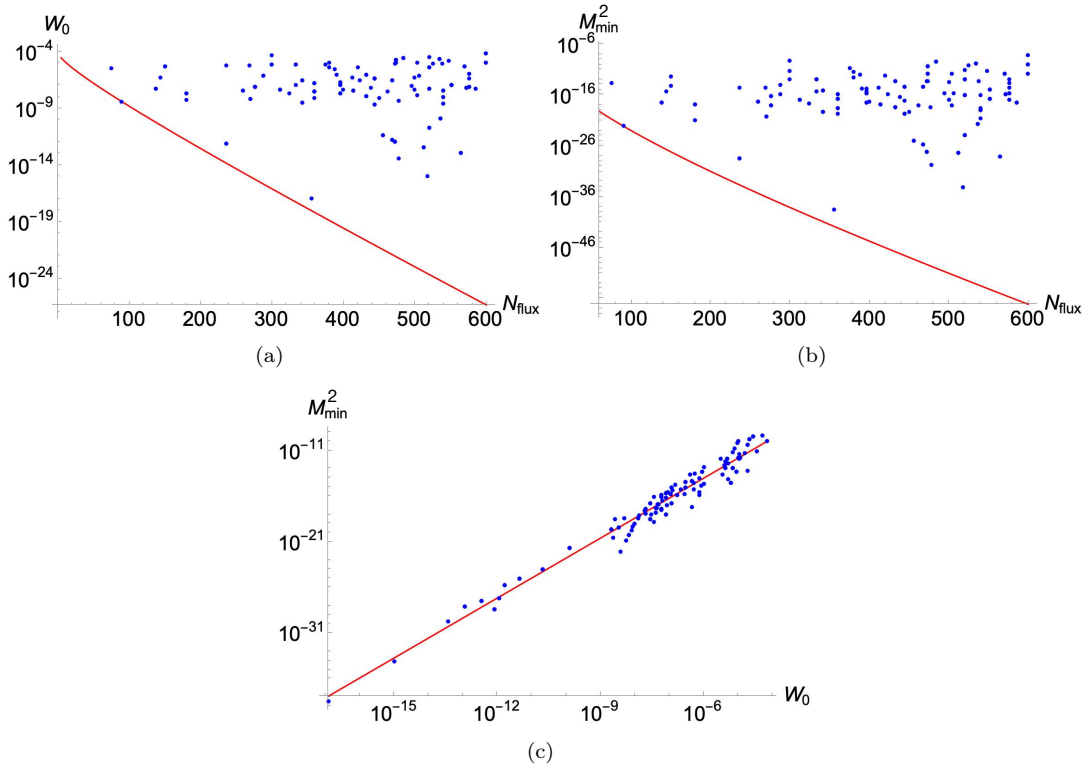

Figure 4.5: (a) The value of the superpotential W_0 for each combination of fluxes as a function of N_{flux}, with the corresponding fit of the boundary in red. (b) The value of the maximal mass eigenvalue (squared) of the canonically normalized mass matrix in units of $M_p^2/4\pi$ as a function of N_{flux}, with the corresponding fits of the upper bound (red) and lower bound (orange). (c) The value of the minimal mass eigenvalue (squared) of the canonically normalized mass matrix in units of $M_p^2/4\pi$ as a function of N_{flux}, with the corresponding fit of the boundary in red. (d) The value of the minimal mass eigenvalue (squared) of the canonically normalized mass matrix in units of $M_p^2/4\pi$ plotted as function of the corresponding value of W_0, with the corresponding fit in red.

4.3.3 Scaling Functions

Now that we have seen the general structure underlying the models under investigation, we can turn to the models used to fit the relevant boundaries of the scatter plots. To fit the boundary of $W_0(N_{\text{flux}})$ in the set of models under consideration, we have chosen to use a fit function of the form

$$W_0(N_{\text{flux}}) = \exp\Big\{\mathrm{a}\sqrt{N_{\text{flux}}} + \mathrm{b}N_{\text{Flux}} + \mathrm{c}\Big\}. \tag{4.41}$$

The approach we take here is conservative in the following sense. First, we fit the boundary envelope of the scatter graph according to Equation 4.41. We consequently adjust the parameter c in such a way that all points are within this boundary. It is important to note here that there is no one-fits-all recipe. The fit function has been chosen by trial and error, and it was found to be a suitable function that could capture the general scaling behavior in all examples. The parameter settings for our models are presented in Table D.1. Some geometries did not give valid solutions to the F-term equations. These are represented by a $-$ in the respective table entries. Interestingly, these models admitted solutions without the addition of the Kähler

modulus.

For the boundary region describing the minimal mass eigenvalue with respect to N_{flux} we use the same functional structure. In particular,

$$M^2_{\text{min}}(N_{\text{flux}}) = \exp\Big\{\text{a}\sqrt{N_{\text{flux}}} + \text{b}N_{\text{Flux}} + \text{c}\Big\}. \tag{4.42}$$

In Table D.2 the parameter settings for this fit have been presented. For both the upper and lower bounding regions of the distribution of M^2_{max} we use the following functional format

$$M^2_{\text{max}}(N_{\text{flux}}) = \exp\{a\log(x) + b\}. \tag{4.43}$$

The parameter settings for these regions are presented in Table D.4 and Table D.3 for the lower- and upper bounding regions, respectively. Finally, the power-law-behavior between the minimal mass eigenvalue and W_0 are described through a fit of the form

$$M^2_{\text{min}} = b \cdot (W_0)^a. \tag{4.44}$$

The parameter settings for these fits are presented in Table D.5.

4.3.4 Moduli Spectroscopy

In the process of going from our ten-dimensional string theory to models of four-dimensional physics, we discard certain modes. In the first place, we integrate out all massive string excitations. We are consequently left with all the massless modes. Upon the compactification, these massless modes generate another infinite tower of massive states that are proportional to the compactification volume. We again assume that the compactification volume is sufficiently small, such that the masses of these massive states are sufficiently large. Since we are looking at very concrete examples, it is important to check that we indeed generate the correct *mass hierarchy* that justifies the compactification procedure in the first place.

In particular, we want to check that

$$M_{\text{Pl}} > M_{\text{s}} > M_{\text{KK}} > M_{\text{mod}}. \tag{4.45}$$

Here we denote by M_{Pl} the Planck mass, M_{s} is the string scale, M_{KK} is the Kaluza-Klein (or compactification) scale and M_{mod} is the moduli mass. We can express the string scale and the KK-scale in terms of the Planck mass in the following way [50]

$$m_s = \frac{g_s}{\sqrt{4\pi\mathcal{V}_s^0}}M_P, \quad M_{\text{KK}} = \frac{g_s\sqrt{\pi}}{(\mathcal{V}_s^0)^{\frac{2}{3}}}M_P. \tag{4.46}$$

Here s is the real part of the axio-dilaton τ, which is related to the string coupling through $s = g_s^{-1}$. Furthermore, $\mathcal{V}$ is the volume of the compactification space, which is related to the real part of the Kähler modulus through $\mathcal{V} = (\rho)^{3/2}$. Our goal now is to explicitly check if this hierarchy is satisfied for the flux vacua that we find for the models under investigation. Let us consider again Calabi-Yau 11 and look at the numerical results. We can compute the *hierarchy vector*, given in terms of the Planck mass, that we define as

$$\{M_{\text{Planck}}, M_s, M_{KK}, M_{\text{max}}, M_{\text{min}}\}, \tag{4.47}$$

where $M_{\text{max}}, M_{\text{min}}$ correspond to the heaviest and lightest moduli, respectively. For each of the allowed fluxes, we can analyze this hierarchy vector. The best we can do if we want to separate scales on each level yields the following hierarchy vector

$$\{1, 0.0043179, 0.000027775, 0.0065709, 3.6368 \cdot 10^{-20}\}. \tag{4.48}$$

We immediately see that the scale of the M_{max} exceeds the Kaluza-Klein scale. It turns out that this is a bottleneck for *each* flux vacuum that we find in this particular model. Indeed, for each combination of fluxes, we can compute the mass ratio. The result of this analysis is presented in Figure 4.6.

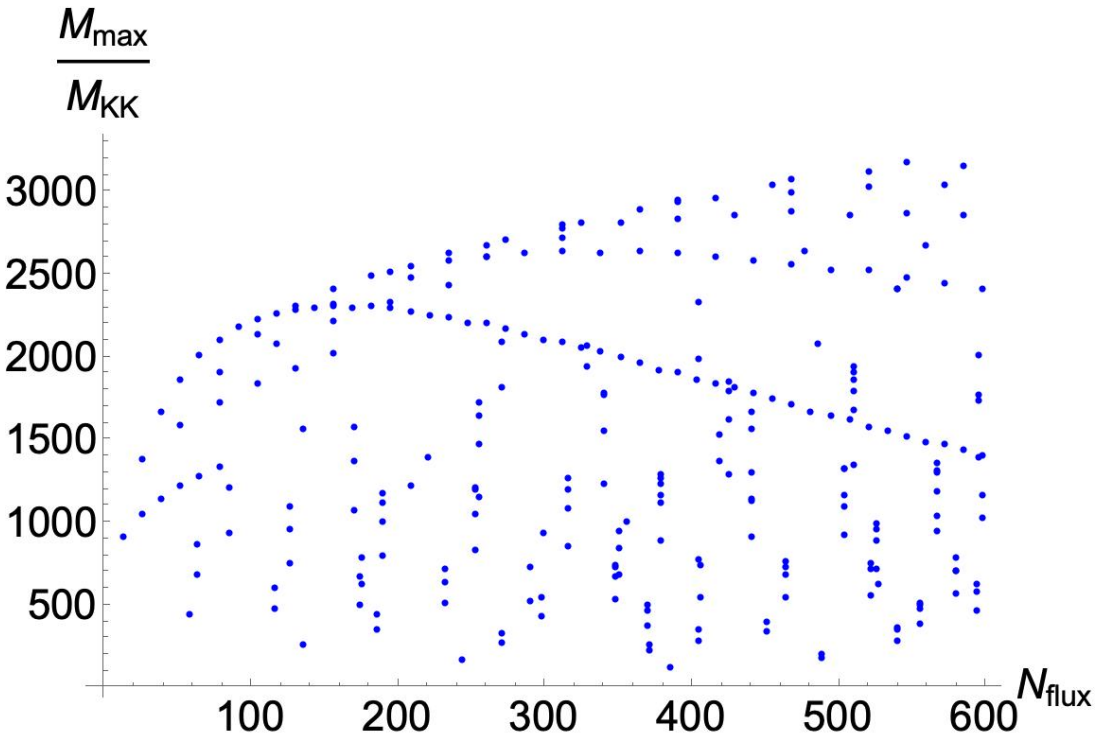

Figure 4.6: Visualization of the scale separation between the heaviest modulus mass M_{max} and the Kaluza-Klein scale M_{KK} as a function of the total flux number.

We can subsequently extend this analysis to all other viable Calabi-Yau models. In particular, we compute for each flux vacuum the ration of $\frac{M_{\text{max}}}{M_{KK}}$ and take the minimal value. The results of this analysis are presented in Figure 4.7. We see that only Calabi-Yau 31 exhibits a vacuum solution in which we obtain the correct hierarchy.

4.3.5 Constraining N_{flux}

We can consider the distribution of the separation M_{max}/M_{KK} as function of N_{flux}, as visualized for CY 11 in Figure 4.6 for all the models under investigation. Instructing *Mathematica* to find the boundary we suggest the following fit function

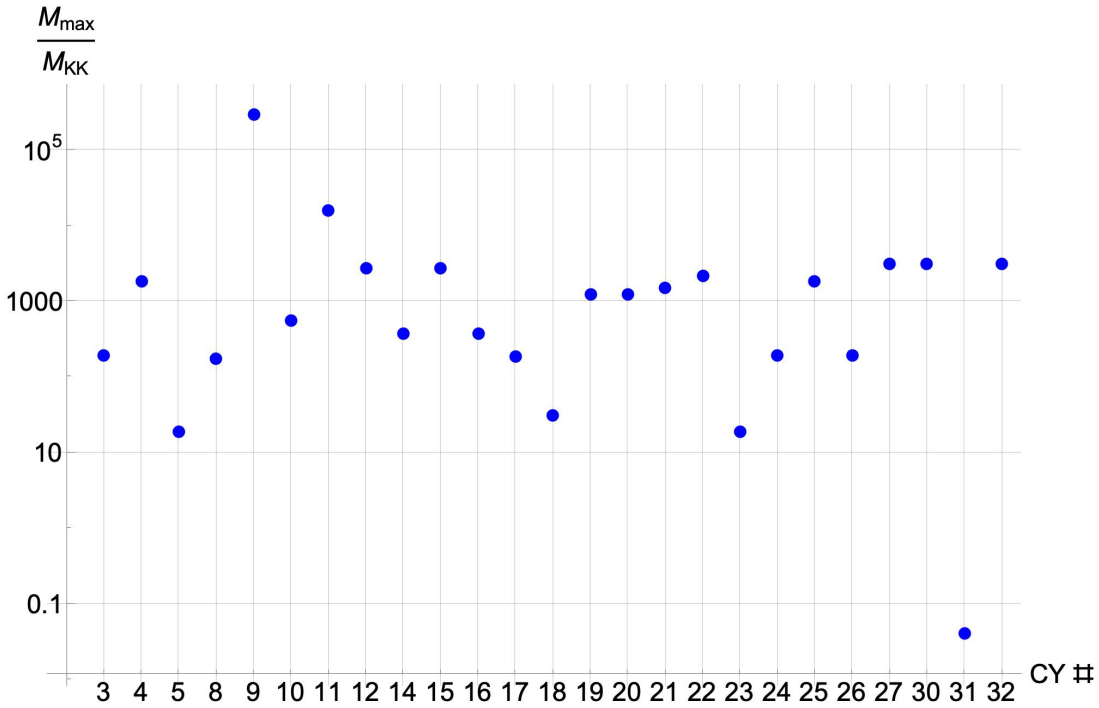

Figure 4.7: Plotted is the hierarchy M_{max}/M_{KK} for combination of fluxes that gives a valid solution to the F-term equations of Calabi-Yau 11. It is clear that none of these solutions give rise to a correct separation of mass scales.

$$\frac{M_{\text{max}}}{M_{KK}}(N_{\text{flux}}) = \exp\{a + b\log N_{\text{flux}} + c(\log N_{\text{flux}})^2\}. \tag{4.49}$$

Not all models have such a well-defined boundary, and fitting them would be speculative work. However, some models admit a clear bounding envelope. These models can be fitted using Equation 4.49. The result of this analysis, for this subset of models, are presented in Table 4.1

Calabi-Yau Geometry	a	b	c
3	5.66986	−0.175063	−0.0480654
5	6.99099	−0.572094	−0.0465246
9	8.78947	−0.252128	−0.0330848
11	7.49274	−0.119376	−0.0551720
17	3.34858	1.10097	−0.192603
18	6.45495	0.502354	−0.199666
19	4.99637	0.388431	−0.100877
20	4.99637	0.388431	−0.100877
23	6.99099	−0.572094	−0.0465246
24	5.66986	−0.175063	−0.0480654
26	5.66986	−0.175063	−0.0480654

Table 4.1: Parameter values for the proposed model of Equation 4.49

We can consequently use the scaling behaviour to put a bound on the flux charge N_{flux} for this set of models. In particular, we solve the inequality

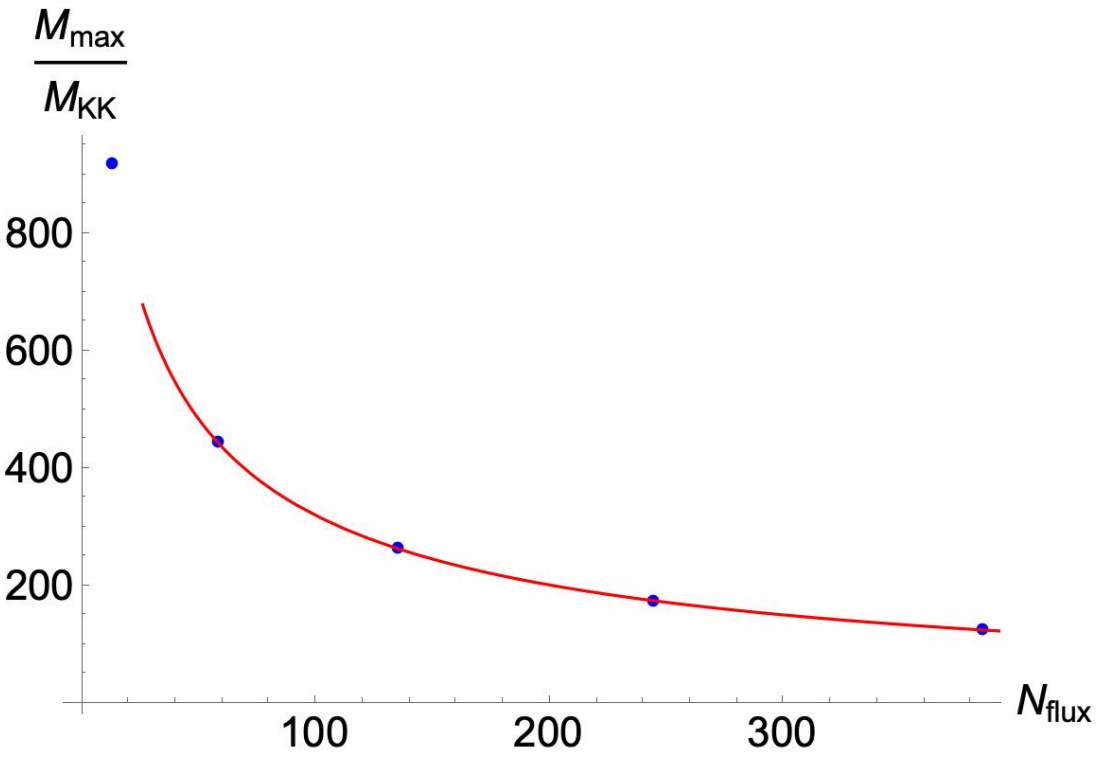

Figure 4.8: The boundary of the distribution of $M_{\max}/M_{KK}$ including the fit in red for Calabi-Yau 11. The parameters for this fit are presented in Table 4.1.

$$\frac{M_{\text{mod}}}{M_{KK}} < \sqrt{\frac{1}{10}}. \tag{4.50}$$

This is already a conservative number, and it would be better to have an even better separation of scales. Solving for this value already gives unrealistically high values for the tadpole charge N_{flux}. The results are presented in Table 4.2.

Calabi-Yau Geometry	Flux Constraint
3	$N_{\text{flux}} > 27724$
5	$N_{\text{flux}} > 4627$
9	$N_{\text{flux}} > 10^6$
11	$N_{\text{flux}} > 96932$
17	$N_{\text{flux}} > 4786$
18	$N_{\text{flux}} > 1914$
19	$N_{\text{flux}} > 21284$
20	$N_{\text{flux}} > 21284$
23	$N_{\text{flux}} > 4627$
24	$N_{\text{flux}} > 27724$
26	$N_{\text{flux}} > 27724$

Table 4.2: Constraints on fluxes from solving Equation 4.50.

We can see that for all models that admit a sufficiently nice boundary, the flux number would have to be extremely high in order to obtain the correct hierarchy of masses. Flux numbers ranging from $10^3 - 10^6$ are unlikely to satisfy the tadpole bound.

Chapter 5

Conclusion and Discussion

Realizing exponentially small flux superpotential W_0 plays a central role in many compactification models. Explicitly exhibiting W_0 is a difficult problem in general, and finding recipes to systematically accomplish this is an important part of string theory research. In this thesis, we considered the DKMM-recipe proposed in [41]. This procedure starts with general constraints on the fluxes in the compactification to ensure the vanishing of W along a particular direction in moduli space. This flat valley is consequently lifted via the inclusion of non-perturbative effects, realizing an exponentially small value in the minimum.

This proposed mechanism has consequently been studied in [34, 44]. They performed an extensive analysis for a broad class of Calabi-Yau manifolds with two complex structure moduli. The results gave insight into the vacuum structure of these compactifications. The authors found that especially $K3$-fibred Calabi-Yau manifolds give rise to an abundance of such perturbatively flat flux vacua.

In this thesis, we extended this analysis in two ways. In the first place, we went beyond the effective approach by solving the complete set of F-term equations. Secondly, we stabilized a single Kähler modulus via the inclusion of additional non-perturbative effects. The upshot of this is that we could compute the canonically normalized mass matrix, allowing us to explicitly compute the masses of the moduli. The stabilized value of the Kähler modulus is a measure of the volume of the compactification space, and its value allows us to compute the Kaluza-Klein scale of these models. This analysis allowed us to say more about the effectiveness of the proposed method in finding physical flux vacua.

The research was originally motivated by the question if we can say something about the scaling of W_0 to N_{flux}. At least in the class of models we have considered, we can answer this question in the affirmative. In particular, W_0 becomes exponentially smaller with the increase of N_{flux}. In these models, we find low values of W_0 for relatively low values of N_{flux} already. In general, we can state that the proposed recipe is extremely convenient for finding vacua with exponentially small W_0. What is interesting, however, is to go one step beyond the computation of the GVW superpotential. This leads us to the most important conclusion we can draw from our research, that non of the $K3$-fibred Calabi-Yau geometries investigated in [34, 44] give rise to physically realistic string compactifications. For each flux vacuum for every single one of these models, the heaviest modulus exceeds the Kaluza-Klein scale set by compactification.

We consequently computed, for each particular flux combination, the ratio M_{mod}/M_{KK} as a function of N_{flux}. By considering the boundaries of the resulting scatter plots we could, for a subset of the models under consideration, put some general bounds on N_{flux}. This analysis

is far from perfect. In the range $0 < N_{\text{flux}} < 600$ we had to fit a boundary behaviour using approximately six data point. The general behavior for this subset of models was quite similar. The ratio fell off as N_{flux} got larger. While it is debatable whether the fit functions are valid far outside of this specified domain, they at least indicate the order of magnitude of N_{flux} at which we can expect a scale separation of at least

$$\frac{M_{\text{mod}}^2}{M_{KK}^2} < \frac{1}{10}.$$

We find that N_{flux} needs, in the best models, to be of order 10^3. At worst, it needs to exceed 10^6. These are many orders of magnitude larger than the highest flux tadpole charge described in the literature, and it is inconceivable that fluxes this large will satisfy the tadpole bound. While we cannot draw any conclusive discussions ruling out all models with $h^{(1,1)} = 2$, we have found that the general structure of the solutions is *very* similar. We can say that finding *physically valid* solutions for these models is much harder than expected. The recent work of [53] investigated two refined DKMM mechanisms. These scenarios are much like the original DKMM recipe. Interestingly, they found that for this mechanism to work one needs unnaturally high flux numbers likely violating the tadpole bound. This finding is closely related to our main result and might indicate that there are indeed structural problems with all of these models.

One important aspect making the KKLT scenario attractive is the fact that the stabilized value of the Kähler modulus provides a supersymmetric AdS vacuum that can be uplifted to a metastable dS vacuum. It turns out that in order to perform the uplift of this minimum we need to consider a different part of moduli space. In particular, we need one of the complex structure moduli to approach the so-called conifold locus for this mechanism to work. The generalizations of the DKMM recipe that give a controllable way to realize exponentially small W_0 in this coni-LCS regime have been studied in [43, 42]. It would be interesting to see how the mass hierarchies behave in this regime. As has already been pointed out in [54], realizing exponentially small W_0 in this regime might make one of the complex structure moduli exponentially heavy. It is not unthinkable that this will spoil the mass hierarchy for these models as well.

Besides the heaviest modulus, we have also discovered the power-law scaling of M_{min}^2 with respect to W_0. In particular, realizing exponentially smaller and smaller values of W_0 makes the lightest modulus lighter and lighter as well. The reason for this is not completely elusive, but it resides in the way that we generate exponentially small W_0 in the first place. We initially start with a flat valley, along which W is zero. Via the introduction of the non-perturbative corrections, we generate a non-zero superpotential along this direction in moduli space. This potential needs to be so shallow, however, that W_0 becomes exponentially small. The lightest modulus is then associated with this shallow direction in moduli space.

This does pose an additional issue that one has to deal with. In essence, this lightest modulus starts competing with the mass of the Kähler modulus if we perform the two-step KKLT procedure. To circumvent this problem, we need to add the non-perturbative corrections that can account for the stabilization of the Kähler modulus from the beginning.

For future research one could proceed along similar lines as done in this thesis, only for geometries with more complex structure moduli. In this thesis we have considered a couple of Calabi-Yau geometries with $h^{(1,1)} = 3$. Interestingly, we have found one geometry giving rise to a vacuum with exponentially small superpotential as well as a correct mass hierarchy. What makes the higher models interesting, but also more complex in their analysis, is the fact that, in contrast to the models with $h^{(1,1)} = 2$, the amount of flux combinations with N_{flux} smaller than some fixed value N_{max} does not have any obvious bound. While it is expected to be finite, it is much harder to find enough of these vacua for our predictions. For three complex structure moduli we already have five free entries one needs to loop over, so we necessarily have to make a choice as to how many fluxes we wish to compute. In addition to this problem, the

computational complexity to solve the full F-term equations also rises significantly in models with increasingly many complex structure moduli. One could also take these geometries and study them in the setting proposed in [43], [42]. It would be interesting to see if the same problems with the mass hierarchies arise in this refined DKMM setting.

As a last note, we want to point out that one could also raise concerns about the DKMM recipe as originally proposed. As is also briefly mentioned in the discussion of [55], the theory about Hodge loci proposed in [56] points out that in an appropriate coordinate system moduli stabilization occurs at zeros of *polynomials*. In practice, we use exponential contributions up to order four in our analysis. It could well be that the Gopakumar-Vafa invariants start conspiring when one includes higher and higher orders, possibly spoiling the mechanism used to lift the flat valley and generate the exponentially small value of W_0. One possible way of investigating this is to use the algorithm proposed in this thesis, including higher and higher orders of the Gopakumar-Vafa invariants. One could consequently analyze how the moduli masses scale as a function of the order of GV-invariants. It remains to be seen, however, if this is computationally achievable. Both the computation of these invariants to a high order, as well as solving the F-term equations using them quickly becomes computationally complex.

Appendix A

Differential Geometry Identities

In this appendix we summarize identities and facts that are useful for the computations done in Chapter 1.

Coordinates and Differential Forms

- The coordinates of Minkowski space are denoted by x^μ, where $\mu = 0, \ldots 3$. On a Calabi-Yau manifold Y we use complex coordinates that are denoted by $(y^\alpha, \bar{y}^{\bar{\alpha}})$, with $\alpha(\bar{\alpha}) = 1, 2, 3$.
- Using a complex basis, (p, q)-forms are expressed as

$$A_{p,q} = \frac{1}{p!q!} A_{i_1 \ldots i_p \bar{p}_1 \ldots \bar{z}_q} dy^{i_1} \wedge \ldots \wedge dy^{i_p} \wedge d\bar{y}^{\bar{i}_1} \wedge \ldots \wedge d\bar{y}^{\bar{i}_q} \tag{A.1}$$

- We can define the Dolbeault operators

$$\partial : A^{p,q} \to A^{p+1,q}, \quad \bar{\partial} : A^{p,q} \to A^{p,q+1}, \tag{A.2}$$

  whose action on a (p, q)-form is given by

$$\begin{aligned} \partial\omega &= \frac{1}{p!q!} \partial_i \omega_{i_1 \cdots i_p \bar{J}_1 \cdots \bar{j}_q} dz^i \wedge dz^{i_1} \wedge \cdots \wedge d\bar{z}^{j_q} \\ \bar{\partial}\omega &= \frac{1}{p!q!} \bar{\partial}_j \omega_{i_1 \ldots i_p \bar{J}_1 \cdots \bar{j}_q} d\bar{z}^j \wedge dz^{i_1} \wedge \cdots \wedge d\bar{z}^{j_q}. \end{aligned} \tag{A.3}$$

- Using the exterior derivative $d = \partial + \bar{\partial}$, the Laplacian is defined to be

$$\Delta = dd^* + d^*d. \tag{A.4}$$

Hodge Decomposition

- On compact orientable Riemannian manifolds any p-form ω_p has a unique decomposition given by

$$\omega_p = h_p + d\alpha_{p-1} + d * \beta_{p+1}, \tag{A.5}$$

where h_p is a zero mode of the Laplacian (i.e. $\Delta h_p = 0$). Since closed forms satisfy $d * \beta_{r+1} = 0$, each cohomology class possesses a unique harmonic representative. This is known as the *Hodge decomposition theorem*. This is precisely the statement that finding Laplace zero-modes on a Calabi-Yau is a cohomology problem.

Weyl Rescaling

- Under a rescaling of the metric defined by $g_{\mu\nu} = \Omega^{-2}\hat{g}_{\mu\nu}$, the inverse metric and the factor of $\sqrt{-g}$ change according to

$$\begin{aligned} g^{\mu\nu} &= \Omega^2 \hat{g}^{\mu\nu} \\ \sqrt{-g} &= \Omega^{-d}\sqrt{-\hat{g}}. \end{aligned} \tag{A.6}$$

- Implementing this on the Ricci scalar in the d-dimensional integration yields

$$\int \mathrm{d}x^d \sqrt{-g}\Omega^{d-2}\mathcal{R} = \int \mathrm{d}x^d \sqrt{-\hat{g}} \left(\mathcal{R} + (d-1)(d-2)\left(\frac{\partial\Omega}{\Omega}\right)^2 \right). \tag{A.7}$$

Reduction of gravity details

We present here the details of computing a term of the dimensionally reduced Ricci scalar, supplementing the discussion in Section 1.4. In the following we will use $\{\mu, \nu, \rho, \sigma\}$ for indices on M_4 and $\{\alpha, \beta, \gamma, \delta, \epsilon\}$ and their conjugates as indices on Y. The Christoffel symbols are defined as

$$\Gamma^M_{NK} = \frac{1}{2} g^{MP} \left(\partial_N g_{KP} + \partial_K g_{NP} - \partial_P g_{NK} \right). \tag{A.8}$$

From the form of the metric it is readily seen that there are 4 non-vanishing Christoffel symbols having one $\mathcal{M}_4$ index. They are given by:

$$\begin{aligned}
\Gamma^{\mu}_{\alpha\bar{\beta}} &= \frac{1}{2}g^{\mu\nu}\left(\partial_{\alpha}g_{\bar{\beta}\nu} + \partial_{\bar{\beta}}g_{\alpha\nu} - \partial_{\nu}g_{\alpha\bar{\beta}}\right) && \text{(A.9)}\\
&= -\frac{1}{2}g^{\mu\nu}\partial_{\nu}\left(\mathring{g}_{\alpha\bar{\beta}} - iv^{A}(\omega_{A})_{\alpha\bar{\beta}}\right)\\
&= \frac{i}{2}g^{\mu\nu}(\partial_{\nu}v^{A})(\omega_{A})_{\alpha\bar{\beta}}\\
\Gamma^{\mu}_{\alpha\beta} &= \frac{1}{2}g^{\mu\nu}\left(\partial_{\alpha}g_{\beta\nu} + \partial_{\beta}g_{\alpha\nu} - \partial_{\nu}g_{\alpha\beta}\right) && \text{(A.10)}\\
&= -\frac{1}{2}g^{\mu\nu}(\partial_{\nu}\overline{z}^{K})(\overline{b}_{K})_{\alpha\beta}\\
\Gamma^{\bar{\beta}}_{\mu\alpha} &= \frac{1}{2}g^{\bar{\beta}A}\left(\partial_{\mu}g_{\alpha A} + \partial_{\alpha}g_{\mu A} - \partial_{A}g_{\mu\alpha}\right) && \text{(A.11)}\\
&= \frac{1}{2}g^{\bar{\beta}\gamma}\left(\partial_{\mu}g_{\alpha\gamma}\right) + \frac{1}{2}g^{\bar{\beta}\bar{\gamma}}\left(\partial_{\mu}g_{\alpha\bar{\gamma}}\right)\\
&= \frac{1}{2}\left(\mathring{g}^{\bar{\beta}\gamma} + iv^{A}(\omega_{A})_{\beta\bar{\gamma}}\mathring{g}^{\beta\bar{\beta}}\mathring{g}^{\gamma\bar{\gamma}}\right)\left(\overline{b}_{K}\right)_{\alpha\gamma}\left(\partial_{\mu}\overline{z}^{K}\right)\\
&\quad + \frac{1}{2}\left(-\overline{z}^{K}(\overline{b}_{K})_{\beta\gamma}\mathring{g}^{\beta\bar{\beta}}\mathring{g}^{\gamma\bar{\gamma}}\right)\left(-i\partial_{\mu}v^{A}\right)\left(\omega_{A}\right)_{\alpha\bar{\gamma}}\\
&= \frac{1}{2}\left(\overline{b}_{K}\right)_{\alpha\beta}\mathring{g}^{\beta\bar{\beta}}\partial_{\mu}\overline{z}^{K} + \frac{i}{2}\left(\omega_{A}\right)_{\gamma\bar{\gamma}}\left(\overline{b}_{K}\right)_{\alpha\beta}\mathring{g}^{\beta\bar{\gamma}}\mathring{g}^{\gamma\bar{\beta}}v^{A}\partial_{\mu}\overline{z}^{K}\\
&\quad + \frac{i}{2}\left(\omega_{A}\right)_{\alpha\bar{\gamma}}\left(\overline{b}_{K}\right)_{\gamma\beta}\mathring{g}^{\beta\bar{\gamma}}\mathring{g}^{\gamma\bar{\beta}}\partial_{\mu}v^{A}\overline{z}^{K}\\
\Gamma^{\beta}_{\mu\alpha} &= \frac{1}{2}g^{\beta A}\left(\partial_{\mu}g_{\alpha A} + \partial_{\alpha}g_{\mu A} - \partial_{A}g_{\mu\alpha}\right) && \text{(A.12)}\\
&= \frac{1}{2}g^{\beta\gamma}\left(\partial_{\mu}g_{\alpha\gamma}\right) + \frac{1}{2}g^{\beta\bar{\gamma}}\left(\partial_{\mu}g_{\alpha\bar{\gamma}}\right)\\
&= \frac{1}{2}\left(-z^{K}(b_{K})_{\bar{\beta}\bar{\gamma}}\mathring{g}^{\gamma\bar{\gamma}}\mathring{g}^{\beta\bar{\beta}}\right)\left((\overline{b}_{L})_{\alpha\gamma}\partial_{\mu}\overline{z}^{L}\right)\\
&\quad + \frac{1}{2}\left(\mathring{g}^{\beta\bar{\gamma}} + i(v^{A})(\omega_{A})_{\gamma\bar{\beta}}\mathring{g}^{\beta\bar{\beta}}\mathring{g}^{\gamma\bar{\gamma}}\right)\left(-i(\partial_{\mu}v^{B})(\omega_{B})_{\alpha\bar{\gamma}}\right)\\
&= -\frac{1}{2}z^{K}(b_{K})_{\bar{\beta}\bar{\gamma}}\mathring{g}^{\beta\bar{\beta}}\mathring{g}^{\gamma\bar{\gamma}}(\overline{b}_{L})_{\alpha\gamma}\partial_{\mu}\overline{z}^{L} - \frac{i}{2}\mathring{g}^{\beta\bar{\gamma}}(\omega_{A})_{\alpha\bar{\gamma}}(\partial_{\mu}v^{A})\\
&\quad + \frac{1}{2}(\omega_{A})_{\gamma\bar{\beta}}(\omega_{B})_{\alpha\bar{\gamma}}v^{A}(\partial_{\mu}v^{B})\mathring{g}^{\beta\bar{\beta}}\mathring{g}^{\gamma\bar{\gamma}}
\end{aligned}$$

The Ricci scalar is given by

$$\begin{aligned}
R_{10} =& R_{4} + g^{\mu\nu}R^{\alpha}_{\mu\alpha\nu} + g^{\alpha\beta}\left(R^{\mu}_{\alpha\mu\beta} + R^{\gamma}_{\alpha\gamma\beta} + R^{\bar{\gamma}}_{\alpha\bar{\gamma}\beta}\right)\\
&+ g^{\alpha\bar{\beta}}\left(R^{\mu}_{\alpha\mu\bar{\beta}} + R^{\gamma}_{\alpha\gamma\bar{\beta}} + R^{\bar{\gamma}}_{\alpha\bar{\gamma}\bar{\beta}}\right) + \text{ conjugate terms .}
\end{aligned} \tag{A.13}$$

The exact form of the first term is given by

$$g^{\mu\nu}R^{\alpha}_{\mu\alpha\nu} = g^{\mu\nu}\left(\partial_{\mu}\Gamma^{\alpha}_{\alpha\nu} + \Gamma^{\alpha}_{\mu\gamma}\Gamma^{\gamma}_{\alpha\nu} + \Gamma^{\alpha}_{\mu\bar{\gamma}}\Gamma^{\bar{\gamma}}_{\alpha\nu} - \Gamma^{\alpha}_{\alpha\lambda}\Gamma^{\lambda}_{\mu\nu}\right). \tag{A.14}$$

Let us work out every term separately, working up to second order in the Kähler and complex structure deformations. To ease notation, we define the following quantities, following [6]

$$\begin{aligned}(\omega_A g) &= (\omega_A)_{\alpha\bar{\beta}}\, \mathring{g}^{\alpha\bar{\beta}} \\ \omega_A \omega_B &= (\omega_A)_{\alpha\bar{\alpha}}\, (\omega_B)_{\beta\bar{\beta}}\, \mathring{g}^{\alpha\bar{\beta}} \mathring{g}^{\beta\bar{\alpha}} \\ b_A \bar{b}_B &= (b_A)_{\bar{\alpha}\bar{\beta}}\, \left(\bar{b}_B\right)_{\alpha\beta}\, \mathring{g}^{\alpha\bar{\beta}} \mathring{g}^{\beta\bar{\alpha}}.\end{aligned} \tag{A.15}$$

Using these definitions the first term reads

$$\begin{aligned}\partial_\mu \Gamma^\alpha_{\alpha\nu} = \partial_\mu \Bigg(&\frac{1}{2}(\omega_A)_{\gamma\bar{\gamma}} (\omega_B)_{\alpha\bar{\beta}} \mathring{g}^{\gamma\bar{\beta}} \mathring{g}^{\alpha\bar{\gamma}} v^A \partial_\nu v^B - \frac{i}{2}(\omega_A)_{\alpha\bar{\beta}} \mathring{g}^{\alpha\bar{\beta}} \partial_\nu v^A \\ &- \frac{1}{2}(b_K)_{\bar{\beta}\bar{\gamma}} (\bar{b}_L)_{\alpha\gamma} \mathring{g}^{\gamma\bar{\beta}} \mathring{g}^{\alpha\bar{\gamma}} z^K \partial_\nu \bar{z}^L \Bigg) \\ = \frac{1}{2}(\omega_A)(\omega_B) &\left(\partial_\mu v^A \partial_\nu v^B + v^A \partial_\mu \partial_\nu v^B\right) - \frac{i}{2}(\omega_A g) \partial_\mu \partial_\nu v^A \\ &- \frac{1}{2}(b_K \bar{b}_L) \left(\partial_\mu z^K \partial_\nu \bar{z}^L + z^K \partial_\mu \partial_\nu \bar{z}^L\right).\end{aligned} \tag{A.16}$$

The second and third terms are given by

$$\begin{aligned}\Gamma^\alpha_{\mu\gamma} \Gamma^\gamma_{\alpha\nu} &= \left(-\frac{i}{2}(\omega_A)_{\gamma\bar{\gamma}} \mathring{g}^{\alpha\bar{\gamma}} \partial_\mu v^A\right) \left(-\frac{i}{2}(\omega_B)_{\alpha\bar{\beta}} \mathring{g}^{\gamma\bar{\beta}} \partial_\nu v^B\right) + \mathcal{O}(3) \\ &= -\frac{1}{4}(\omega_A \omega_B) \partial_\mu v^A \partial_\nu v^B,\end{aligned} \tag{A.17}$$

$$\begin{aligned}\Gamma^\alpha_{\mu\bar{\gamma}} \Gamma^{\bar{\gamma}}_{\alpha\nu} &= \left(\frac{1}{2}(b_K)_{\bar{\gamma}\bar{\beta}} \mathring{g}^{\alpha\bar{\beta}} \partial_\mu z^K\right) \left(\frac{1}{2}(\bar{b}_L)_{\alpha\gamma} \mathring{g}^{\gamma\bar{\gamma}} \partial_\nu \bar{z}^L\right) + \mathcal{O}(3) \\ &= \frac{1}{4}(b_K \bar{b}_L) \partial_\nu \bar{z}^K \partial_\mu z^L.\end{aligned} \tag{A.18}$$

For the last term we obtain

$$\Gamma^\lambda_{\mu\nu} \Gamma^\alpha_{\alpha\lambda} = \Gamma^\lambda_{\mu\nu} \left(\frac{1}{2}(\omega_A \omega_B) v^A \partial_\lambda v^B - \frac{i}{2}(\omega_A g) \partial_\lambda v^A - \frac{1}{2}(b_K \bar{b}_L) z^K \partial_\lambda \bar{z}^L\right), \tag{A.19}$$

and we note that we can combine these term with the ones looking like $\partial^2 z$ and $\partial^2 v$ in Equation A.16 to form a four-dimensional covariant derivative ∇_μ. Doing this gives the expression

$$\begin{aligned}g^{\mu\nu} R^\alpha_{\mu\alpha\nu} = &-\frac{i}{2}(\omega_A g) \nabla_\mu \partial^\mu v^A + \frac{1}{2}(\omega_A \omega_B) v^A \nabla_\mu \partial^\mu v^B - \frac{1}{2}(b_K \bar{b}_L) z^K \nabla_\mu \partial^\mu \bar{z}^L \\ &+ \frac{1}{4}(\omega_A)(\omega_B)(\partial_\mu v^A \partial^\mu v^B) - \frac{1}{4}(b_K \bar{b}_L)(\partial_\mu z^K \partial^\mu \bar{z}^L).\end{aligned} \tag{A.20}$$

We recall that everything appears in a ten-dimensional integration as in Equation 1.20. For that reason we are free to perform a four-dimensional integration by parts to move the covariant

derivatives and write the expression in terms of partial derivatives. This can be done in the following way

$$\nabla_\mu \sqrt{-\hat{g}} = \sqrt{-g_4}\partial_\mu \sqrt{g_6} = \sqrt{-\hat{g}} \times (\text{terms linear and quadratic in the moduli}). \tag{A.21}$$

To see how this helps us we consider the second term given by Equation A.20 as it appears in the action

$$\begin{aligned} \frac{1}{2}\int_{M_4\times Y} \sqrt{|\hat{g}|}\,(\omega_A\omega_B)\, v^A \nabla_\mu \partial^\mu v^B &\sim -\frac{1}{2}\int_{M_4\times Y} (\omega_A\omega_B)\,\partial^\mu v^B \nabla_\mu \left(\sqrt{|\hat{g}|}v^A\right) \\ &= -\frac{1}{2}\int_{M_4\times Y} \sqrt{|\hat{g}|}\,(\omega_A\omega_B)\,\partial_\mu v^A \partial^\mu v^B + O(3), \end{aligned} \tag{A.22}$$

where $\sim$ denotes equality modulo a total derivative term. Repeated application of this trick yields the following expressions for the remaining terms that contribute:

$$\begin{aligned} g^{\mu\nu}R^\alpha_{\mu\alpha\nu} \sim& \frac{1}{2}\left((\omega_A g)\,(\omega_B g) - \frac{1}{2}\omega_A\omega_B\right)\partial_\mu v^A \partial^\mu v^B \\ &+ \frac{1}{4} b_K \bar{b}_L \partial_\mu z^K \partial^\mu \bar{z}^L \\ g^{\alpha\beta}R^\mu_{\alpha\mu\beta} \sim& \frac{1}{2} b_K \bar{b}_L \partial_\mu z^K \partial^\mu \bar{z}^L \\ g^{\alpha\bar{\beta}}R^\mu_{\alpha\mu\bar{\beta}} \sim& \frac{1}{2}\left((\omega_A g)\,(\omega_B g) - \frac{1}{2}\omega_A\omega_B\right)\partial_\mu v^A \partial^\mu v^B \\ &- \frac{1}{4} b_K \bar{b}_L \partial_\mu z^K \partial^\mu \bar{z}^L \\ g^{\alpha\bar{\beta}}R_{\alpha\gamma\bar{\beta}^\gamma} =& -\frac{1}{4}\left((\omega_A g)\,(\omega_B g) - \omega_A\omega_B\right)\partial_\mu v^A \partial^\mu v^B \\ g^{\alpha\bar{\beta}}R_{\alpha\bar{\gamma}\bar{\beta}^{\bar{\gamma}}} =& -\frac{1}{4}(\omega_A g)\,(\omega_B g)\,\partial_\mu v^A \partial^\mu v^B \\ &- \frac{1}{4} b_K \bar{b}_L \partial_\mu z^K \partial^\mu \bar{z}^L. \end{aligned} \tag{A.23}$$

All other terms are at least of order three in the moduli and omitted. Plugging everything into Equation 1.20 and integrating over Y gives the final result for the dimensionally reduced Einstein-Hilbert term

Appendix B

Basic Propeties of Calabi-Yau Manifolds

This appendix summarizes the most important properties of Calabi-Yau manifolds used in this thesis. It does not serve as a pedagogical introduction into the vast subject of this interesting field of complex geometry. The reader interested in the basics of complex geometry can consult [57]. Many string theory textbooks provide excellent explanations of how Calabi-Yau manifolds are used in string theory. This list includes, but is not limited to, [1, 3, 2]. This Appendix is based primarily on the relevant sections of these references.

Definition B.0.1 *A Calabi-Yau manifold.*

A Calabi-Yau manifold is a compact Kähler manifold with vanishing first Chern class. ♣

Conjectured by Calabi, and consequently proved by Yau, Calabi-Yau manifolds admit a Ricci flat metric. Furthermore, they have $SU(N)$-holonomy. In this thesis we will be mainly concerned with Calabi-Yau threefolds, where the three refers to the complex dimension. The $SU(3)$-holonomy is important, as it ensures that the CY admits exactly one covariantly constant spinor [3]. Together with the Ricci-flatness of the metric, this is the reason why Calabi-Yau manifolds are considered a viable candidate for superstring compactifications.

There are a couple of differential forms that are of great importance to us. In the following z^μ and $\overline{z}^{\bar{\nu}}$ denote the holomorphic and anti-holomorphic coordinates on the CY-manifold of dimension m, respectively. Then a Calabi-Yau has mutually compatible Riemannian, complex and symplectic structures. For a fixed complex structure this results in the following forms:

1. The Hermitean metric $g = g_{\mu\bar{\nu}} dz^\mu \otimes d\overline{z}^{\bar{\nu}} + g_{\bar{\mu}\nu} d\overline{z}^{\bar{\mu}} \otimes dz^\nu$.
2. The Kähler form $J = i g_{\mu\bar{\nu}} dz^\mu \wedge d\overline{z}^{\bar{\nu}}$.
3. A nowhere vanishing m-form, given by:

$$\Omega = \underbrace{J \wedge \ldots \wedge J}_{m}.$$

Owing to the fact that on a Kähler manifold $dJ = 0$, one can establish the existence of a

Kähler potential $K(z,\overline{z})$, such that

$$g_{\mu\bar{\nu}} = \partial_\mu \partial_{\bar{\nu}} K \tag{B.1a}$$

$$J = i\partial\overline{\partial}K, \tag{B.1b}$$

where ∂ and $\overline{\partial}$ denote the holomorphic and anti-holomorphic Dolbeault operators, respectively.

Topologically Calabi-Yau manifolds are characterized by their Dolbeault cohomology groups $H^{(p,q)}$. If we denote $h^{(p,q)} = \dim_{\mathbb{C}}(H^{(p,q)})$, one finds that for a Calabi-Yau threefold only the Hodge numbers $h^{(1,1)}$ and $h^{(2,1)}$ are independent. The Hodge diamond of the Calabi-Yau then takes the form [11]

$$\begin{array}{ccccccc} & & h^{(0,0)} & & & & \\ & h^{(1,0)} & & h^{(0,1)} & & & \\ h^{(2,0)} & & h^{(1,1)} & & h^{(0,2)} & & \\ h^{(3,0)} & & h^{(2,1)} & & h^{(1,2)} & & h^{(0,3)} \\ & h^{(3,1)} & & h^{(2,2)} & & h^{(1,3)} & \\ & & h^{(3,2)} & & h^{(2,3)} & & \\ & & & h^{(3,3)} & & & \end{array} = \begin{array}{ccccccc} & & 1 & & & & \\ & 0 & & 0 & & & \\ 0 & & h^{(1,1)} & & 0 & & \\ 1 & & h^{(2,1)} & & h^{(2,1)} & & 1 \\ & 0 & & h^{(1,1)} & & 0 & \\ & & 0 & & 0 & & \\ & & & 1 & & & \end{array} . \tag{B.2}$$

In passing we mention that each Calabi-Yau manifold Y admits a mirror Calabi-Yau $\tilde{Y}$. In the setting of Calabi-Yau threefolds, the mirror manifold can be characterized through the interchanged Hodge numbers $h^{(1,1)}$ and $h^{(2,1)}$ of Y. Mirror symmetry is a tremendously powerful tool in string compactifications, as it allows us to translate problems on Y to their mirror $\tilde{Y}$. There are ample examples where these initial problems simplify tremendously under this mirror map. We will not explicitly investigate these powerful tools, but often we will simply use the results. For the interested reader [46] would be a good place to start reading more about this topic.

B.0.1 Metric deformations

As string theory is a theory of quantum gravity, we need to treat the graviton as a dynamical field in its own right. In particular, this means that the Calabi-Yau metric is not fixed but allowed to fluctuate around some background value. To have a sensible string compactification, however, these fluctuations are not allowed to break the Calabi-Yau condition. We therefore have to make sure that the new metric still satisfies the conditions appropriate for a Calabi-Yau. In particular, it must remain Ricci flat. This condition leads to various modes of the graviton describing the volume and shape of the Calabi-Yau manifold. The space of these various deformations is called a *moduli* space and they come naturally equipped with a metric.

Consider now the setting in which we compactify on an internal manifold that is Calabi-Yau. If the metric on this internal space is denoted g_{mn}, we can think about perturbing it according to

$$g_{mn} \to g_{mn} + \delta g_{mn}. \tag{B.3}$$

If our perterubed metric is to satisfy the Calabi-Yau conditions, we require that

$$R_{mn}(g+\delta g)=0. \tag{B.4}$$

Deformations δg satisfying the Condition B.4 change the size and structure of the Calabi-Yau in such a way that preserves both the topology and the admittance of one covariantly constant spinor. The coefficients of these deformations will turn up in the lower dimensional theory as scalar fields called *moduli*.

If we supplement Condition B.4 with a gauge condition that eliminates variations in the metric due to coordinate transformations, we end up with the Lichnerowicz equation [1]:

$$\nabla^k\nabla_k\delta g_{mn}+2R^{pq}_{mn}\delta g_{pq}=0. \tag{B.5}$$

A striking property of the Lichnerowicz equation is that deformations with pure index structure, $\delta g_{\alpha\beta}$, and deformations with mixed index structure $\delta g_{\alpha\bar{\beta}}$, decouple. This means that locally the moduli space of the Calabi-Yau manifold has a product form,

$$\text{Moduli space of Y} = \text{pure index structure} \times \text{mixed index structure}. \tag{B.6}$$

The part parametrized by deformations with a pure index structure is known as the *complex structure moduli space* whereas the part parametrized by the mixed index structure is known as the *Kähler moduli space*.

B.0.2 Complex Structure Moduli Space

The holomorphic and anti-holomorphic components of the background metric on Y are both zero. This can change if we perturb the metric. Since we want our background manifold to still be of the Calabi-Yau type, there must be a coordinate system in which the new metric $g+\delta g$ has only mixed index structure components. Since holomorphic functions do not change the index structure, we conclude that the metric is Hermitean with respect to a *new complex structure*. We therefore associate the metric deformations of the form $\delta g_{\bar{\alpha}\bar{\beta}}$ and $\delta g_{\alpha\beta}$ with a change of complex structure.

Via the unique holomorphic three form Ω, we can associate the complex structure variations with a $(2,1)$-form

$$\Omega_{abc}g^{c\bar{d}}\delta g_{\bar{d}\bar{e}}dz^a\wedge dz^b\wedge d\bar{z}^{\bar{e}}. \tag{B.7}$$

If the deformation $\delta g_{\bar{d}\bar{e}}$ satisfies the Lichnerowicz equation B.5 then this form is actually harmonic. By the Hodge decomposition we can conclude that the complex structure deformations are in one-to-one correspondence with the $(2,1)$ forms, via Equation B.7.

Using this fact, it is convenient to define the following basis of the $(2,1)$-forms:

$$\eta_A=\frac{1}{2}(b_A)_{\alpha\beta\bar{\gamma}}dz^\alpha\wedge dz^\beta\wedge d\bar{z}^{\bar{\gamma}}, \tag{B.8}$$

where the components are given by

$$(\eta_A)_{\alpha\beta\bar{\gamma}} = -\frac{1}{2}\Omega^{\bar{\delta}}_{\alpha\beta}\frac{\partial g_{\bar{\gamma}\bar{\delta}}}{\partial z^A}. \tag{B.9}$$

The z^A denote the local coordinates on the complex structure moduli space. If we consequently define

$$(b_A)_{\bar{\alpha}\bar{\beta}} = -\frac{i}{\|\Omega\|^2}\,(\eta_A)_{\bar{\alpha}\gamma\delta}\,\Omega^{\gamma\delta}_{\bar{\beta}}, \tag{B.10}$$

we find that

$$\delta g_{\bar{\alpha}\bar{\beta}} = z^A (b_A)_{\bar{\alpha}\bar{\beta}}. \tag{B.11}$$

It turns out that the manifold of complex structure comes equipped with the Weil-Peterson metric

$$-\frac{\int_Y \eta_A \wedge \eta_B}{\int_Y \Omega \wedge \overline{\Omega}} = \frac{1}{2V}\int g^{a\bar{b}} g^{c\bar{d}}\left[\delta g_{ac}\delta g_{bd}\right], \tag{B.12}$$

where from the second definition it becomes clear that Q_{AB} in the effective action 1.22 that couples the moduli z^A and $\overline{z}^A$ indeed appears as a metric on the complex structure moduli space. It turns out that this metric is also Kähler, with potential given by

$$K = -\log\left[-\mathrm{i}\int_Y \Omega\wedge\bar{\Omega}\right]. \tag{B.13}$$

A striking feature of the complex structure moduli space is the fact that it is *special Kähler*. This means that we can write the Kähler potential in terms of a *prepotential* $\mathcal{F}$. In order to see how this work, let us first introduce a basis of homology three-cycles $\{\rho_{\hat{K}}, \sigma^{\hat{L}}\}$ (see also Table 2.1) such that they intersect according to the following rules

$$\rho_{\hat{K}}\bigcap\sigma^{\hat{L}} = -\sigma^{\hat{L}}\bigcap\rho_{\hat{K}} = \delta^{\hat{L}}_{\hat{K}}, \quad \rho_{\hat{K}}\bigcap\rho_{\hat{L}} = \sigma^{\hat{L}}\bigcap\sigma^{\hat{K}} = 0. \tag{B.14}$$

We can consequently consider the dual cohomology basis $\{\alpha_{\hat{K}}, \beta^{\hat{L}}\}$. Their integration relations with respect to the homology elements of Equation B.14 are given by

$$\begin{aligned}
&\int_{\sigma^{\hat{L}}}\alpha_{\hat{K}} = \int_Y \alpha_{\hat{K}}\wedge\beta^{\hat{L}} = \delta^{\hat{L}}_{\hat{K}}, \quad \int_{\rho_{\hat{K}}}\beta^{\hat{L}} = \int_Y \beta^{\hat{L}}\wedge\alpha_{\hat{K}} = -\delta^{\hat{L}}_{\hat{K}} \\
&\int_{\sigma^{\hat{L}}}\beta^{\hat{K}} = \int_{\rho_{\hat{K}}}\alpha_{\hat{L}} = 0.
\end{aligned} \tag{B.15}$$

Having these at our disposal, we can define the *periods* of the holomorphic three from Ω. These are defined as

$$\mathcal{X}^\Lambda = \int_{\sigma^\Lambda}\Omega_3 = \int_Y \Omega_3\wedge\beta^\Lambda, \qquad \mathcal{F}_\Lambda = \int_{\rho_\Lambda}\Omega_3 = \int_Y \Omega_3\wedge\alpha_\Lambda. \tag{B.16}$$

Using both Equations B.14 and B.15 we see that the holomorphic three-form can be expanded as

$$\Omega_3 = \mathcal{X}^\Lambda \alpha_\Lambda - \mathcal{F}_\Lambda \beta^\Lambda. \tag{B.17}$$

The *prepotential* is a homogeneous degree two polynomial in the moduli that satisfies

$$\mathcal{F}_\Lambda = \frac{\partial}{\partial \mathcal{X}^\Lambda} \mathcal{F}. \tag{B.18}$$

In the large complex structure regime we can explicitly write this prepotential as

$$\mathcal{F} = -\frac{\kappa^0_{ijk} \mathcal{X}^i \mathcal{X}^j \mathcal{X}^k}{3! \mathcal{X}^0} + \frac{1}{2} \tilde{p}_{ij} \mathcal{X}^i \mathcal{X}^j + \tilde{p}_i \mathcal{X}^i \mathcal{X}^0 - \frac{i}{2} \tilde{p}_0 \left(\mathcal{X}^0\right)^2. \tag{B.19}$$

The projective coordinates $\mathcal{X}^i$ are related through the complex structure moduli z^i through $\mathcal{X}^I = (1, z^i)$. The coefficients appearing in Equation B.19 are topological numbers characterizing the *mirror* Calabi-Yau. They are related through the so-called mirror map [46, 1]. Using this prepotential in the expansion of the holomorphic three form in Equation B.17 the Kähler potential can then be written as

$$K = -\ln\left[-i\left(\mathcal{X}^\Lambda \bar{\mathcal{F}}_\Lambda - \bar{\mathcal{X}}^\Lambda \mathcal{F}_\Lambda\right)\right]. \tag{B.20}$$

Given the prepotential, the gauge coupling function $\mathcal{M}$ appearing in Equation 1.32 is given by

$$\mathcal{M} = \overline{\mathcal{F}}_{AB} + \frac{2i}{(\mathrm{Im}\,\mathcal{F})_{PQ} \mathcal{X}^P \mathcal{X}^Q} (\mathrm{Im}\,\mathcal{F})_{AC} (\mathrm{Im}\,\mathcal{F})_{BD} \mathcal{X}^C \mathcal{X}^D. \tag{B.21}$$

B.0.3 Kähler structure moduli space

We have seen that the variations in the metric corresponding to pure index structures are related to changes in the complex structure. The next step is to consider the variations $\delta g_{a\bar{b}}$ that have a mixed index structure. Since these correspond to elements of $H^{(1,1)}(Y)$, the mixed index variations change the Kähler form J and are therefore called Kähler deformations. By convention we consider the complexified Kähler class, combining the mixed index metric deformations with the magnetic two form B_2. That is, the variation of the Kähler form

$$g_{i\bar{\jmath}} + \delta g_{i\bar{\jmath}} = -i J_{i\bar{\jmath}} = -i v^A \left(\omega_A\right)_{i\bar{\jmath}}, \quad A = 1, \ldots, h^{(1,1)} \tag{B.22}$$

is combined with the scalars b^A of the magnetic two form B_2 to give the Kähler moduli t^A

$$t^A = b^A + i v^A. \tag{B.23}$$

The relevant integrals over the harmonic one forms are then given by

$$\begin{aligned} \mathcal{K} &= \frac{1}{6}\int_Y J\wedge J\wedge J, \quad \mathcal{K}_i = \int_Y \omega_i\wedge J\wedge J \\ \mathcal{K}_{ij} &= \int_Y \omega^i\wedge\omega^j\wedge J, \quad \mathcal{K}_{ijk} = \int_Y \omega^i\wedge\omega^j\wedge\omega^k. \end{aligned} \tag{B.24}$$

The moduli space defined by the Kähler deformations is again a Kähler manifold and the metric is defined by [6]

$$g_{ij} = \frac{1}{4\mathcal{K}}\int_Y \omega_i\wedge *\omega_j. \tag{B.25}$$

Using the identity [58]

$$*\omega_i = -J\wedge\omega_i + \frac{\mathcal{K}_i}{4\mathcal{K}}J\wedge J \tag{B.26}$$

we can rewrite the metric as

$$g_{ij} = -\frac{1}{4\mathcal{K}}\left(\mathcal{K}_{ij} - \frac{1}{4\mathcal{K}}\mathcal{K}_i\mathcal{K}_j\right). \tag{B.27}$$

For Calabi-Yau compactifications the Kähler moduli space is again special Kähler. The prepotential can then be written as

$$\mathcal{F} = -\frac{1}{3!}\frac{\mathcal{K}_{ijk}X^iX^jX^k}{X^0}, \tag{B.28}$$

where now the projective coordinates are related to the Kähler moduli as $X^I = (1, t^i)$. Using above definitions one can show that the coupling P_{AB} in Equation 1.24 can be written as

$$P_{ij} = 2\mathcal{K}g_{ij} - \frac{1}{4\mathcal{K}}\mathcal{K}_i\mathcal{K}_j. \tag{B.29}$$

Appendix C

Calabi-Yau Data

In this section we provide the topological data of the Calabi-Yau manifolds studied in Chapter 4. The information for the examples with $h^{(1,1)} = 2$ were taken from [34, 44]. For $h^{(1,1)} = 3$ we used the topological data from [51, 59, 60] combined with the pyCICY package supplementing [61]. These CICY's carry an identification following [62], and their Gopakumar-Vafa invariants can be found in the database supplementing [52]. All topological numbers are written down in the Kähler basis, following the conventions of [34, 44].

C.0.1 CY's with $h^{(1,1)} = 2$

Further info in [34].

CY # / Identifier	- χ	Intersection Tensor	$c_2(J)$
1 / $\mathcal{M}_{2,8}$	- 168	{{{8, 4}, {4, 0}}, {{4, 0}, {0, 0}}}	$\{56, 24\}$
2 / $\mathcal{M}_{2,9}$	- 168	{{{8, 4}, {4, 0}}, {{4, 0}, {0, 0}}}	$\{56, 24\}$
3 / $\mathcal{M}_{2,10}$	- 168	{{{0, 0}, {0, 4}}, {{0, 4}, {4, 8}}}	$\{24, 56\}$
4 / $\mathcal{M}_{2,11}$	- 168	{{{0, 0}, {0, 4}}, {{0, 4}, {4, 2}}}	$\{24, 44\}$
5 / $\mathcal{M}_{2,12}$	- 168	{{{0, 0}, {0, 4}}, {{0, 4}, {4, 5}}}	$\{24, 50\}$
6 / $\mathcal{M}_{2,30}$	- 252	{{{4, 2}, {2, 0}}, {{2, 0}, {0, 0}}}	$\{52, 24\}$
7 / $\mathcal{M}_{2,31}$	- 252	{{{4, 2}, {2, 0}}, {{2, 0}, {0, 0}}}	$\{52, 24\}$
8 / $\mathcal{M}_{2,32}$	- 252	{{{0, 0}, {0, 2}}, {{0, 2}, {2, 4}}}	$\{24, 52\}$
9 / $\mathcal{M}_{2,33}$	- 252	{{{0, 0}, {0, 2}}, {{0, 2}, {2, 0}}}	$\{24, 36\}$
10 / $\mathcal{M}_{2,34}$	- 252	{{{0, 0}, {0, 2}}, {{0, 2}, {2, 2}}}	$\{24, 44\}$

Table C.1: Topological data of the Calabi-Yau's with $h^{(1,1)} = 2$. The Identifier corresponds to the number in [34], where these are the $K3$-fibred ones.

C.0.2 CICY's with $h^{(1,1)} = 2$

Further info in [44].

CY # / Identifier	- χ	Intersection Tensor	$c_2(J)$
11 / $\mathcal{M}_{2,10}$ / 7860	- 108	{{{0, 0}, {0, 6}}, {{0, 6}, {6, 6}}}	$\{24, 48\}$
12 / $\mathcal{M}_{2,14}$ / 7816	- 112	{{{0, 0}, {0, 8}}, {{0, 8}, {8, 8}}}	$\{24, 56\}$
13 / $\mathcal{M}_{2,15}$ / 7817	- 112	{{{0, 0}, {0, 8}}, {{0, 8}, {8, 12}}}	$\{24, 60\}$
14 / $\mathcal{M}_{2,16}$ / 7819	- 112	{{{0, 0}, {0, 8}}, {{0, 8}, {8, 16}}}	$\{24, 64\}$
15 / $\mathcal{M}_{2,18}$ / 7822	- 112	{{{0, 0}, {0, 8}}, {{0, 8}, {8, 8}}}	$\{24, 56\}$
16 / $\mathcal{M}_{2,19}$ / 7823	- 112	{{{0, 0}, {0, 8}}, {{0, 8}, {8, 16}}}	$\{24, 64\}$
17 / $\mathcal{M}_{2,21}$ / 7840	- 120	{{{0, 0}, {0, 6}}, {{0, 6}, {6, 9}}}	$\{24, 54\}$
18 / $\mathcal{M}_{2,24}$ / 7875	- 128	{{{0, 0}, {0, 6}}, {{0, 6}, {6, 5}}}	$\{24, 50\}$
19 / $\mathcal{M}_{2,26}$ / 7867	- 132	{{{0, 0}, {0, 6}}, {{0, 6}, {6, 12}}}	$\{24, 60\}$
20 / $\mathcal{M}_{2,28}$ / 7869	- 132	{{{0, 0}, {0, 6}}, {{0, 6}, {6, 12}}}	$\{24, 60\}$
21 / $\mathcal{M}_{2,29}$ / 7873	- 140	{{{0, 0}, {0, 6}}, {{0, 6}, {6, 8}}}	$\{24, 56\}$
22 / $\mathcal{M}_{2,30}$ / 7882	- 148	{{{0, 0}, {0, 6}}, {{0, 6}, {6, 4}}}	$\{24, 52\}$
23 / $\mathcal{M}_{2,33}$ / 7885	- 168	{{{0, 0}, {0, 4}}, {{0, 4}, {4, 5}}}	$\{24, 50\}$
24 / $\mathcal{M}_{2,34}$ / 7886	- 168	{{{0, 0}, {0, 4}}, {{0, 4}, {4, 8}}}	$\{24, 56\}$
25 / $\mathcal{M}_{2,35}$ / 7887	- 168	{{{0, 0}, {0, 4}}, {{0, 4}, {4, 2}}}	$\{24, 44\}$
26 / $\mathcal{M}_{2,56}$ / 7888	- 168	{{{0, 0}, {0, 4}}, {{0, 4}, {4, 8}}}	$\{24, 52\}$

Table C.2: Topological data of the Calabi-Yau's with $h^{(1,1)} = 2$. The Identifier corresponds to the number in [44], where they used the numbering originally proposed in [62].

C.0.3 CICY's with $h^{(1,1)} = 3$

The data for these CICY's was constructed using the database of [51, 59, 60] and the pyCICY package of [61].

CY # / Identifier	- χ	Intersection Tensor	$c_2(J)$
27 / 7872	- 138	{{{0, 0, 0}, {0, 0, 3}, {0, 3, 4}}, {{0, 0, 3}, {0, 0, 0}, {3, 0, 4}}, {{0, 3, 4}, {3, 0, 4}, {4, 4, 5}}}	$\{24, 24, 50\}$
28 / 7874	- 144	{{{0, 0, 0}, {0, 0, 3}, {0, 3, 2}}, {{0, 0, 3}, {0, 0, 0}, {3, 0, 4}}, {{0, 3, 2}, {3, 0, 4}, {2, 4, 2}}}	$\{24, 24, 44\}$
29 / 7875	- 144	{{{0, 0, 0}, {0, 0, 3}, {0, 3, 2}}, {{0, 0, 3}, {0, 0, 3}, {3, 3, 3}}, {{0, 3, 2}, {3, 3, 3}, {2, 3, 0}}}	$\{24, 24, 36\}$
30 / 7877	- 144	{{{0, 0, 0}, {0, 6, 3}, {0, 3, 0}}, {{0, 6, 3}, {6, 4, 2}, {3, 2, 0}}, {{0, 3, 0}, {3, 2, 0}, {0, 0, 0}}}	$\{24, 24, 52\}$
31 / 7880	- 144	{{{0, 0, 0}, {0, 0, 3}, {0, 3, 2}}, {{0, 0, 3}, {0, 0, 0}, {3, 0, 2}}, {{0, 3, 2}, {3, 0, 2}, {2, 2, 0}}}	$\{24, 24, 36\}$
32 / 7881	- 144	{{{0, 0, 0}, {0, 6, 3}, {0, 3, 0}}, {{0, 6, 3}, {6, 4, 2}, {3, 2, 0}}, {{0, 3, 0}, {3, 2, 0}, {0, 0, 0}}}	$\{24, 24, 52\}$

Table C.3: Topological data of the Calabi-Yau's with $h^{(1,1)} = 3$.

Appendix D

Fit Parameters

Calabi-Yau Geometry	a	b	c
1	–	–	–
2	–	–	–
3	−4.20294	0.10426	−0.08952
4	−4.63451	0.11466	15.72183
5	−0.54211	−0.09082	0.34887
6	–	–	–
7	–	–	–
8	−5.16931	0.14210	4.78786
9	−3.28989	0.07205	4.78264
10	−3.98856	0.09174	2.50147
11	−2.34126	0.01585	−1.90496
12	−3.20881	0.06018	12.29477
13	–	–	–
14	−3.59785	0.07807	2.34874
15	−3.20881	0.06018	12.29477
16	−3.59785	0.07807	2.34874
17	−4.88672	0.12846	2.68414
18	−0.49527	−0.04889	0.62336
19	−3.74791	0.08082	−0.87777
20	−3.74791	0.08082	−0.87777
21	−6.232434	0.16751	23.73144
22	−2.70194	0.05032	9.21037
23	−0.54211	−0.09082	0.34887
24	−4.20294	0.10426	−0.08952
25	−4.63451	0.11466	15.72183
26	−4.20294	0.10426	−0.08952
27	−0.423924	−0.068461	−9.154524
28	–	–	–
29	–	–	–
30	−19.718599	0.551861	85.51697
31	−7.41115	0.2182168	34.128653
32	−19.718599	0.551861	85.51697

Table D.1: Parameter settings for the model defined by Equation 4.41 for all 32 Calabi-Yau geometries investigated, representing the scaling of W_0 with respect to N_{flux}.

Calabi-Yau Geometry	a	b	c
1	–	–	–
2	–	–	–
3	−9.753035	0.25281	1.901020
4	−10.55544	0.26033	38.54870
5	−10.03593	0.205769	43.3325
6	–	–	–
7	–	–	–
8	−10.13079	0.266725	3.225086
9	−7.04154	0.14924	12.1764
10	−8.08865	0.177118	1.993767
11	−4.849378	0.0314722	−5.410354
12	−1.00365	−0.03907	−21.19424
13	–	–	–
14	−10.17023	0.21985	25.65089
15	−1.00365	−0.03907	−21.19424
16	−10.17023	0.21985	25.65089
17	−9.683946	0.2074655	13.02949
18	−1.06192	−0.09769	−4.11469
19	−8.21151	0.17478	−2.22712
20	−8.21151	0.17478	−2.22712
21	−11.90508	0.307117	40.00581
22	−0.90354	−0.03849	−17.29690
23	−10.03593	0.205769	43.3325
24	−9.753035	0.25281	1.901020
25	−10.55544	0.26033	38.54870
26	−9.753035	0.25281	1.901020
27	−2.18888	−0.09344	−21.7134959
28	–	–	–
29	–	–	–
30	−26.86069	0.70097988	93.81479
31	−8.7041256	0.17782	26.35305
32	−26.86069	0.70097988	93.81479

Table D.2: Parameter settings for the model defined by Equation 4.42 for all 32 Calabi-Yau geometries investigated, representing the scaling of M^2_{min} with respect to N_{flux}. The empty entries correspond to models that did not admit any solutions.

Calabi-Yau Geometry	a	b
1	–	–
2	–	–
3	4.00000	−17.75555
4	3.99999	−19.67677
5	3.99999	−24.86004
6	–	–
7	–	–
8	3.999999	−18.94479
9	4.00000	−16.57476
10	3.99999	−18.25533
11	3.99999	−13.82452
12	4.00000	−24.58234
13	–	–
14	4.00184	−21.21490
15	4.00000	−24.58234
16	4.00184	−21.21490
17	3.99999	−19.43065
18	3.999999	−24.79225
19	4.000000	−16.91920
20	4.000000	−16.91920
21	4.000578	−18.96495
22	3.999999	−22.668517
23	3.99999	−24.86004
24	4.00000	−17.75555
25	3.99999	−19.67677
26	4.00000	−17.75555
27	–	–
28	–	–
29	–	–
30	–	–
31	–	–
32	–	–

Table D.3: Parameter settings for the model defined by Equation 4.43 for all 32 Calabi-Yau geometries investigated, representing the scaling of the upper boundary of M^2_{max} with respect to N_{flux}. The empty entries correspond to models that did not admit any solutions.

Calabi-Yau Geometry	a	b
1	–	–
2	–	–
3	−1.692140	−1.303736
4	−1.61968	2.739722
5	−1.656419	0.207017
6	–	–
7	–	–
8	−1.657491	−1.715677
9	−1.681597	4.6205711
10	−1.6586443	0.401894
11	−1.585089	0.4996058
12	−1.852590	4.0921336
13	–	–
14	−1.597698	−0.721343
15	−1.852590	4.0921336
16	−1.597698	−0.721343
17	−1.646110	−0.227977
18	−1.571493	1.8914033
19	−1.7643601	−0.590592
20	−1.7643601	−0.590592
21	−1.5438675	0.43597675
22	−1.800346	5.2104519
23	−1.656419	0.207017
24	−1.692140	−1.303736
25	−1.61968	2.739722
26	−1.692140	−1.303736
27	–	–
28	–	–
29	–	–
30	–	–
31	–	–
32	–	–

Table D.4: Parameter settings for the model defined by Equation 4.43 for all 32 Calabi-Yau geometries investigated, representing the scaling of the lower boundary of M^2_{max} with respect to N_{flux}. The empty entries correspond to models that did not admit any solutions or that did not admit a clear boundary region to fit.

Calabi-Yau Geometry	a	b
1	–	–
2	–	–
3	0.0683473	2.1248882
4	0.1814214	2.14074124
5	0.0037455	2.0712002
6	–	–
7	–	–
8	0.376120	2.221312
9	8.2030637	2.2216796
10	0.80770714	2.2244397
11	239.681496	2.5210463
12	0.00331384	1.9790171
13	–	–
14	0.00697314	2.0758698
15	0.00331384	1.9790171
16	0.00697314	2.0758698
17	0.02388102	2.09279784
18	0.00273291	2.03662475
19	0.55216128	2.23595847
20	0.55216128	2.23595847
21	0.7469129	2.2620552
22	0.01633044	2.018057
23	0.0037455	2.0712002
24	0.0683473	2.1248882
25	0.1814214	2.14074124
26	0.0683473	2.1248882
27	0.1216724	2.18653729
28	–	–
29	–	–
30	0.2487028	0.2487028
31	1.75147	2.2535075
32	0.2487028	0.2487028

Table D.5: Parameter settings for the model defined by Equation 4.44 for all 32 Calabi-Yau geometries investigated, representing the scaling of M^2_{min} with respect to W_0. The empty entries correspond to models that did not admit any solutions or that did not admit a clear boundary region to fit.

Bibliography

[1] R. Blumenhagen, D. Lüst, and S. Theisen. *Basic concepts of string theory*. Vol. 17. Springer, 2013.

[2] K. Becker, M. Becker, and J. H. Schwarz. *String theory and M-theory: A modern introduction*. Cambridge University Press, Dec. 2006. ISBN: 978-0-511-25486-4, 978-0-521-86069-7, 978-0-511-81608-6. DOI: 10.1017/CBO9780511816086.

[3] M. B. Green, J. H. Schwarz, and E. Witten. *Superstring Theory: 25th Anniversary Edition*. Vol. 1. Cambridge Monographs on Mathematical Physics. Cambridge University Press, 2012. DOI: 10.1017/CBO9781139248563.

[4] J. Polchinski. *String theory*. 2005.

[5] D. Tong. *Lectures on String Theory*. 2009. DOI: 10.48550/ARXIV.0908.0333. URL: https://arxiv.org/abs/0908.0333.

[6] S. Gurrieri. "N= 2 and N= 4 supergravities as compactifications from string theories in 10 dimensions". In: *arXiv preprint hep-th/0408044* (2004).

[7] C. Li. "Geometric derivations of quantum corrections for gauge coupling functions". MA thesis. 2017.

[8] R. Böhm et al. "Compactification of type IIB string theory on Calabi–Yau threefolds". In: *Nuclear Physics B* 569.1-3 (Mar. 2000), pp. 229–246. ISSN: 0550-3213. DOI: 10.1016/s0550-3213(99)00796-8. URL: http://dx.doi.org/10.1016/S0550-3213(99)00796-8.

[9] J. Michelson. "Compactifications of Type IIB strings to four dimensions with non-trivial classical potential". In: *Nuclear Physics B* 495.1-2 (June 1997), pp. 127–148. ISSN: 0550-3213. DOI: 10.1016/s0550-3213(97)00184-3. URL: http://dx.doi.org/10.1016/S0550-3213(97)00184-3.

[10] M. Graña and H. Triendl. "String Theory Compactifications". In: 2017.

[11] T. Grimm. "The effective action of type II Calabi-Yau orientifolds". In: *Fortschritte der Physik* 53.11-12 (Nov. 2005), pp. 1179–1271. ISSN: 1521-3978. DOI: 10.1002/prop.200510253. URL: http://dx.doi.org/10.1002/prop.200510253.

[12] T. W. Grimm and J. Louis. "The effective action of Calabi–Yau orientifolds". In: *Nuclear Physics B* 699.1-2 (Nov. 2004), pp. 387–426. ISSN: 0550-3213. DOI: 10.1016/j.nuclphysb.2004.08.005. URL: http://dx.doi.org/10.1016/j.nuclphysb.2004.08.005.

[13] I. Brunner and K. Hori. "Orientifolds and Mirror Symmetry". In: *Journal of High Energy Physics* 2004.11 (Nov. 2004), pp. 005–005. ISSN: 1029-8479. DOI: 10.1088/1126-6708/2004/11/005. URL: http://dx.doi.org/10.1088/1126-6708/2004/11/005.

[14] B. Acharya et al. "Orientifolds, mirror symmetry and superpotentials". In: *arXiv preprint hep-th/0202208* (2002).

[15] A. Sen. "F-theory and orientifolds". In: *Nuclear Physics B* 475.3 (Sept. 1996), pp. 562–578. ISSN: 0550-3213. DOI: 10.1016/0550-3213(96)00347-1. URL: http://dx.doi.org/10.1016/0550-3213(96)00347-1.

[16] R. Blumenhagen et al. "Four-dimensional string compactifications with D-branes, orientifolds and fluxes". In: *Physics Reports* 445.1–6 (July 2007), pp. 1–193. ISSN: 0370-1573. DOI: 10.1016/j.physrep.2007.04.003. URL: http://dx.doi.org/10.1016/j.physrep.2007.04.003.

[17] J. Polchinski. *TASI Lectures on D-Branes*. 1997. arXiv: hep-th/9611050 [hep-th].

[18] R. C. Myers. "Non-Abelian phenomena on D-branes". In: *Classical and Quantum Gravity* 20.12 (May 2003), S347–S372. ISSN: 1361-6382. DOI: 10.1088/0264-9381/20/12/302. URL: http://dx.doi.org/10.1088/0264-9381/20/12/302.

[19] C. P. Bachas. *Lectures on D-branes*. 1998. DOI: 10.48550/ARXIV.HEP-TH/9806199. URL: https://arxiv.org/abs/hep-th/9806199.

[20] E. Plauschinn. "Type IIB Orientifolds, D-Brane Instantons And The Large Volume Scenario". In: *Fortsch. Phys.* 58 (2010), pp. 913–1019. DOI: 10.1002/prop.200900109.

[21] D. Z. Freedman and A. Van Proeyen. *Supergravity*. Cambridge University Press, 2012. DOI: 10.1017/CBO9781139026833.

[22] S. B. Giddings, S. Kachru, and J. Polchinski. "Hierarchies from fluxes in string compactifications". In: *Physical Review D* 66.10 (Nov. 2002). ISSN: 1089-4918. DOI: 10.1103/physrevd.66.106006. URL: http://dx.doi.org/10.1103/PhysRevD.66.106006.

[23] J. A. Harvey and G. Moore. *Superpotentials and Membrane Instantons*. 1999. arXiv: hep-th/9907026 [hep-th].

[24] L. Goerlich et al. "Gaugino Condensation and Nonperturbative Superpotentials in Flux Compactifications". In: *Journal of High Energy Physics* 2004.12 (Jan. 2005), pp. 074–074. ISSN: 1029-8479. DOI: 10.1088/1126-6708/2004/12/074. URL: http://dx.doi.org/10.1088/1126-6708/2004/12/074.

[25] M. Graña. "Flux compactifications in string theory: A comprehensive review". In: *Physics Reports* 423.3 (Jan. 2006), pp. 91–158. ISSN: 0370-1573. DOI: 10.1016/j.physrep.2005.10.008. URL: http://dx.doi.org/10.1016/j.physrep.2005.10.008.

[26] L. E. Ibanez and A. M. Uranga. *String theory and particle physics: An introduction to string phenomenology*. Cambridge University Press, Feb. 2012. ISBN: 978-0-521-51752-2, 978-1-139-22742-1.

[27] S. Gukov, C. Vafa, and E. Witten. "CFT's from Calabi–Yau four-folds". In: *Nuclear Physics B* 584.1–2 (Sept. 2000), pp. 69–108. ISSN: 0550-3213. DOI: 10.1016/s0550-3213(00)00373-4. URL: http://dx.doi.org/10.1016/S0550-3213(00)00373-4.

[28] E. Plauschinn. "The tadpole conjecture at large complex-structure". In: *Journal of High Energy Physics* 2022.2 (Feb. 2022). ISSN: 1029-8479. DOI: 10.1007/jhep02(2022)206. URL: http://dx.doi.org/10.1007/JHEP02(2022)206.

[29] S. Lüst et al. *Holography and the KKLT Scenario*. 2022. DOI: 10.48550/ARXIV.2204.07171. URL: https://arxiv.org/abs/2204.07171.

[30] S. Kachru et al. "de Sitter vacua in string theory". In: *Physical Review D* 68.4 (Aug. 2003). ISSN: 1089-4918. DOI: 10.1103/physrevd.68.046005. URL: http://dx.doi.org/10.1103/PhysRevD.68.046005.

[31] I. Bena et al. "The tadpole problem". In: *Journal of High Energy Physics* 2021.11 (Nov. 2021). DOI: 10.1007/jhep11(2021)223. URL: https://doi.org/10.1007%2Fjhep11%282021%29223.

[32] E. Plauschinn. "The tadpole conjecture at large complex-structure". In: *Journal of High Energy Physics* 2022.2 (Feb. 2022). DOI: 10.1007/jhep02(2022)206. URL: https://doi.org/10.1007%2Fjhep02%282022%29206.

[33] E. Witten. "Non-perturbative superpotentials in string theory". In: *Nuclear Physics B* 474.2 (Aug. 1996), pp. 343–360. DOI: 10.1016/0550-3213(96)00283-0. URL: https://doi.org/10.1016%2F0550-3213%2896%2900283-0.

[34] F. Carta, A. Mininno, and P. Shukla. "Systematics of perturbatively flat flux vacua". In: *Journal of High Energy Physics* 2022.2 (Feb. 2022). ISSN: 1029-8479. DOI: 10.1007/jhep02(2022)205. URL: http://dx.doi.org/10.1007/JHEP02(2022)205.

[35] S. K. Ashok and M. R. Douglas. "Counting Flux Vacua". In: *Journal of High Energy Physics* 2004.01 (Jan. 2004), pp. 060–060. DOI: 10.1088/1126-6708/2004/01/060. URL: https://doi.org/10.1088%2F1126-6708%2F2004%2F01%2F060.

[36] F. Denef and M. R. Douglas. "Distributions of flux vacua". In: *Journal of High Energy Physics* 2004.05 (May 2004), pp. 072–072. DOI: 10.1088/1126-6708/2004/05/072. URL: https://doi.org/10.1088%2F1126-6708%2F2004%2F05%2F072.

[37] F. Denef and M. R. Douglas. "Distributions of nonsupersymmetric flux vacua". In: *Journal of High Energy Physics* 2005.03 (Mar. 2005), pp. 061–061. DOI: 10.1088/1126-6708/2005/03/061. URL: https://doi.org/10.1088%2F1126-6708%2F2005%2F03%2F061.

[38] M. R. Douglas, B. Shiffman, and S. Zelditch. "Critical Points and Supersymmetric Vacua I". In: *Communications in Mathematical Physics* 252.1-3 (Oct. 2004), pp. 325–358. DOI: 10.1007/s00220-004-1228-y. URL: https://doi.org/10.1007%2Fs00220-004-1228-y.

[39] M. R. Douglas, B. Shiffman, and S. Zelditch. "Critical points and supersymmetric vacua, II: Asymptotics and extremal metrics". In: (2004). DOI: 10.48550/ARXIV.MATH/0406089. URL: https://arxiv.org/abs/math/0406089.

[40] M. R. Douglas and S. Kachru. "Flux compactification". In: *Reviews of Modern Physics* 79.2 (May 2007), pp. 733–796. DOI: 10.1103/revmodphys.79.733. URL: https://doi.org/10.1103%2Frevmodphys.79.733.

[41] M. Demirtas et al. "Vacua with Small Flux Superpotential". In: *Physical Review Letters* 124.21 (May 2020). ISSN: 1079-7114. DOI: 10.1103/physrevlett.124.211603. URL: http://dx.doi.org/10.1103/PhysRevLett.124.211603.

[42] M. Demirtas et al. "Conifold Vacua with Small Flux Superpotential". In: *Fortschritte der Physik* 68.11–12 (Oct. 2020), p. 2000085. ISSN: 1521-3978. DOI: 10.1002/prop.202000085. URL: http://dx.doi.org/10.1002/prop.202000085.

[43] R. Álvarez-García et al. "Small Flux Superpotentials for Type IIB Flux Vacua Close to a Conifold". In: *Fortschritte der Physik* 68.11–12 (Oct. 2020), p. 2000088. ISSN: 1521-3978. DOI: 10.1002/prop.202000088. URL: http://dx.doi.org/10.1002/prop.202000088.

[44] F. Carta, A. Mininno, and P. Shukla. "Systematics of perturbatively flat flux vacua for CICYs". In: (Jan. 2022). arXiv: 2201.10581 [hep-th].

[45] L. Schlechter. "Computational methods in string theory and applications to the swampland conjectures". PhD thesis. Munich U., Munich U., 2021. DOI: 10.5282/edoc.28084.

[46] S. Hosono, A. Klemm, and S. Theisen. "Lectures on mirror symmetry". In: *Lecture Notes in Physics* (), pp. 235–280. DOI: 10.1007/3-540-58453-6_13. URL: http://dx.doi.org/10.1007/3-540-58453-6_13.

[47] P. Candelas et al. "Mirror symmetry for two-parameter models — II". In: *Nuclear Physics B* 429.3 (Nov. 1994), pp. 626–674. ISSN: 0550-3213. DOI: 10.1016/0550-3213(94)90155-4. URL: http://dx.doi.org/10.1016/0550-3213(94)90155-4.

[48] J. P. Conlon and F. Quevedo. "Astrophysical and cosmological implications of large volume string compactifications". In: *Journal of Cosmology and Astroparticle Physics* 2007.08 (Aug. 2007), pp. 019–019. DOI: 10.1088/1475-7516/2007/08/019. URL: https://doi.org/10.1088%2F1475-7516%2F2007%2F08%2F019.

[49] R. Blumenhagen et al. *Large field inflation and string moduli stabilization*. 2015. DOI: 10.48550/ARXIV.1510.04059. URL: https://arxiv.org/abs/1510.04059.

[50] J. Conlon. "Moduli stabilisation and applications in IIB string theory". In: *Fortschritte der Physik* 55.3 (Mar. 2007), pp. 287–422. DOI: 10.1002/prop.200610334. URL: https://doi.org/10.1002%2Fprop.200610334.

[51] R. Altman et al. "A Calabi-Yau database: threefolds constructed from the Kreuzer-Skarke list". In: *Journal of High Energy Physics* 2015.2 (Feb. 2015). DOI: 10.1007/jhep02(2015)158. URL: https://doi.org/10.1007%2Fjhep02%282015%29158.

[52] F. Carta et al. "Gopakumar-Vafa hierarchies in winding inflation and uplifts". In: *Journal of High Energy Physics* 2021.5 (May 2021). DOI: 10.1007/jhep05(2021)271. URL: https://doi.org/10.1007%2Fjhep05%282021%29271.

[53] R. Blumenhagen, A. Gligovic, and S. Kaddachi. "Mass Hierarchies and Quantum Gravity Constraints in DKMM-refined KKLT". In: (June 2022). arXiv: 2206.08400 [hep-th].

[54] B. Bastian, T. W. Grimm, and D. van de Heisteeg. "Engineering Small Flux Superpotentials and Mass Hierarchies". In: (Aug. 2021). arXiv: 2108.11962 [hep-th].

[55] M. Graña et al. "The Tadpole Conjecture in Asymptotic Limits". In: (Apr. 2022). arXiv: 2204.05331 [hep-th].

[56] E. Cattani, P. Deligne, and A. Kaplan. *On the Locus of Hodge Classes*. 1994. DOI: 10.48550/ARXIV.ALG-GEOM/9402009. URL: https://arxiv.org/abs/alg-geom/9402009.

[57] M. Nakahara. *Geometry, topology and physics*. CRC press, 2018.

[58] A. Strominger. "Yukawa Couplings in Superstring Compactification". In: *Phys. Rev. Lett.* 55 (1985), p. 2547. DOI: 10.1103/PhysRevLett.55.2547.

[59] R. Altman et al. "New large volume Calabi-Yau threefolds". In: *Physical Review D* 97.4 (Feb. 2018). DOI: 10.1103/physrevd.97.046003. URL: https://doi.org/10.1103%2Fphysrevd.97.046003.

[60] R. Altman et al. "Orientifold Calabi-Yau threefolds with divisor involutions and string landscape". In: *Journal of High Energy Physics* 2022.3 (Mar. 2022). DOI: 10.1007/jhep03(2022)087. URL: https://doi.org/10.1007%2Fjhep03%282022%29087.

[61] M. Larfors and R. Schneider. "Line Bundle Cohomologies on CICYs with Picard Number Two". In: *Fortschritte der Physik* 67.12 (Nov. 2019), p. 1900083. DOI: 10.1002/prop.201900083. URL: https://doi.org/10.1002%2Fprop.201900083.

[62] L. B. Anderson et al. "Fibrations in CICY threefolds". In: *Journal of High Energy Physics* 2017.10 (Oct. 2017). DOI: 10.1007/jhep10(2017)077. URL: https://doi.org/10.1007%2Fjhep10%282017%29077.